



NTNU – Trondheim
Norwegian University of
Science and Technology

Fatigue Capacity of partially loaded Areas in Concrete Structures submerged in Water

Erlend Bognøy
Tor Magne Søilverød Mo
Vegard Vee

Civil and Environmental Engineering (2 year)

Submission date: June 2014

Supervisor: Jan Arve Øverli, KT

Norwegian University of Science and Technology
Department of Structural Engineering

Master thesis in Structural Design 2014

by

Erlend Bognøy, Tor Magne Søilverød Mo and Vegard Vee

Fatigue capacity of partially loaded areas in concrete structures submerged in water

In the Eurocode (NS-EN-1992-1-1) and DNV design code (DNV-OS-C502) there are requirements to control the resistance of partially loaded areas. Since the load spreads out from the loaded area an increased compressive capacity compared to uniaxial strength is allowed due to confinement. To control the bursting forces below the loaded area, reinforcement must be provided to avoid spalling.

In design of wind turbines, the connection between steel shaft and the concrete foundation is subjected to a line load. The static capacity of this partially loaded area is given in Eurocode and DNV design code. However, wind turbines are also subjected to dynamic loading. The fatigue capacity of partially loaded area is not documented in either of the codes.

This study is a continuation of the work carried out in Furnes and Hauges master thesis in 2011. The main goal of this thesis is to gain more insight and knowledge of the capacity of partially loaded areas in structures submerged in water, subjected to both static and dynamic loading. Of special interest is to see if the increased contact pressure capacity of static loading also is valid in fatigue.

A major part of the work is to carry out an experimental program to investigate the static and fatigue capacity. The production of concrete elements will be performed at NTNU. The experimental testing of the elements will be done in the laboratory at DNV-GL in Oslo. The setup of the experiments must be done in close collaboration with the supervisors and the technicians of the laboratories. The concrete elements are designed so the splitting reinforcement is activated, but the failure is governed by compression. Both static and dynamic loads are applied to the elements.

The study can be divided in the following tasks:

- A literature study to understand, and find the background and mechanics in partially loaded areas both for static and dynamic loading
- Production of elements
- Testing of elements
- Evaluation of experimental results

The work is carried out in collaboration with DNV-GL. Contact and co-supervisor at DNV-GL is Ole Martin Hauge.

This thesis must be completed before 10. June 2014.

Trondheim 13.01.2014

Jan Arve Øverli

Associate Professor

Preface

This thesis was written for The Department of Structural Engineering at the Norwegian University of Science and Technology (NTNU) in collaboration with Det Norske Veritas (DNV-GL).

This thesis is an investigation regarding fatigue response of concrete submerged in water subjected to partial compression. In addition, the effect of splitting reinforcement in concrete for both static and fatigue loads is being investigated.

The thesis was divided into four main parts. The first part was a literature study to understand the background and mechanics in partially loaded areas exposed to static and dynamic loading. The second and third part were the practical work, which involved producing and testing the specimens. The fourth and last part was the evaluation of the experimental data from the testing.

We would like to thank DNV-GL for the opportunity to conduct this study and for the collaboration during this period. A special thanks to Jonny Nikolaisen who was invaluable in the testing period and to Hege Berg Thurmann for organizing our stay. We would also like to thank staff engineer Ove Loraas and his laboratory crew for all the assistance during production. Finally, we would like to thank our supervisors Jan Arve Øverli and Ole-Martin Hauge for guidance throughout this project.

Trondheim, 10.06.2014

Erlend Bognøy

Tor Magne Sølverød Mo

Vegard Vee

Abstract

As the world develops, the energy demand grows from day to day. With the climate changes as a concern, production of renewable energy is the future. The suppliers of wind turbines need to create larger turbines which requires higher towers. Hence higher stresses act under the tower shaft on the foundation. This is the starting point for this thesis.

The thesis is an extension of the work started by Alexander Furnes and Ole Martin Hauge in their master thesis in 2011. As a part of this further work a higher amount of specimens were tested submerged in water. Reinforced and unreinforced specimens were subjected to partial static and dynamic compressive loads. This should document the contribution from the confinement effect by the splitting reinforcement.

A part of the thesis is to validate the design code factors for increased compression strength for partially loaded concrete exposed to dynamic loading (fatigue). Static tests of the specimens were performed to determine an average static strength and the effect of reinforcement on the static strength. The main focus of the thesis is the specimens' performance in fatigue while exposed to water. A total of 6 specimens were tested statically (3 reinforced, 3 unreinforced), while 12 were tested dynamically (6 reinforced, 6 unreinforced). All the specimens had the measurements 210(length) x210(width) x525(height) mm. In addition reference cubes (100x100x100) were tested throughout the testing period to track the concrete strength development.

To be able to plot the result in a Wöhler-curve the specimens had to be tested with a minimum of two different load levels. In this thesis these two load levels were divided in short term and long term. The short term tests had a higher load level and therefore a shorter fatigue life. The long term tests had a lower load level and therefore a longer fatigue life. Three reinforced and three unreinforced were tested in both short term and long term.

As the concrete strength became greater than planned, the calculated need for splitting reinforcement turned out to be lower than required. This affected the confinement of the partially loaded area. Although too little splitting reinforcement was mounted in the reinforced specimens, the trend is that the partially loaded area have an increase in strength if properly confined/reinforced. In the unreinforced specimens the factor for increase in capacity due to partially loading were ≈ 1 , while in the reinforced specimens this factor was 1,48. The factor achieved was higher than the factor allowed in DNV-OS-C502, but lower than the factor allowed in NS-EN-1992-1-1. This factor would probably have been higher if the specimens were reinforced according to the actual concrete strength.

The results from the dynamic testing were plotted in a Wöhler-curve and compared to the expected results according to the DNV design code. The C1-factor used in the DNV design code takes environmental effects on the fatigue life into account. The C1-factor is different for air (C1=12) and water (C1=10). The results from the dynamic tests showed that the design code is just conservative enough, with an indication of C1 \approx 10 which is the same as in

the design code. This applied for both reinforced and unreinforced specimens. However, when accounting for concrete strength development, some results indicate that the DNV design code might be inadequate.

Thus, the C1-factor in the DNV design code is much more conservative with regard to air than to water (Furnes and Hauges testing estimated a C1-factor much higher than $C1=12$, for air). This indicates that the water effect is absolutely present, and might be of greater importance than commonly thought. Other codes and formulas do not even consider the environmental effect of water.

As of now, the DNV design code does not cover the topic of partially loaded areas in dynamic loading. Paola Mayorca and DNV-GL is currently conducting a study to find appropriate rules on this topic. At the moment a partial amplification factor of 1,3 is suggested. By including both this new amplification factor and the concrete strength development, one unreinforced specimen is inadequate according to DNV design code. The partial effect is not present in unreinforced specimens. Therefore the partial factor will not affect their endurance. Hence, reinforcement in top layers is crucial.

The reinforcement bars never reached yielding during the dynamic tests. This is mainly because the applied load in the dynamic tests were lower than the load which led to yielding in the static tests. Another reason is that the critical cracks is prevented from occurring within the reinforcement by the reinforcement, and occurs outside of the reinforcement bars. In comparison the critical cracks on the unreinforced specimens occurred in the middle of the specimens and develop towards the sides.

The investigation have some limitations. The specimens are only an approach to a real wind turbine foundation. The threaded bars will affect the crack development. In addition, a higher number of specimens would have been beneficial to achieve results with a better statistical certainty. Though the limitations are present, the results give good indications of fatigue behaviour.

Results from the investigation:

Static test results						
Specimens without splitting reinforcement (specimen number)	Load rate [mm/min]	Maximum load [P_{fail}]	Test duration to max load	Test date	Sampling rate	
1	0,4	552,72	11 min 17,4 sec	06.03.14	5 Hz	
2	0,4	460,64	7 min 52 sec	07.03.14	5 Hz	
3	0,4	504,04	8 min 29,2 sec	07.03.14	5 Hz	
Specimens with splitting reinforcement						
4	0,4	753,28	15 min 49,4 sec	07.03.14	5 Hz	
5	0,4	743,36	15 min 42 sec	07.03.14	5 Hz	
6	0,4	713,44	14 min 19 sec	10.03.14	5 Hz	

Dynamic test results							
Specimens without splitting reinforcement	Max dynamic load [kN]	Min dynamic load [kN]	Cycles until failure	Stroke [mm]	LVDT [mm]	Load level	Average cylinder strength [N/mm²]
7	379,4	50,6	2872	3,7	2,4	0,75/0,10	35,2
8	379,4	50,6	7099	3,2	2,4	0,75/0,10	35,8
9	379,4	50,6	2595	3,3	2,5	0,75/0,10	34,7
10	328,8	50,6	21675	3,5	-	0,65/0,10	36,7
11	328,8	50,6	7821	4,7	3,2	0,65/0,10	35,9
12	328,8	50,6	46407	3,7	2,9	0,65/0,10	35,9
Specimens with splitting reinforcement							
13	625,5	73,6	231	5,8	-	0,85/0,10	34,8
14	551,9	73,6	4749	4,0	4,0	0,75/0,10	34,6
15	551,9	73,6	5023	7,6	6,0	0,75/0,10	36,2
16	478,9	73,6	40523	5,7	-	0,65/0,10	37,0
17	478,9	73,6	26040	7,7	6,7	0,65/0,10	37,9
18	478,9	73,6	61854	7,5	6,4	0,65/0,10	37,4

Sammendrag

En verden i stadig utvikling krever stadig større tilgang til energi. Derfor er det ønskelig at vindmøller kan produsere mye fornybar energi. Dette medfører et behov for større vindmøller med større produksjonskapasitet. Større vindmøller forårsaker større opptredende krefter i overgangen mellom ståltårn og betongfundament, noe som gjør at betongens egenskaper må kartlegges nærmere. Dette er utgangspunktet for denne tesen.

Denne oppgaven bør sees i sammenheng med Alexander Furnes og Ole Martin Hauges masteroppgave fra 2011, ettersom dette på flere måter er en videreføring av deres arbeid. Hovedforskjellen er at i denne oppgaven ble flere prøvestykker testet, i tillegg var de neddykket i vann. Både armerte og uarmerte prøvestykker er blitt påført partiell dynamisk last i trykk. Dette gjøres for å dokumentere splittarmeringens effekt mot betongens tverrutvidelse.

En del av oppgaven besto av å verifisere faktorene som uttrykker betongens økte trykkapasitet i partielt belastede områder, utsatt for dynamisk last. Statistiske tester ble utført for å bestemme gjennomsnittlig styrke i prøvestykkene, samt armeringens bidrag til statisk styrke. Hovedfokuset i oppgaven er prøvestykkenes oppførsel i utmatting i vann. 6 prøvestykker ble testet statisk (3 armerte, 3 uarmerte). 12 prøvestykker ble testet dynamisk (6 armerte, 6 uarmerte). Prøvestykkene hadde målene 210mm x 210mm x 525mm. I tillegg ble referanseterninger testet underveis for å overvåke utviklingen i betongens styrke.

Prøvestykkene måtte testes på minst to ulike lastnivå for å ha mulighet til å plote resultatene i en Wöhlerkurve. I denne oppgavene er disse lastnivåene inndelt i langtids og korttids utmatting. Korttidstestene hadde høyest lastnivå og derfor kortere levetid. Tre armerte og tre uarmerte prøvestykker ble testet i både langtids og korttids utmatting.

Betongkvaliteten ble høyere enn planlagt. Derfor ble den forhåndskalkulerte armeringsmengden utilstrekkelig. Dette påvirket fastholdingen mot tverrutvidelse. Indikasjonen er uansett at partielt belastede områder fører til økt betongstyrke dersom fastholdingseffekten/armeringen er stor nok. I uarmerte prøvestykker var faktoren som uttrykker økt kapasitet i partielt belastede områder ≈ 1 . I armerte prøvestykker var den 1,48. Denne faktoren er høyere enn hva DNV-OS-C502 anbefaler, men lavere enn hva NS-EN-1992-1-1 anbefaler. Faktoren ville mest sannsynlig vært høyere i armerte prøvestykker dersom armeringsmengden hadde vært tilstrekkelig i forhold til betongkvaliteten.

Resultatene fra dynamiske tester ble plottet i Wöhlerkurver og sammenlignet med forventet levetid fra DNVs standard. C1 faktoren i DNVs standard tar miljømessige hensyn for betong i utmatting. For luft er $C1=12$, for vann er $C1=10$ når det gjelder trykk-trykk utmatting. Resultatene antydte $C1 \approx 10$, for både armerte og uarmerte prøvestykker. På en annen side viste resultatene at $C1=10$ ikke er konservativt nok for uarmerte prøvestykker, dersom utviklingen i betongstyrke ble hensyntatt.

Basert på resultatene fra denne oppgaven, samt fra Furnes og Hauges oppgave, er det tydelig at DNV standarden er mye mer konservativ når det gjelder utmatting i luft, i forhold til utmatting i vann. Dette tilsier at vannets effekt kanskje er viktigere enn tidligere antatt.

I skrivende stund er det ikke en partiell faktor for dynamiske laster inkludert i DNVs standard. Paola Mayorca og DNV-GL ønsker å utarbeide en slik faktor. Faktoren er foreløpig foreslått å være 1,3. Dersom både denne faktoren og betongens styrkeutvikling tas med, resulterer det i at en av de uarmerte prøvestykkene ikke har god nok utmattingskapasitet i forhold til DNVs standard. Den partielle effekten neglisjerbar i uarmerte prøvestykker. Derfor vil ikke partiell belastning påvirke kapasiteten i disse prøvestykkene. Dette beviser viktigheten av armering i topplagene.

Armeringen nådde ikke flytegrense i de dynamiske testene. Hovedgrunnen til dette er at den påførte dynamiske lasten er lavere enn påført last som ga flytning i de statiske testene. I tillegg oppsto de kritiske rissene på utsiden av armeringen, noe som førte til liten påvirkning i armeringen.

Denne avhandlingen har noen begrensninger. Prøvestykkene er kun en tilnærming til et faktisk vindmøllefundament. Gjengestagene påvirker rissenes utvikling. I tillegg er det gunstig med et stort antall tester for å innføre en bedre statistisk sikkerhet i resultatene. Selv om disse begrensningene er tilstede bør resultatene likevel gi en god indikasjon på betongens utmattingssegenskaper.

Resultater:

Statiske testresultater						
Prøvestykker uten splittarmering	Lastrate [mm/min]	Maksimum last [P_{fail}]	Varighet til maksimum last	Testdato	Loggingsrate	
1	0,4	552,72	11 min 17,4 sec	06.03.14	5 Hz	
2	0,4	460,64	7 min 52 sec	07.03.14	5 Hz	
3	0,4	504,04	8 min 29,2 sec	07.03.14	5 Hz	
Prøvestykker med splittarmering						
4	0,4	753,28	15 min 49,4 sec	07.03.14	5 Hz	
5	0,4	743,36	15 min 42 sec	07.03.14	5 Hz	
6	0,4	713,44	14 min 19 sec	10.03.14	5 Hz	

Dynamiske testresultater							
Prøvestykker uten splittarmering	Maksimum dynamisk last [kN]	Minimum dynamisk last [kN]	Sykler før brudd	Stroke [mm]	LVDT [mm]	Lastnivå	Sylinderstyrke [N/mm^2]
7	379,4	50,6	2872	3,7	2,4	0,75/0,10	35,2
8	379,4	50,6	7099	3,2	2,4	0,75/0,10	35,8
9	379,4	50,6	2595	3,3	2,5	0,75/0,10	34,7
10	328,8	50,6	21675	3,5	-	0,65/0,10	36,7
11	328,8	50,6	7821	4,7	3,2	0,65/0,10	35,9
12	328,8	50,6	46407	3,7	2,9	0,65/0,10	35,9
Prøvestykker med splittarmering							
13	625,5	73,6	231	5,8	-	0,85/0,10	34,8
14	551,9	73,6	4749	4,0	4,0	0,75/0,10	34,6
15	551,9	73,6	5023	7,6	6,0	0,75/0,10	36,2
16	478,9	73,6	40523	5,7	-	0,65/0,10	37,0
17	478,9	73,6	26040	7,7	6,7	0,65/0,10	37,9
18	478,9	73,6	61854	7,5	6,4	0,65/0,10	37,4

Symbols, Notation and Definition

A_{c0}, A_1	The partially loaded area
A_{c1}, A_2	Maximum design distribution area
C1	Factor that takes environment into account in calculations of fatigue life
F_{Rdu}	Capacity for partially loaded area
F_{Rd}	Capacity for fully loaded area
N	Amount of load cycles at given/respective time
N_f	Amount of load cycles at failure
P_{fail}	Static capacity, static load at failure on static tests
P_{max}	Maximum dynamic load
P_{min}	Minimum dynamic load
S_{max}	Maximum dynamic load level
S_{min}	Minimum dynamic load level
β	Material constant
σ_{max}	Maximum stress attained during the cycle
σ_{min}	Minimum stress attained during the cycle
Reinforced specimen	Splitting reinforcement in the top of the specimen
Unreinforced specimen	No splitting reinforcement in the top of the specimen
Stroke	Vertical deformation of concrete specimens, measured by test machine
LVDT	Linear variable differential transformer. More accurate measurement of vertical deformation in concrete specimens

Table of contents

1. Introduction.....	1
1.1 General	1
1.2 Purpose of investigation	2
1.3 Range of investigation	3
1.4 Limitations of the investigation	3
1.5 Previous work	4
2. Literature review	5
2.1 Introduction	5
2.2 Fatigue	5
2.2.1 Fatigue in general.....	5
2.2.1.1 Miners hypothesis	7
2.2.2 Fatigue in concrete	8
2.2.2.1 Historical perspective.....	9
2.2.2.2 Environmental effect.....	10
2.2.2.3 Frequency effect and resting periods	10
2.2.3 Calculating fatigue life	11
2.2.3.1 Calculating fatigue life according to DNV-OS-C502	12
2.2.3.2 Calculating fatigue life according to NS-EN-1992-1-1.....	15
2.2.3.3 Calculating fatigue life according to Model Code 2010	19
2.3 Effect of confinement on fatigue.....	24
2.4 Partially loaded areas in concrete	27
2.4.1 Introduction	27
2.4.2 Some design codes.....	27
2.4.2.1 NS-EN-1992-1-1.....	27
2.4.2.2 NS 3473 & DNV-OS-C502 (offshore concrete structures).....	31
2.4.2.3 Model code 2010	33
2.4.3 Partially loaded areas exposed to fatigue.....	34
3. Materials, Test Specimens and Instrumentation	35
3.1 Introduction	35
3.2 Materials and concrete mix.....	35
3.2.1 Casting frame	35

3.2.2 Concrete mix	36
3.2.3 Reinforcement	36
3.2.4 Threaded bars	37
3.2.5 Test specimens.....	38
3.2.5.1 Size of specimens	38
3.2.5.2 Casting	39
3.2.5.3 Instrumentation	39
3.2.5.4 Storage and curing	40
4. Testing	41
4.1 Introduction	41
4.2 Testing equipment.....	42
4.3 Test cubes	44
4.4. Problems due to higher cube strength than expected.....	45
4.5 Static testing	45
4.6 Dynamic testing	45
4.6.1 Introduction	45
4.6.2 Preliminary calculations	46
4.6.2.1 Load levels	46
4.6.2.2 Calculation of load levels	46
4.6.2.3 Short term reinforced	46
4.6.2.4 Short term unreinforced	48
4.6.2.5 Long term reinforced	49
4.6.2.6 Long term unreinforced	50
4.6.2.7 Pre-cyclic routine.....	50
5. Static test results	51
5.1 Introduction	51
5.2 Results.....	51
5.2.1 Maximal static load at fracture	51
5.2.2 Capacity of partially loaded areas.....	51
5.2.3 Force deformation relation.....	53
5.2.3.1 Force deformation relation in reinforced specimens	53
5.2.3.2 Force deformation relation in unreinforced specimens	55

5.2.4 Force strain relation in concrete.....	56
5.2.5 Strain in reinforced tests.....	58
5.2.6 Strain in unreinforced tests	61
5.2.7 Crack patterns in static tests.....	62
6. Dynamic test results	65
6.1 Introduction	65
6.2 Results.....	65
6.2.1 Wöhler-diagram	67
6.2.1.1 Results compared to DNV design code	67
6.2.1.2 C1-factor	68
6.2.1.3 Wet/dry comparison	69
6.2.1.4 Results compared to other formulas and design codes	70
6.2.1.5 Effect of concrete strength development.....	71
6.2.1.6 General tendency of data points.....	75
6.2.2 Life cycle development	76
6.2.2.1 Reinforced specimens	76
6.2.2.2 Unreinforced specimens	80
6.2.2.3 Comparison between reinforced and unreinforced specimens	83
6.3 Strain gauges	84
6.3.1 Strain in reinforced specimens	84
6.3.1.1 Strain 1 – stirrup in the 2 nd layer from the top	86
6.3.1.2 Strain 2 – splitting reinforcement in the 2 nd layer from the top.....	88
6.3.1.3 Strain 3 – splitting reinforcement in the 1 st layer from the top	90
6.3.1.4 Strain 4 – threaded bar in the 2 nd layer from the top.....	92
6.3.2 Strain in unreinforced specimens	94
6.4 Cracks.....	95
6.4.1 Crack patterns	95
6.4.2 Crack initiation versus fatigue life.....	98
7. Conclusion	101
7.1 Introduction	101
7.2 Conclusions static tests.....	101
7.3 Conclusions dynamic tests.....	102

7.4 Suggestions for further work.....	103
8. References.....	105
9. Attachments.....	107

Figure list

Figure 1 - Transferring forces to the foundation	1
Figure 2 - Simplification from wind turbine to test specimen	2
Figure 3 - Sketch of test specimen	2
Figure 4 - Example of an S-N curve	5
Figure 5 – Example of a modified Goodman-diagram	6
Figure 6 - Example on passive confinement, taken from Furnes and Hauges thesis	24
Figure 7 - Example on active confinement, taken form Furnes and Hauges thesis.....	24
Figure 8 - Taken from Eurocode 2, NS-EN-1992-1-1 [3.1.9 (2)]	27
Figure 9 - Design distribution for partially loaded areas (figure taken from Eurocode 2).....	28
Figure 10 - Strut and tie-models of partial and full discontinuity (taken from Eurocode 2) ...	29
Figure 11 - Stress field under concentrated load according to linear analysis	30
Figure 12 - Transverse stresses including splitting forces.....	30
Figure 13 - Loaded area smaller in only one direction, taken from Furnes and Hauges Thesis	31
Figure 14 - Geometrical limitations for partial loaded areas, taken from DNV-OS-C502.....	32
Figure 15 - Casting frame	35
Figure 16 - With and without splitting reinforcement.....	37
Figure 17 - Threaded bars	38
Figure 18 - Strain gauges mounted on reinforcement.....	39
Figure 19 - Soaked burlap sacks, plastic wrapped shipment	40
Figure 20 - Hydraulic jack "MTS", Instron 8500 controller, Spider8 logger and a computer ..	42
Figure 21 - Rigging of the LVDT's, load transferring plates and spherical bearing	44
Figure 22 - Development of cube strength	44
Figure 23 - The sinusoidal load for short term reinforced tests with a maximum load level of 75% for an excerpt of 10 seconds	47
Figure 24 - The sinusoidal load for short term unreinforced tests with a maximum load level of 75% for an excerpt of 10 seconds.....	48
Figure 25 - The sinusoidal load for short term reinforced tests with a maximum load level of 65% for an excerpt of 10 seconds.	49
Figure 26 - The sinusoidal load for short term reinforced tests with a maximum load level of 65% for an excerpt of 10 seconds.	50
Figure 27 - Force deformation relation - with splitting reinforcement	53
Figure 28 - Stroke in the machine and equipment	54
Figure 29 - Modified force deformation relation - with splitting reinforcement	55
Figure 30 - Force deformation relation - without splitting reinforcement.....	55
Figure 31 - Modified force deformation relation - without splitting reinforcement.....	56
Figure 32 - Force strain relation in concrete - with splitting reinforcement	57
Figure 33 - Force strain relation in concrete - without splitting reinforcement.....	57
Figure 34 - Strain in reinforcement (NB! Strain 3 illustrated using larger strain values).....	59

Figure 35 - Strain in reinforcement vs time (NB! Strain 3 illustrated using larger strain values)	60
Figure 36 - Strain in threaded bars in unreinforced specimens	61
Figure 37 – Spalling of cover concrete	62
Figure 38 - First critical cracks	62
Figure 39 - Critical cracks in reinforced (left) and unreinforced (right) specimens	63
Figure 40 - Crushing of the top in static specimens	63
Figure 41 - Load vs number of cycles	65
Figure 42 – Results compared to DNV-OS-C502	67
Figure 43 - Results compared to DNV-OS-C502 with different C1-factors	68
Figure 44 - Results from Furnes and Hauges thesis compared to DNV-OS-C502 (C1=10)	69
Figure 45 - Results compared to other formulas	70
Figure 46 - Effect of concrete strength development	72
Figure 47 - Results in design situation compared to DNV-OS-C502	74
Figure 48 – General tendency of data points	75
Figure 49 - Stroke development for short term reinforced	76
Figure 50 - Stroke development for long term reinforced	77
Figure 51 - LVDT development for short term reinforced	78
Figure 52 - LVDT development for long term reinforced	79
Figure 53 - Deformation under the loading area on specimen 17	79
Figure 54 - Superimposing of short term (left) and long term (right) reinforced	80
Figure 55 - Stroke development of short term unreinforced	81
Figure 56 - Stroke development of long term unreinforced	81
Figure 57 - LVDT development of short term unreinforced	82
Figure 58 - LVDT development of long term unreinforced	82
Figure 59 - Superimposing of short term (left) and long term (right) unreinforced	83
Figure 60 – Short term specimen 9 unreinforced (left) and short term specimen 15 reinforced (right)	84
Figure 61 - Short term reinforced: strain 1	86
Figure 62 - Long term reinforced: strain 1	86
Figure 63 - Short term reinforced: strain 2	88
Figure 64 - Long term reinforced: strain 2	88
Figure 65 - Short term reinforced: strain 3	90
Figure 66 - Long term reinforced: strain 3	90
Figure 67 – Explanation of crack details	91
Figure 68 - Short term reinforced: strain 4	92
Figure 69 - Long term reinforced: strain 4	92
Figure 70 - Short term unreinforced: strain in threaded bars	94
Figure 71 - Long term unreinforced: strain in threaded bars	94
Figure 72 - Local crushing at the top	95
Figure 73 - Crack initiation in reinforced (left) and unreinforced (right) specimens	96

Figure 74 - Crack at failure in reinforced (left) and unreinforced (right) specimens.....	96
Figure 75 - Crack at failure (disassembled) in reinforced (left) and unreinforced (right) specimens.....	97
Figure 76 – Cracks appeared between steel and concrete	97
Figure 77 - Crack initiation vs cycles to failure.....	99

1. Introduction

1.1 General

The energy demands of the world are growing from one day to the next. More and more developing countries are rising into modern societies where energy is vital. With the climate change as a big concern, the production of renewable energy needs to increase. As a part of this, the suppliers of wind turbines need to create larger turbines, which also require higher towers. Higher towers have larger loading areas for the wind, which causes larger bending moments at the base shaft. The bending moment and the axial force are taken by a concrete foundation as compressive forces.

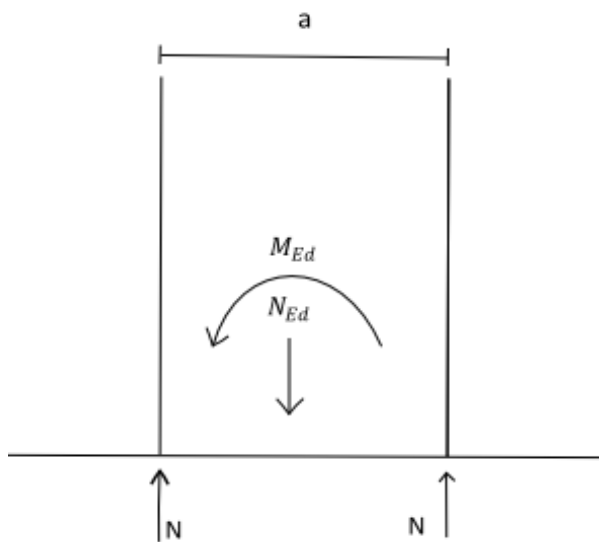


Figure 1 - Transferring forces to the foundation

The wind turbines are mostly subjected to dynamic wind loads, which causes dynamic compressive forces in the concrete foundation. Because of that, the fatigue capacity of the concrete foundation is of great significance. Higher wind turbines require larger distribution areas in the concrete. This distribution occurs in the connection between shaft and foundation. Unfortunately, the steel shafts have a maximum diameter, due to transportation limitations. Therefore, at some point, the optimal size of the steel shaft is not achievable. Hence compressive forces in the concrete will increase with increasing heights.

This study is based on wind turbines with a circular concrete foundation. It is assumed that dead load and wind load acts as a circular line load on the foundation in hoop direction. Thus, the partial loading can only spread in the radial direction. To examine the foundation, one can isolate a small piece of the circular area and simulate its behaviour. To secure the correct boundary conditions the specimen needs to be restrained in direction parallel to the line load. The simplification from wind turbine to test specimen is illustrated below.

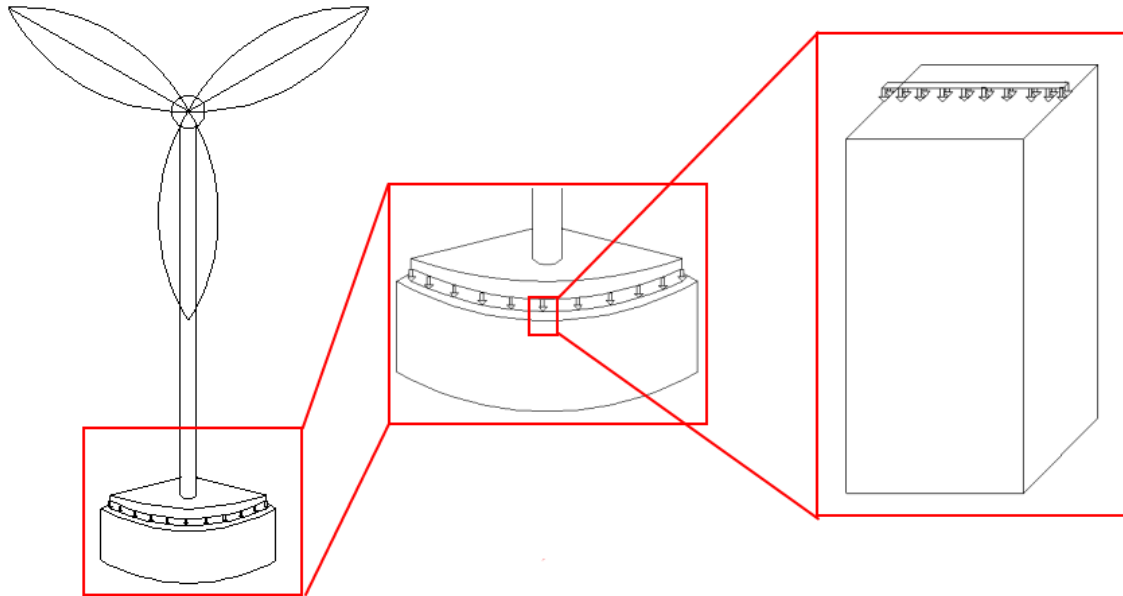


Figure 2 - Simplification from wind turbine to test specimen

1.2 Purpose of investigation

The purpose of this thesis is to control the validity of the increase in concrete strength under partially loaded areas in fatigue. In addition, the effect of splitting reinforcement in concrete for both static and dynamic loads is investigated.

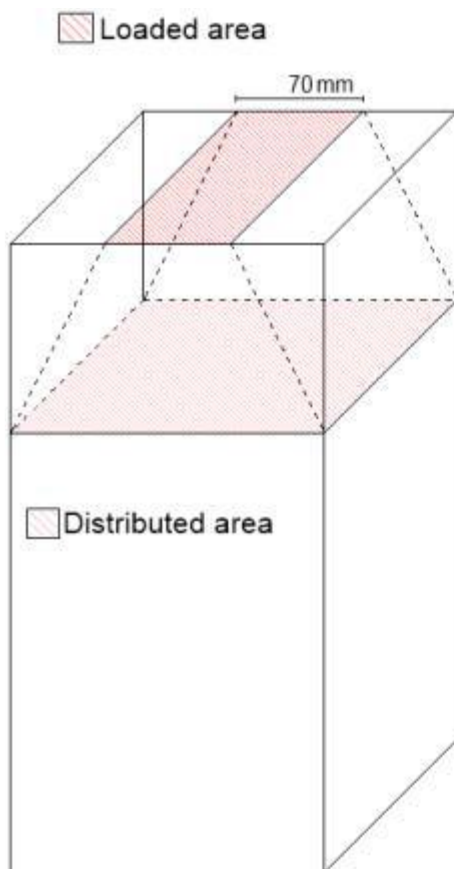


Figure 3 - Sketch of test specimen

1.3 Range of investigation

The size of the specimens used in this investigation are 210x210x525mm. These dimensions are typical for connections between concrete foundation and steel shaft in wind turbines. In total, there are 18 concrete specimens. In the investigation there are 2 groups of specimens. 9 are reinforced with stirrups and splitting reinforcement, and 9 are not reinforced. In each group, 3 of the specimens are tested statically in compression to determine the ultimate limit strength. In the static tests the load rate is 0.4 mm/min and the failure is reached when the deformation is increasing while loading is decreasing. 12 of the specimens are tested dynamically in compression until failure. In the dynamic test, the failure criteria is set as an upper limit of the stroke in the hydraulic jack. At this upper limit, the deformation increases rapidly as the specimens are no longer able to support the load.

1.4 Limitations of the investigation

To be able to perform the study, some simplifications must be made. As long as it is not possible to perform full-scale tests, there will of course be flaws and limitations. The limitations are mainly connected to the size, confinement and the number of tests.

By reducing the size and isolating a small piece, some of the stress components in the foundation will not be accounted for. In order to obtain realistic conditions, the concrete has to be restrained from deformation in one direction. This is achieved by using threaded bars, which leads to a confinement of the concrete. This method gives some uncertainties due to the bonding between concrete and steel, and the fact that crack patterns may be effected by the bars.

The dimension of the study is another limitation. The fatigue strength of concrete are known to have quite large variations between two identical specimens. This means that to fully understand the results of the problem the amount of tests must be high. This study only consists of 9 reinforced and 9 unreinforced specimens. This is due to the limited time of the study. In addition, because of the limited time, no tests with low stress levels and a high amount of cycles are performed.

A high strength concrete is normally used in the foundation of wind turbines. Unfortunately, it is not possible to use high strength concrete in this study. The hydraulic jacks, where the tests are to be performed, have a limited capacity, which means that the compressive cube strength of the concrete have to be kept below 30 MPa. This leads to an uncertainty about the transferability between the study and the high concrete strength foundations.

1.5 Previous work

In 2011, Furnes and Hauge¹ did a similar thesis, in collaboration with the Norwegian University of Science and Technology (NTNU) and Det Norske Veritas (DNV). Their main goal was to check the validity of factors used to increase concrete strength under partially loaded areas in fatigue, and secondarily investigate the role of splitting reinforcement in concrete both for static loads and in fatigue. During their study they conducted 12 tests of concrete specimens exposed to air. Half of the tests were static tests while the second half were dynamic tests.

This thesis is also in collaboration with the Norwegian University of Science and Technology (NTNU) and Det Norske Veritas (DNV-GL), and can be seen as a continuation of their work. The main difference between the two studies is the environmental conditions, where in this study the concrete specimens will be submerged in water during testing. The reason for this continuation is that DNV-OS-C502 standard distinguishes between concrete exposed to air and water. This effect needs further study, which this report will provide.

¹ "Fatigue capacity of partially loaded areas in concrete structures" by Alexander Furnes and Ole Martin Hauge

2. Literature review

2.1 Introduction

To give an insight to the topics covered by this thesis, a literature review of the theory will follow. This includes topics such as fatigue mechanics, fatigue in concrete, confinement effects and partially loaded areas in concrete.

2.2 Fatigue

2.2.1 Fatigue in general

In material science fatigue is defined as weakening of the material caused by cyclic loading. It is a structural damage that occurs when a material is subjected to repeated loading and unloading. This phenomenon can take place at stress levels below the static yield limit.

Fatigue life is the number of stress cycles the specimen can withstand at a specified stress level before failure. The most common analysis of fatigue uses S-N relationships. The relationship can be described in an S-N curve, also known as a Wöhler curve. This is a graph that describes the maximum stress level against the logarithmic scale of cycles to failure. An S-N curve proves how the lifetime is reduced when the average stress increases. Each curve is only applicable for a specific minimum load level.



Figure 4 - Example of an S-N curve

These curves are derived by doing tests on the material where a cyclic stress is applied. A testing machine counts the number of cycles before failure at different stress levels. These test results create the fatigue data. Statistical analyses of the data is required to obtain the S-N curve for a specific material. From these curves the endurance limit can be found. The

endurance limit of a material is the level of stress where failure will not occur even after an infinite number of cycles. However, some materials, including concrete, do not have an endurance limit and will fail due to fatigue no matter how low the stress level is, provided enough cycles is applied.

Another way of presenting fatigue data, which is often used for fatigue design, is the modified Goodman-diagram.

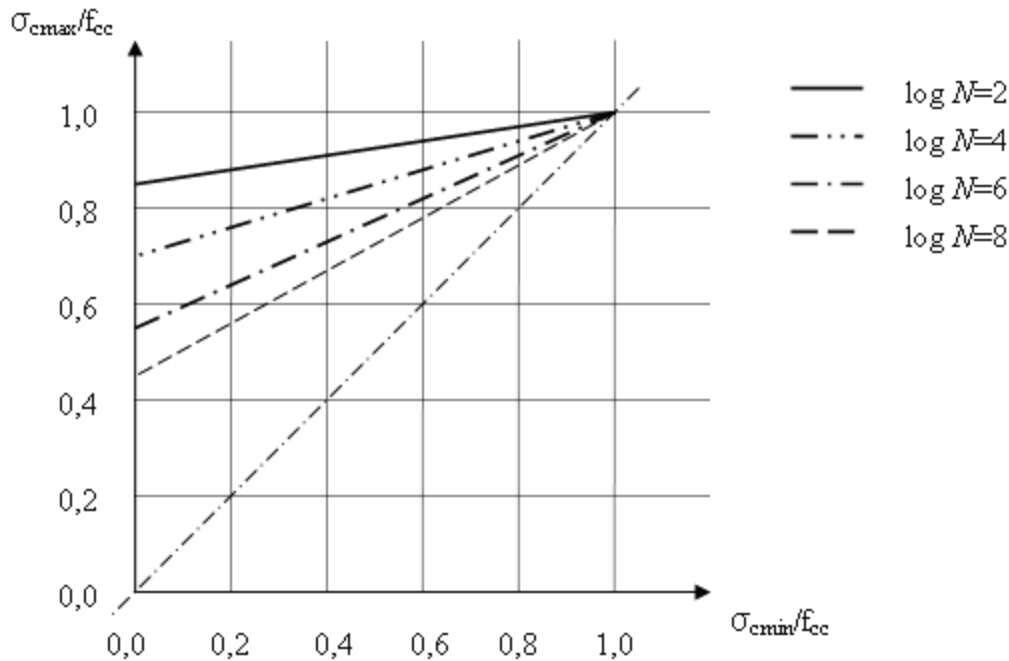


Figure 5 – Example of a modified Goodman-diagram²

The Goodman-diagram, as the Wöhler-diagram, is derived by experimental testing on the material where a cyclic load is applied. The data needed is the maximum and minimum stress level. In difference from the Wöhler-diagram, a single Goodman-diagram can be used for all possible minimum stress levels. The 45° line expresses the endurance limit. All variations of maximum and minimum stress level below this line will never fail due to fatigue, and this zone is called the safe zone.

Determining the fatigue life of a structure without testing is a complex matter. There are a lot of factors that affect the fatigue life. The most important ones are listed below:

- **Cyclic stress state**, load level, stress amplitude, mean stress and load sequence.
- **Geometry**, geometrical discontinuity leads to stress concentrations where cracks initiate
- **Material type**, ductile materials initiate micro cracks more rapidly

² "Fatigue in plain concrete – Phenomenon and Method of analysis" – Payman Ameen & Mikael Szymanski

- **Surface quality**, roughness in the surface can cause microscopic stress concentrations
- **Residual stresses**, welding, cutting and other processes involving heat decreases the fatigue strength
- **Direction of loading**, for non-isotropic materials the load direction must be taken into account
- **Environment**, environmental conditions can cause erosion and corrosion
- **Temperature**, extreme high or low temperature can decrease fatigue strength
- **Air or water**, water attacks the material and speed up the propagation of cracks

When a specimen fails due to fatigue, its life can be split into three phases; crack initiation, slow crack propagation and sudden propagation leading to fracture. The significance of each of the phases depends on the stress amplitude, geometry, nature of the material, temperature, previous loading and environment. In general, ductile materials are known to initiate micro cracks more rapidly. The crack initiations usually occurs in the inclusions and are dependent on their quantity, size, nature, distribution and shape regarding load direction.

After the first phase, the compressive strength is often increased and in some cases even an increase in the modulus of elasticity is measured. The strengthening effects is assumed to be caused by three phenomena. Limited micro-cracking gives a release of local stress concentrations, movements on the sub-microscopic levels gives an increase in interparticle attraction forces, and by forced hydration due to compaction of the material structure.

In general, experimental testing of fatigue is known to have results with a wide scatter. The scatter is caused by three main factors. The preparation of the specimen seems to be the obvious cause. This includes all the steps in making and preparing the specimen for testing. The next cause is the uncertainty during testing, which includes settings of test machines, applied loading, cycle frequency and other influences of the surroundings. The last cause of scatter is those within the material. These causes are less well known and include factors like inclusions and structure heterogeneities.

2.2.1.1 Miners hypothesis

Damages will appear in the material due to fluctuating loading. There are several theories on how to calculate the sum of the contributions from the loading. Miners hypothesis is the most common. In 1924 A. Palmgren proposed a hypothesis, which M. A. Miner made common in 1945.

Palmgren-Miner is a linear damage accumulation law. The hypothesis states that with k different stress magnitudes S_i in a spectrum, each contributing with $n_i(S_i)$ cycles, and $N_i(S_i)$ is the number of cycles to failure at stress magnitude S_i , failure occurs when Miners sum M_S :

$$M_S = \sum_{i=1}^k \frac{n_i}{N_i} = C$$

For design purposes C is assumed to be 1, even though it is experimentally found to be between 0,7 and 2,2³. The thought behind this hypothesis is that each cycle contributes to the damage with a size $\frac{1}{N_i}$. The contributions can be randomly summed, and failure occur when the sum is equal to C.

However, the hypothesis was determined on aluminium alloys. Because of that, the hypothesis can not be used for all kinds of materials without moderation. For some materials, there is an effect in the order of the stress levels. The sum can therefore not be randomly summed. High stress cycles followed by low stress cycles may have less damage than low stress followed by high stress cycles, due to compressive residual stresses is present. The hypothesis also underestimates the effect of very low load levels by considering them as non-damaging. In addition, the hypothesis considers each cycle to cause equal amount of damage, even though the damage varies on where in the fatigue life it occurs.

Concrete is one of the materials that does not suit the Miner hypothesis that well. Tests of the changes in material parameters have found three major weaknesses to the hypothesis in concrete. Concrete is a heterogeneous material made from cement paste and aggregate. Both materials fail in a brittle manner and are linear. However, under cyclic loading the damage development of concrete follows a three-stage non-linear curve. This non-linearity is due to the poor bond between the two materials and the cracking of the material. Miners rule is as know based on a linear damage accumulation. In addition, the sequence of loading blocks and the influence from small loading can not be neglected. This has later been confirmed by Weigler and Klausen⁴. However, research has shown that in combination with TNO method of counting⁵, Miners hypothesis gives a good indication of total fatigue life for concrete structures.

2.2.2 Fatigue in concrete

Concrete fatigue is the well-known phenomenon where concrete can deteriorate with a stress level lower than its initial strength. Concrete fatigue is not a sudden change of the material, but a gradual destruction and loosening of the structure. The exposure to repeated loading causes the bond between the cement paste and the aggregate in the concrete to break before the structure eventually collapses. The cyclic loading leads to an initial decrease of concrete volume (structure compression) before it increases (structure loosening). When rupture occurs, the volume is larger than in unloaded condition. Within the entire lifetime, the time of compression and loosening varies depending on the stress level. In some cases at

³ URL: <http://core.materials.ac.uk/search/detail.php?id=3180>

⁴ "High strength concrete SP3 - Fatigue - Report 3.2" – SINTEF (Page 74)

⁵ For more about TNO method of counting, please see "Fatigue of normal weight concrete and lightweight concrete" - Eurolightcon, part 2.3.9: "TNO method for counting cycles".

lower stresses, the concrete volume will decrease, while at stresses close to static strength only loosening is observed. The speed of the fatigue process is determined by the intensity of the repeated loading and the number of load cycles. The different forms of fatigue failure in concrete are bending, shear, compression, tension and bond failures.

Fatigue strength is usually defined as a fraction of the static strength that the structure can withstand for a given number of repeated cycles. The fatigue strength is commonly taken as the upper stress level at 2 million cycles on the S-N curve. The ratio between this fatigue strength and the static strength is known as the fatigue strength factor.

More importantly is the fatigue life. The fatigue life is normally measured as the number of cycles required at a specified load level before rupture. The load level is determined by S_{max} (σ_{max} / f_{rd}) and S_{min} (σ_{min} / f_{rd}), which are ratios between 0 and 1. The specified load level is described by the maximum load and the load amplitude the structure is subjected to. It is common to present the fatigue resistance in an S-N curve, which is a coordinate system represented by S_{max} and the number of cycles before failure. There will be a different curve for each value of S_{min} . These curves gives an estimation on how many cycles the structure can withstand before rupture.

The fatigue strength of concrete is affected, in a similar manner as the ultimate limit strength, by material properties such as cement content, water-cement ratio, age at loading, air content, curing conditions and type of aggregates. For instance, increasing air content and increasing water-cement ratio decreases fatigue life.

2.2.2.1 Historical perspective

Historically the fatigue of concrete in compression have hardly been mentioned in design specifications. The concrete quality was for a long time low compared to the self-weight, which lead to failure due to other factors than fatigue. Today the availability of high strength concrete means that the constructions get lighter and slender, which can lead to failure due to fatigue. Because of that a lot of research and experiments have been conducted, and today most of the design specifications includes fatigue of concrete.

One of the main problems in making general rules for fatigue in concrete is that most of the experimental work are located at high maximum load levels. In addition, fatigue tests at low levels gives a big scatter of results and requires a great amount of time to conduct. High and lower maximum load levels also gives different failure mechanisms.

In 1973 Freitag⁶ performed a series of tests to find the effect of different load levels in fatigue. The conclusion was that, with a maximum stress level less than 80% of static strength and amplitudes less than 35%, the structure will never fail in fatigue.

⁶ "High strength concrete SP3 - Fatigue - Report 3.2" – SINTEF (Page 72)

2.2.2.2 Environmental effect

The fatigue life of a structure is highly dependent on the environment. In concrete fatigue we differ between structures in air, water or sealed in high humidity. Experiments conducted by Van Leeuwen and Siemes⁷ in 1979 proved that there is a significant reduction in fatigue strength at higher humidity. When in compression, specimens in water seems to have a significantly shorter lifetime than specimens in air and specimens which are sealed, while sealed specimens have shorter lifetime than specimens in air.

The specimens in air gets dried out, while the two other types have pore water. The pore water pressure will increase during compression, due to the water's incompressibility, causing the bond between cement and aggregate to break faster. The difference between watered and sealed specimens can be explained by extra water penetrating the cracks by capillary suction. The penetration reduces the friction, which increases the crack propagation rate. However, tests have shown that water penetration under tension loading does not have significant effect on the fatigue life.

However, DNV-OS-C502 is the only code which takes the environment into account, and it is accounted for by a multiplication factor. This factor differs for structures in water and structures in air. However, the water content of the specimen itself is not taken into account. This means that aired and sealed structures are considered equal, which is not exactly correct.

The fatigue strength is also effected by the temperature⁸. At very low surrounding temperatures the fatigue life will have a significant increase. This increase will also be experienced in the static strength, but the effect is larger for fatigue life.

The environmental effects teach us that it is important to be certain of the environment at the building site, and to ensure controlled environment to secure similar conditions during experimental testing.

2.2.2.3 Frequency effect and resting periods

During fatigue, the frequency of loading have a noteworthy effect. Several researchers have confirmed this. Lower frequencies results in less cycles to failure. However, there is a difference between high stress and low stress cases. Research shows that at stress ratios less than 75% of static strength, frequencies from 1 to 15 Hz have little effect on fatigue life. The fatigue strength at higher stress ratios will decrease with decreasing frequency. Decreasing the frequency with a factor X will decrease the number of cycles before failure with the square root of X.

Tests conducted by Hilsdorf and Kesler⁹ have shown that the effect of rest periods during fatigue is dependent on the duration of the resting period and when in the loading history it

⁷ "Miner's rule with respect to plain concrete" - Van Leeuwen and Siemes

⁸ "Fracture energy and fatigue strength of unreinforced concrete beams at normal and low temperatures" - Ohlsson U., Daerga P. A., Elfgren L.

occurs. The conclusion is that a resting period with duration of up to 5 minutes have a beneficial effect on fatigue life, increasing from 0 to 5 minutes, while longer periods do not give any additional effect. Petkovic¹⁰ however, gave evidence for the fact that the rest periods have to be dependent on when in the loading history it occurs and which loading levels it is acting in combination with.

2.2.3 Calculating fatigue life

During the last 50 years there have been many studies with the goal of defining a way of calculating fatigue life in concrete. All of them points towards the same type of variables. The Aas-Jakobsen Formula, made by Aas-Jakobsen and Lenschow¹¹ in 1973, is a generally accepted formula for calculating fatigue life of concrete. Through observations, they discovered that the fatigue strength for a given number of identical cycles varies in a linear way with the loading ratio R, between the minimum and maximum intensity of the cyclic stress.

$$\frac{\sigma_{\max}}{f_c} = 1 - \beta (1 - R) \text{Log } N_f$$

where:

σ_{\max} : maximum stress attained during the cycle;

σ_{\min} : minimum stress attained during the cycle;

f_c : short-term resistance under static loading;

$R = \sigma_{\min}/\sigma_{\max}$: loading ratio;

β : material constant;

$\text{Log } N_f$: decimal logarithm of the number of cycles to failure.

At the time they defined the material constant β as 0.064, which have later been changed to 0.0685. Its validity has been verified for a wide range of frequencies for load levels up to 80% and for number of failures up to $2 * 10^6$.

In 1979 Jan Ove Holmen published "Fatigue of Concrete by constant and variable amplitude"¹² in collaboration with The Norwegian Institute of Technology. The purpose of the study was to find an empirical method of calculating fatigue life in concrete. The study included static and dynamic testing of 462 cylindrical specimens, with varying stress levels and varying load amplitudes. On the basis of the results, a new basic design formula was proposed.

$$\log N = (1 - S_{\max}) * (12 + 16 * S_{\min} + 8 * S_{\min}^2)$$

⁹ "Flexural fatigue behaviour of concrete containing various sources of fly ash" - Tarun R. Naik, V.M. Malhotra, Shiw S. Singh, and Bruce W. Ramme (Page 8)

URL: <https://www4.uwm.edu/cbu/Papers/1997%20CBU%20Reports/REP-337.pdf>

¹⁰ "Properties of concrete related to fatigue damage : with emphasis on high strength concrete" – G. Petkovic

¹¹ "ACI Journal March 1973: Behavior of Reinforced Columns Subjected to Fatigue Loading" – Knut Aas-Jakobsen and Rolf Lenschow

¹² "Fatigue of Concrete by constant and variable amplitude" - Jan Ove Holmen

In Holmens formula $\log N$ is defined as the decimal logarithm of the number of cycles to failure, while the load levels is defined as S_{max} (σ_{max} / f_{rd}) and S_{min} (σ_{min} / f_{rd}). In the later years, different methods have been developed. They are all based on the same factors with maximum stress level and minimum stress level as the main part. Some formulas also considers the environmental effects.

The design codes base the characteristic concrete strength on the strength 28 days after casting. However, the strength will continue to rise after the 28 days and this effect normally gives a 10% increase in strength. This increase is smaller for high strength concrete than for normal strength concrete. Anyway, during static loading this effect is neglected. That is due to the fact that static loads often have a long duration which decreases the concrete strength. These two effects are assumed to be of same magnitude and is therefore ignored. In fatigue loading each cycle is assumed to be a short term load, and the probability of heavy cyclic loads at an early age of structure is low. This implies that for fatigue loading it is possible to use the long term strength.

2.2.3.1 Calculating fatigue life according to DNV-OS-C502

In concrete structures the DNV-OS-C502¹³ consider the case of concrete fatigue as well as fatigue of the reinforcement bars.

When a structure is subjected to constant stress blocks the DNV-standard have a simple straight forward way of calculating the expected fatigue life of the concrete. The fatigue life is given as a number of cycles before failure.

M 200 Fatigue strength, design life

Concrete and grout

201 The design life of concrete and grout subjected to cyclic stresses may be calculated from:

$$\log_{10} N = C_1 \left(\frac{1 - \frac{\sigma_{max}}{C_5 \cdot f_{rd}}}{1 - \frac{\sigma_{min}}{C_5 \cdot f_{rd}}} \right)$$

where:

- f_{rd} = the compression strength for the type of failure in question
- σ_{max} = the numerically largest compressive stress, calculated as the average value within each stress-block
- σ_{min} = the numerically least compressive stress, calculated as the average value within each stress-block
- C_5 = fatigue strength parameter. For concrete, C_5 shall be taken equal to 1.0. For grout, C_5 shall be determined by testing.

The environmental effects is taken into account by the factor C1. Structures in water, either compression-compression or compression-tension, and structures in air have different factors.

¹³ "Offshore standard DNV-OS-C502 Offshore concrete structures" – Det Norske Veritas

When σ_{\min} is tension, it shall be taken as zero when calculating the design life.

The factor C_1 shall be taken as:

12.0 for structures in air

10.0 for structures in water for those stress-blocks having stress variation in the compression-compression range

8.0 for structures in water for those stress-blocks having stress variation in the compression-tension range.

In addition the standard gives a possibility for an increase in fatigue life under certain circumstances.

If the calculated design life $\log N$ is larger than the value of X given by the expression:

$$X = \frac{C_1}{1 - \frac{\sigma_{\min}}{C_2 \cdot f_{rd}} + 0.1 \cdot C_1}$$

The design life may be increased further by multiplying the value of $\log N$ by the factor C_2 where this is taken as:

$$C_2 = (1 + 0.2 (\log_{10} N - X)) > 1.0$$

When a structure is subjected to varying stress blocks the DNV-standard is using a linear damage accumulation law to check how big of a damage the concrete in the structure has taken.

107 Calculation of design life at varying stress amplitudes and/or mean stress can be based on cumulative linear damage theory. The stresses due to cyclic actions may be arranged in stress blocks. Each stress block can be defined by the peak stress and trough stress and a corresponding number of stress cycles. A minimum of 10 blocks is recommended for each stress level even distributed so that each block provides a significant contribution to the total damage ratio.

108 If the random nature of the loads implies that the stress ranges, mean stress and durations vary, a linear damage accumulation law may be assumed:

$$D = \sum_{i=1}^k \frac{n_i}{N_i} \leq \eta$$

109 where k is the number of stress blocks used (≥ 10) per load ratio, n_i is the number of cycles in stress block i , N_i is the number of uniform cycles with the same mean, stress range and duration which causes failure.

This method adds the contributions from each of the stress ranges, and the structure fails due to fatigue when the sum reaches the limit η .

112 The limit for the cumulative damage ratio (η) to be used in the design shall depend on the access for inspection and repair. Limits for cumulative damage ratios according to Table M1 are normally acceptable for concrete and steel reinforcement.

Table M1 Limit of cumulative damage ratios (η)		
<i>No access for inspection and repair</i>	<i>Below or in the splash zone¹⁾</i>	<i>Above splash zone²⁾</i>
0.33	0.5	1.0
<p>1) In typical harsh environment (e. g. the North Sea or equivalent) structural details exposed to seawater in the splash zone are normally to be considered to have no access for inspection and repair, i.e. the limit for the cumulative damage ratios shall be reduced to 0.33.</p> <p>2) For reinforcement, which cannot be inspected and repaired; the limit for the cumulative damage ratio for reinforcement above splash zone is reduced to 0.5.</p>		

The limit η takes into account where the structure is located. The limit η differs between structures with no access for inspection and repair, structures below or in the splash zone,

and structures above splash zone. This method gives an understanding on how much more damage the structure can withstand before failure.

The DNV-standard also have rules for fatigue of the steel reinforcement bars. The basic formula for calculating fatigue life is rather simple.

Steel reinforcement

202 The design life of reinforcement subjected to cyclic stresses may be calculated based on:

$$\log_{10}N = C_3 - C_4 \log_{10}\Delta\sigma$$

where:

$\Delta\sigma$ is the stress variation of the reinforcement (MPa)

C_3 and C_4 are factors dependent on the reinforcement type, bending radius and corrosive environment.

The maximum stress σ_{\max} in the reinforcement shall be less than f_{sk}/γ_s , where γ_s is taken from Table C1.

The stress range in the reinforcement is $\Delta\sigma$, while C_3 and C_4 is dependent on the reinforcement type, bending radius and the corrosive environment.

203 For straight reinforcement bars in a concrete structure under exposure classes X0, XC1, XC2, XC3, XC4, XF1, XA1 and XA2 the value of $C_3 = 19.6$ and $C_4 = 6.0$ shall be used. See O200 for exposure class definitions.

For reinforcement bent around a mantel of diameter less than $3 \cdot \phi$ and used in a structure under exposure class X0, XC1, XC2, XC3, XC4, XF1, XA1 and XA2 the value of $C_3 = 15.9$ and $C_4 = 4.8$ shall be used. See O200 for exposure class definitions.

For intermediate bending diameters between $3 \cdot \phi$ and straight bars, interpolated values may be used.

Infinite fatigue life may be assumed if the calculated value of N is greater than $2 \cdot 10^8$ cycles.

204 Values of C_3 and C_4 for straight bars in a concrete structure under exposure class XD1, XD2, XD3, XS1, XS2, XS3, XF2, XF3, XF4, XA3 and XSA are suggested in Table M2. For straight reinforcement bars in a concrete structure exposed to specially or severely aggressive environment, which are not included in the previous list, the influence of corrosion on the fatigue properties shall be assessed separately. See O200 for exposure class definitions.

Special assessment shall also be made for bent bars.

Reinforcement which is protected against corrosion using cathodic protection may be assessed for fatigue life using the values C_3 and C_4 in M203.

Table M2			
	Level of Stress Variations (MPa)		
	$\Delta\sigma > 235$	$235 > \Delta\sigma > 65$	$65 > \Delta\sigma > 40$
C_3	15.7	13.35	16.97
C_4	4.5	3.5	5.5

In most cases the reinforcement will have a longer lifetime than the concrete, and the standard define $N > 2 \cdot 10^8$ cycles as infinite fatigue life.

2.2.3.2 Calculating fatigue life according to NS-EN-1992-1-1

For concrete structures, the NS-EN-1992-1-1¹⁴ consider the cases of both fatigue of concrete and fatigue of reinforcement. The verification for concrete and steel shall be performed separately.

6.8 Fatigue

6.8.1 Verification conditions

- (1)P The resistance of structures to fatigue shall be verified in special cases. This verification shall be performed separately for concrete and steel.
- (2) A fatigue verification should be carried out for structures and structural components which are subjected to regular load cycles (e.g. crane-rails, bridges exposed to high traffic loads).

For reinforcement and prestressing steel in constant stress blocks, the code determines the fatigue life with the help of S-N curves.

6.8.4 Verification procedure for reinforcing and prestressing steel

- (1) The damage of a single stress range $\Delta\sigma$ may be determined by using the corresponding S-N curves (Figure 6.30) for reinforcing and prestressing steel. The applied load should be multiplied by $\gamma_{F,fat}$. The resisting stress range at N^* cycles $\Delta\sigma_{Rsk}$ obtained should be divided by the safety factor $\gamma_{S,fat}$.

Note 1: The value of $\gamma_{F,fat}$ is given in 2.4.2.3 (1).

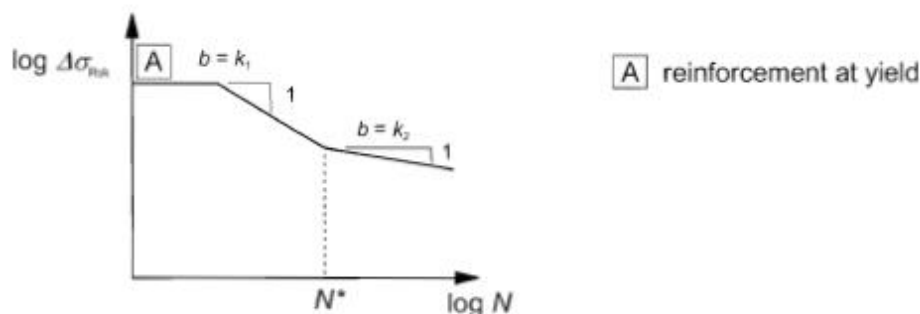


Figure 6.30: Shape of the characteristic fatigue strength curve (S-N-curves for reinforcing and prestressing steel)

Note 2: The values of parameters for reinforcing steels and prestressing steels S-N curves for use in a Country may be found in its National Annex. The recommended values are given in Table 6.3N and 6.4N which apply for reinforcing and prestressing steel respectively.

The code differs between the different types of reinforcements. Straight and bent bars, welded and wire fabrics, and splicing devices have their own S-N curve. Their S-N curves is defined by the factors in table 6.3N.

¹⁴ “Eurocode 2: Design of concrete structures - Part 1-1: General rules and rules for buildings” – Standard Norge

Table 6.3N: Parameters for S-N curves for reinforcing steel

Type of reinforcement	N^*	stress exponent		$\Delta\sigma_{Rsk}$ (MPa) at N^* cycles
		k_1	k_2	
Straight and bent bars ¹	10^6	5	9	162,5
Welded bars and wire fabrics	10^7	3	5	58,5
Splicing devices	10^7	3	5	35

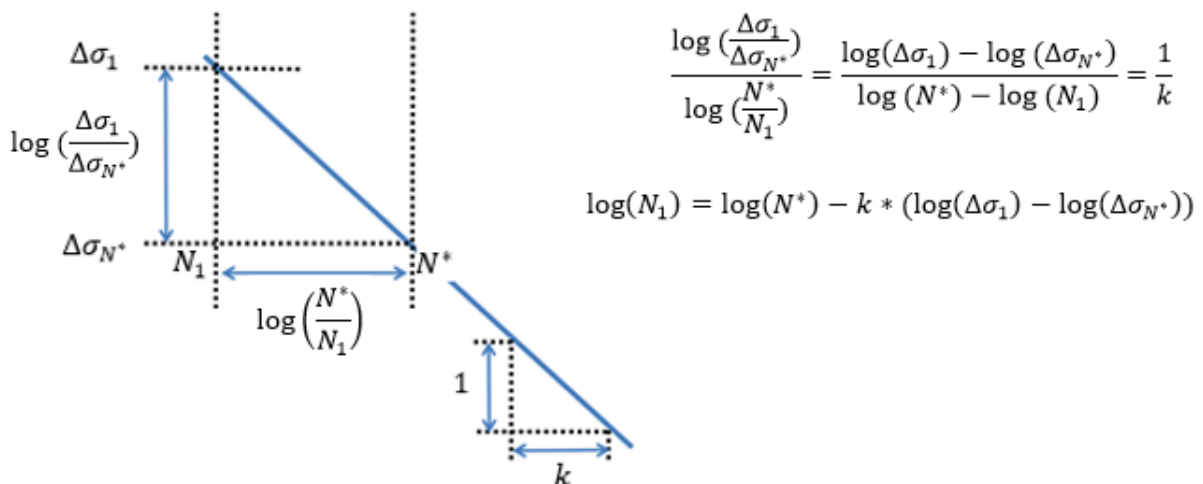
Note 1: Values for $\Delta\sigma_{Rsk}$ are those for straight bars. Values for bent bars should be obtained using a reduction factor $\zeta = 0,35 + 0,026 D / \phi$.
where:
 D diameter of the mandrel
 ϕ bar diameter

The code uses the same type of table for prestressing steel.

Table 6.4N: Parameters for S-N curves of prestressing steel

S-N curve of prestressing steel used for	N^*	stress exponent		$\Delta\sigma_{Rsk}$ (MPa) at N^* cycles
		k_1	k_2	
pre-tensioning	10^6	5	9	185
post-tensioning				
- single strands in plastic ducts	10^5	5	9	185
- straight tendons or curved tendons in plastic ducts	10^6	5	10	150
- curved tendons in steel ducts	10^6	5	7	120
- splicing devices	10^6	5	5	80

With the help of these S-N curves, it is possible to find the number of cycles before failure for the reinforcement and the pre-stressing steel for the specified stress range. The code does not give clear instructions on how to use the curves. In lack of specified formulations, the following formulations can be used to find the fatigue life at stress ranges above $\Delta\sigma_{N^*}$.



When a structure is subjected to varying stress blocks, the Euro Code uses the Palmgren-Miner rule to determine the condition of the reinforcement. Palmgren-Miner is a linear damage accumulation law, which adds the contributions from all the stress blocks.

(2) For multiple cycles with variable amplitudes the damage may be added by using the Palmgren-Miner Rule. Hence, the fatigue damage factor D_{Ed} of steel caused by the relevant fatigue loads should satisfy the condition:

$$D_{Ed} = \sum_i \frac{n(\Delta\sigma_i)}{N(\Delta\sigma_i)} < 1 \quad (6.70)$$

where:

$n(\Delta\sigma_i)$ is the applied number of cycles for a stress range $\Delta\sigma_i$

$N(\Delta\sigma_i)$ is the resisting number of cycles for a stress range $\Delta\sigma_i$

However, the Eurocode does not take the location of the structure into account. When the sum of the contributions reaches 1, the reinforcement fails due to fatigue.

In the case of fatigue of concrete, the Euro Code does not have a method of calculating the fatigue life. Instead, the code does a verification that the concrete can withstand a given number of cycles, which is normally 10^6 cycles. Because of that, the Eurocode does not seem to be very good on weak structures with a low fatigue life.

6.8.7 Verification of concrete under compression or shear

(1) A satisfactory fatigue resistance may be assumed for concrete under compression, if the following condition is fulfilled:

$$E_{cd,max,eqv} + 0,43\sqrt{1 - R_{eqv}} \leq 1 \quad (6.72)$$

where:

$$R_{equ} = \frac{E_{cd,min,eqv}}{E_{cd,max,eqv}} \quad (6.73)$$

$$E_{cd,min,eqv} = \frac{\sigma_{cd,min,eqv}}{f_{cd,fat}} \quad (6.74)$$

$$E_{cd,max,eqv} = \frac{\sigma_{cd,max,eqv}}{f_{cd,fat}} \quad (6.75)$$

where :

- R_{equ} is the stress ratio
- $E_{cd,min,eqv}$ is the minimum compressive stress level
- $E_{cd,max,eqv}$ is the maximum compressive stress level
- $f_{cd,fat}$ is the design fatigue strength of concrete according to (6.76)
- $\sigma_{cd,max,eqv}$ is the upper stress of the ultimate amplitude for N cycles
- $\sigma_{cd,min,eqv}$ is the lower stress of the ultimate amplitude for N cycles

Note: The value of N ($\leq 10^6$ cycles) for use in a Country may be found in its National Annex. The recommended value is $N = 10^6$ cycles.

$$f_{cd,fat} = k_1 \beta_{cc}(t_0) f_{cd} \left(1 - \frac{f_{ck}}{250} \right) \quad (6.76)$$

where:

- $\beta_{cc}(t_0)$ is a coefficient for concrete strength at first load application (see 3.1.2 (6))
- t_0 is the time of the start of the cyclic loading on concrete in days

Note: The value of k_1 for use in a Country may be found in its National Annex. The recommended value for $N = 10^6$ cycles is 0,85.

The Eurocode also gives a second method of controlling fatigue of concrete. But as for the first, the second also base the verification on the ability to withstand 10^6 cycles.

(2) The fatigue verification for concrete under compression may be assumed, if the following condition is satisfied:

$$\frac{\sigma_{c,max}}{f_{cd,fat}} \leq 0,5 + 0,45 \frac{\sigma_{c,min}}{f_{cd,fat}} \quad (6.77)$$

$$\leq 0,9 \text{ for } f_{ck} \leq 50 \text{ MPa}$$

$$\leq 0,8 \text{ for } f_{ck} > 50 \text{ MPa}$$

where:

- $\sigma_{c,max}$ is the maximum compressive stress at a fibre under the frequent load combination (compression measured positive)
- $\sigma_{c,min}$ is the minimum compressive stress at the same fibre where $\sigma_{c,max}$ occurs. If $\sigma_{c,min}$ is a tensile stress, then $\sigma_{c,min}$ should be taken as 0.

With these two methods, the Eurocode does not have general formulations for random structures. The code is only applicable to verify that a structure can withstand 10^6 cycles, neither more or less.

2.2.3.3 Calculating fatigue life according to Model Code 2010

For concrete structures, Model Code 2010¹⁵ have verification methods for both the concrete and the reinforcement. The rules in Model Code 2010 are applicable for the entire lifetime of concrete. For reinforcement and pre-stressing steel, the rules are only applicable for high-cycle fatigue, with more than 10^4 repetitions.

7.4.1 Fatigue design

7.4.1.1 Scope

The following design rules apply for the entire service life of concrete structures. The rules for reinforcing and prestressing steel should be applied if more than 10^4 load repetitions are expected; low-cycle fatigue is not covered.

The verifications can be performed with four different methods with increasing refinement.

4.5.2.3 Fatigue verification

Design principles

Fatigue design shall ensure that in any fatigue endangered cross-section the expected damage D will not exceed a limiting damage D_{lim} . The verifications of this requirement can be performed according to four methods of increasing refinement.

7.4.1.3 Level I of Approximation: the simplified procedure

7.4.1.4 Level II of Approximation: verification by means of a single load level

7.4.1.5 Level III of Approximation: verification by means of a spectrum of load levels

The first method is a qualitative verification that no variable action is able to produce fatigue. If the conclusion of this verification is not positive, a verification according to one of the higher levels shall be made.

The verifications by simplified procedure (Level I) is an indirect verification that the loss of strength will not be significant. The procedure considers both the concrete and the steel, but is limited to structures subjected to less than 10^8 low stress cycles. If the conditions in this procedure are satisfied, detailed fatigue design is not necessary.

¹⁵ Model Code 2010 – CEB-FIP

7.4.1.3 Level I of Approximation: the simplified procedure

This procedure is only applicable to structures subjected to a limited number ($\leq 10^5$) of low stress cycles.

Steel

The fatigue requirements will be met, if the maximum calculated stress range under the frequent combination of loads, $\max \Delta\sigma_{Rsk}$, satisfies the condition

$$\gamma_{Sd} \max \Delta\sigma_{Ss} \leq \Delta\sigma_{Rsk} / \gamma_{s, fat} \quad (7.4-3)$$

where:

$\Delta\sigma_{Rsk}$ is the characteristic fatigue strength at 10^5 cycles.

Values for $\Delta\sigma_{Rsk}$ are given in Table 7.4-1 and Table 7.4-2.

Concrete

Detailed fatigue design needs not be carried out if the maximum calculated stresses under the frequent combination of loads, $\sigma_{c, max}$ (compression), $\sigma_{t, max}$ (tension), respectively, satisfy the following criteria:

Compression

$$\gamma_{Sd} \sigma_{c, max} \eta_c \leq 0.45 f_{cd, fat} \quad (7.4-4)$$

where:

$\sigma_{c, max}$ is the maximum compressive stress;

η_c is an averaging factor considering the stress gradient Eq. (7.4-2);

$f_{cd, fat}$ is the design fatigue reference strength for concrete in compression.

Tension

$$\gamma_{Sd} \sigma_{t, max} \leq 0.33 f_{ctd, fat} \quad (7.4-5)$$

where:

$\sigma_{t, max}$ is the maximum tensile stress in the concrete;

$f_{ctd, fat}$ is the design fatigue reference tensile strength of the concrete.

The verification by means of a single load level (Level II) takes into account the dominant load level for fatigue. For this specific load level, the procedure calculates the lifetime in number of cycles.

7.4.1.4 Level II of Approximation: verification by means of a single load level

This method takes account of the required service life with a foreseen number, n , of cycles. This number intervenes in the verification with the maximum fatigue effects of the action, Q , as defined in subclauses 4.5.2.3(b), subclause 7.4.1.2 and the paragraphs below.

As for the simplified procedure, this method considers both the concrete and the steel. For the steel, the fatigue requirement will be satisfied if a certain fatigue condition is met.

Steel

The fatigue requirement will be met if the calculated maximum acting stress range, $\max \Delta\sigma_{Ss}$, satisfies the condition:

$$\gamma_{Sd} \max \Delta\sigma_{Ss} \leq \Delta\sigma_{Rsk}(n) / \gamma_{s, fat} \tag{7.4-6}$$

where:

$\Delta\sigma_{Ss}$ is the steel stress range under the acting loads;

$\Delta\sigma_{Rsk}(n)$ is the stress range relevant to n cycles obtained from a characteristic fatigue strength function.

Model Code 2010 uses the S-N curve, with a corresponding table for reinforcement, to determine the characteristic fatigue strength. A similar table for prestressing steel is also available.

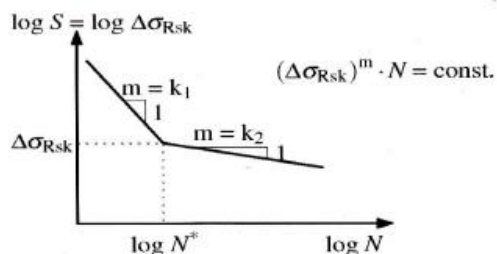


Figure 7.4-2: Shape of the characteristic fatigue strength curves (S-N curves) for steel

Table 7.4-1: Parameters of S-N curves for reinforcing steel (embedded in concrete)

	N^*	Stress exponent		$\Delta\sigma_{Rsk}$ (MPa) ^(e)	
		k_1	k_2	at N^* cycles	at 10^8 cycles
Straight and bent bars $D \geq 25\phi$	10^6	5	9	210	125
Bent bars $D < 25\phi$ ^(b)	10^6	5	9	— ^(e)	— ^(e)
Welded bars ^(b) including tack	10^7	3	5	50	30
Welding and butt joints					
Mechanical connectors					
Marine environment ^{(b),(d)}	10^7	3	5	65	40

For the concrete, the fatigue requirement will be met if the required lifetime is less than the number of cycles to failure. The code have different methods for compression and tension, and the parameters are specified in the code.

Concrete

The fatigue requirements under cyclic loading will be met if the required lifetime (number of cycles) is lower than or equal to the number of cycles to failure:

$$n \leq N$$

where:

n is the foreseen number of cycles during the required design service life;

N is the number of resisting stress cycles, to be calculated from the fatigue strength functions given below.

Compression

For $S_{cd,min} > 0.8$, the S-N relations for $S_{cd,min} = 0.8$ are valid.

For $0 \leq S_{cd,min} \leq 0.8$, Eqs. (7.4-7a)-(7.4-7b) apply.

$$\log N_1 = \frac{8}{Y-1} \cdot (S_{cd,max} - 1) \quad (7.4.7a)$$

$$\log N_2 = 8 + \frac{8 \cdot \ln(10)}{Y-1} \cdot (Y - S_{cd,min}) \cdot \log\left(\frac{S_{cd,max} - S_{cd,min}}{Y - S_{cd,min}}\right) \quad (7.4.7b)$$

with

$$Y = \frac{0.45 + 1.8 \cdot S_{cd,min}}{1 + 1.8 \cdot S_{cd,min} - 0.3 \cdot S_{cd,min}^2}$$

where

(a) if $\log N_1 \leq 8$, then $\log N = \log N_1$;

(b) if $\log N_1 > 8$, then $\log N = \log N_2$;

where:

$\sigma_{c,min}$ is the minimum compressive stress;

$S_{cd,max}$ is the maximum compressive stress level;

$$S_{cd,max} = \gamma_{Ed} \sigma_{c,max} \eta_c / f_{cd,fat}$$

$S_{cd,min}$ is the minimum compressive stress level;

$$S_{cd,min} = \gamma_{Ed} \sigma_{c,min} \eta_c / f_{cd,fat}$$

Compression – tension with $\sigma_{ct,max} \leq 0.026 |S_{cd,max}|$

$$\log N = 9(1 - S_{cd,max}) \quad (7.4.8)$$

Pure tension and tension-compression with $\sigma_{ct,max} > 0.026 |S_{cd,max}|$

$$\log N = 12(1 - S_{td,max}) \quad (7.4.9)$$

where:

$\sigma_{ct,max}$ is the maximum tensile stress;

$S_{td,max}$ is the maximum tensile stress level;

$$S_{td,max} = \gamma_{Ed} \sigma_{ct,max} / f_{cd,fat}$$

Compression

$$f_{cd,fat} = 0.85\beta_{cc}(t) \left[f_{ck} \left(1 - \frac{f_{ck}}{25f_{ck0}} \right) \right] / \gamma_{c,fat}$$

where

$\beta_{cc}(t)$ is the coefficient which depends on the age t of the concrete in days when fatigue loading starts (see subclause 5.1.9.1);

$f_{ck0} = 10$ MPa (reference strength).

In Model Code the static capacity is calculated as $f_{cd,fat}$. This capacity does not consider the effect of any reinforcement, which is the weakness of the code.

Verification by means of spectrum of load levels (Level III) is the most accurate method, which also considers both concrete and steel. According to this method, the load history with its whole load spectrum should be taken into account. The accumulation of fatigue strength is calculated on the basis of the Palmgren-Miner summation. The fatigue requirement is satisfied if $D \leq D_{lim}$.

7.4.1.5 Level III of Approximation: verification by means of a spectrum of load levels

This method takes account of the required service life, the load spectrum (which is divided into j blocks) and the characteristic fatigue strength functions.

Fatigue damage D is calculated using the Palmgren-Miner summation

$$D = \sum_{i=1}^j \frac{n_{Si}}{N_{Ri}} \quad (7.4-10)$$

where:

D is fatigue damage;

n_{Si} denotes the number of acting stress cycles associated with the stress range for steel and the actual stress levels for concrete;

N_{Ri} denotes the number of resisting stress cycles at a given stress level.

The fatigue requirement will be satisfied if $D \leq D_{lim}$.

Appropriate values for D_{lim} should be adopted for concrete. Under increasing stress levels, D_{lim} can be safely used.

2.3 Effect of confinement on fatigue

A specimen can be prevented from expanding in one or more directions by restricting movement, or by applying a load which causes a stress build-up. These two cases are called passive and active confinement. The cases are illustrated below with lateral confinement along the x-axis.

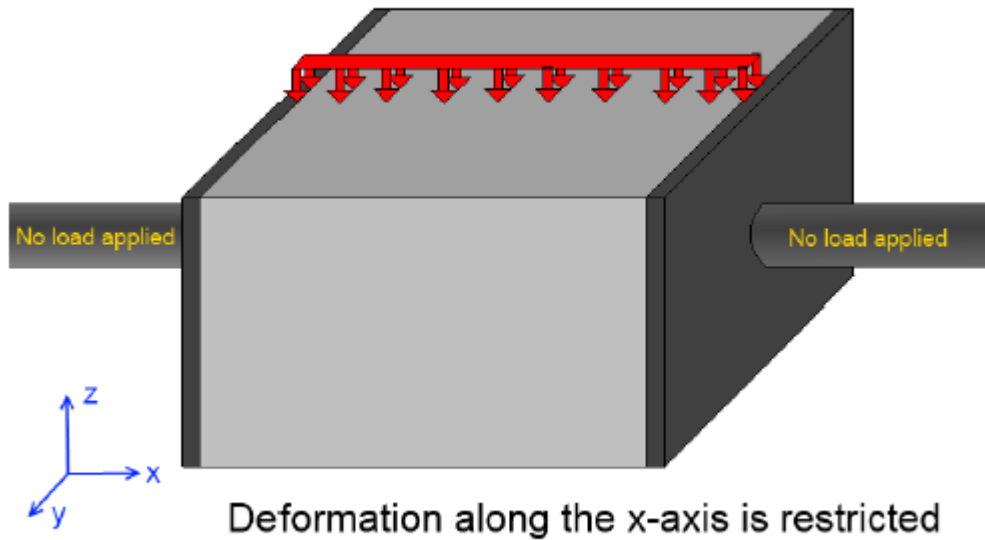


Figure 6 - Example on passive confinement, taken from Furnes and Hauges thesis

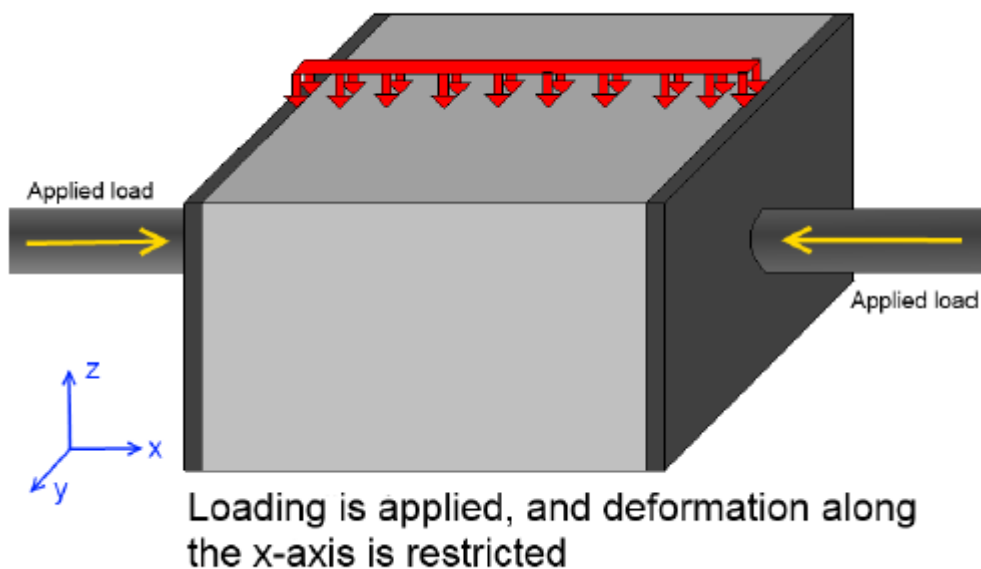


Figure 7 - Example on active confinement, taken form Furnes and Hauges thesis

Most previous research on confinement of concrete has been carried out with static loads. Very little research is carried out on confined concrete with dynamic loads.

On a general basis, it is well known that concrete which is effectively confined will get an increased strength and ductility. The fatigue strength also seems to be affected of confinement, although most research carried out are with a low number of cycles with high stress or strain amplitude to simulate earthquake loading.

For many other load situations, this is not necessarily the most relevant research. For pile driving, sea waves, wind and vehicular traffic a much larger number of load cycles with lower stress amplitude is much more relevant. For plain concrete extensive research have been carried out, but for confined concrete there is very limited research and test results available.

Some research on active confined concrete is however conducted. The only work found on passive confined concrete is the work by Tan Teng Hooi¹⁶, with spirally confined specimens. There is a big difference between how passive and active confinement influences the confining stresses in the concrete that again influences the concrete behaviour.

Tan Teng Hooi investigated the applicability of Aas-Jacobsen's formula to passive confined concrete. Aas-Jacobsen's formula:

$$\frac{f_c^{max}}{f'_{co}} = 1 - \beta(1 - R_f) \log_{10} N_f$$

Where: $R_f = \frac{f_c^{min}}{f_c^{max}}$, $\beta = 0,0685$ (in difference from 0,064 used earlier)

The results of Hooi's work showed the data spread is much lower in the confined test results than in the unconfined. Aas-Jacobsen's formula can be re-expressed to take the effects from the lateral confinement into account¹⁷.

$$\frac{f_c^{max}}{f'_{co}} = \alpha - \beta(1 - R_f) \log_{10} N_f$$

Where α is the predicted value of the confined concrete for monotonic loading ($f_c^{max} = f'_{cc}$)

The research of Hooi shows that the passive lateral confinement increases the strength of the concrete (bigger α) which will lead to lower applied stress ratio, but simultaneously the susceptibility to fatigue damage increases. Although the susceptibility to fatigue damage increases, the enhancement of concrete strength outweighs it and the net effect is that the lateral confinement leads to higher fatigue strength overall, given that the comparison is to

¹⁶ "Effects of passive confinement on fatigue properties of concrete" – Tan Teng Hooi

¹⁷ "Effects of passive confinement on fatigue properties of concrete" – Tan Teng Hooi

unconfined fatigue strength. Hooi's conclusion is that a modified Aas-Jacobsen given by expressions for α and β is adequate to include the effect of the passive confinement:

Where:

$$\alpha = \left[1 + K_1 \left(\frac{f_{le}}{f'_{co}} \right) \right]$$

$$\beta = \left[0,5 \left(\frac{f_{le}}{f'_{co}} \right) + 0,08 \right]$$

Some of the difference between passive and active confinement is that concrete under passive confinement do not experience any remarkable confining pressure until it reaches the beginning of unstable propagation of cracks. First when substantial cracking have occurred, the confining pressure is generated, which prevents the further development of cracks.

The confining pressure will increase continuously as the cracking progresses, but finally the material used to confine the concrete specimen reaches yielding. Loading beyond the yield point will cause a permanent strain even after unloading. On this way the concrete damage may accumulate with each cycle, though the confinement prevents total collapse of the structure.

In active confined concrete the applied confining stress will change the local stress state at the micro-cracks tips, which helps to prevent further crack propagation. This is how the active confinement improves the fatigue behaviour.

The Eurocode briefly discusses confined concrete in point 3.1.9, though the given rules are very conservative. The reason is "the absence of more precise data"¹⁸. The rules given below is given for confinement in x- and y- direction, $\sigma_2 = \sigma_3$. By using the formulas on confinement in one direction the allowed $f_{ck,c}$ will be equal to f_{ck} ($\sigma_2 = 0$), even though it will have an positive effect on the strength with confinement in only one direction as well. To provide lateral confinement in all directions (x & y) closed stirrups or cross-ties is adequate, according to Eurocode.

$$f_{ck,c} = f_{ck} (1,000 + 5,0 \sigma_2/f_{ck}) \quad \text{for } \sigma_2 < 0,05f_{ck}$$

$$f_{ck,c} = f_{ck} (1,125 + 2,50 \sigma_2/f_{ck}) \quad \text{for } \sigma_2 > 0,05f_{ck}$$

$$\varepsilon_{c2,c} = \varepsilon_{c2} (f_{ck,c}/f_{ck})^2$$

$$\varepsilon_{cu2,c} = \varepsilon_{cu2} + 0,2 \sigma_2/f_{ck}$$

¹⁸ Eurocode 2, NS-EN-1992-1-1 [3.1.9 (2)]

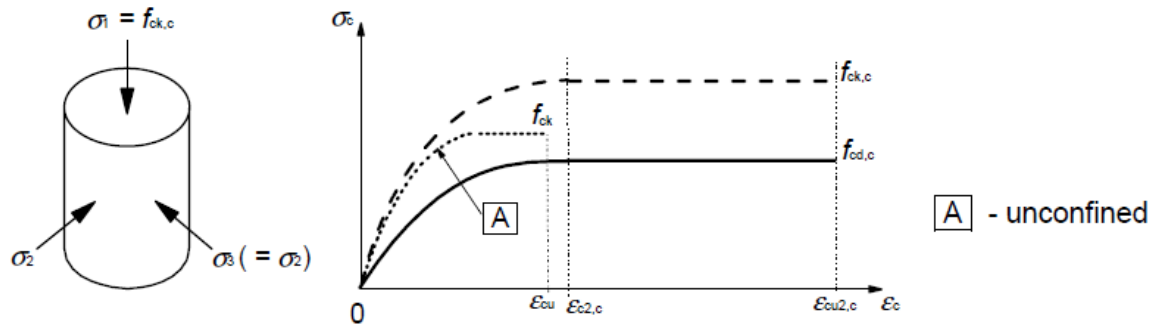


Figure 8 - Taken from Eurocode 2, NS-EN-1992-1-1 [3.1.9 (2)]

2.4 Partially loaded areas in concrete

2.4.1 Introduction

In cases where the concrete specimen has a load surface smaller than the whole concrete surface, the effect of partially loaded areas appear. When only parts of the surface is loaded, the surrounding concrete gives an increasing effect on the compressive strength, compared to the loaded area alone.

This subject is discussed in the design codes and a theoretical background can be found in “Designers’ guide to EN 1992-2”¹⁹. Apart from studies performed by J.A. Øverli²⁰, and Furnes and Hauges²¹ master thesis, the experimental studies in this area are not comprehensive.

2.4.2 Some design codes

2.4.2.1 NS-EN-1992-1-1

In Eurocode²² part 2 partially loaded areas are featured in part 6.7. For partially loaded areas local crushing and transverse tension forces have to be taken into account.

For a partially loaded area exposed to compression, given formula in Eurocode applies:

$$F_{Rdu} = A_{c0} * f_{cd} * \sqrt{A_{c1}/A_{c0}} \leq 3,0 * f_{cd} * A_{c0} \quad (6.63)$$

Where:

A_{c0} = the loaded area

A_{c1} = is the maximum design distribution area with a similar shape to A_{c0}

¹⁹ “Designers guide to EN-1992-2, Eurocode 2: Design of concrete structures, Part 2: Concrete bridges” - C. R. Hendy and D. A. Smith

²⁰ “Static and Fatigue Capacity of Partially Loaded Areas in Concrete Structures” – Jan Arve Øverli

²¹ “Fatigue capacity of partially loaded areas in concrete structures” - Alexander Furnes and Ole Martin Hauge

²² NS-EN 1992-1-1:2004+NA:2008

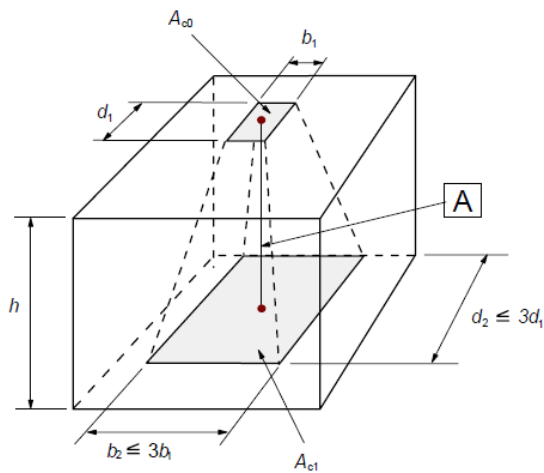


Figure 9 - Design distribution for partially loaded areas (figure taken from Eurocode 2)

As it appears from the formula for $F_{Rd,u}$, elements with partially loaded area have an increase in strength compared to an equivalent fully loaded area, F_{Rd} . The reason is that the compressed area is prevented from expanding by the surrounding non-loaded concrete. The expansion will give transverse tension forces.

Part 6.7(4) requires that the tension forces that occur due to the load propagation should be taken by appropriate reinforcement. It does not emphasize where the reinforcement should be placed or what formula/method to use.

To find appropriate reinforcement for the transverse tension forces a strut and tie model according to part 6.5.3 can be used. The tension force T depends on if the specimen is partly or fully discontinuous (if the load propagation is fully, or limited by the renders of the specimen).

a) for partial discontinuity regions $\left(b \leq \frac{H}{2}\right)$, see Figure 6.25 a:

$$T = \frac{1}{4} \frac{b-a}{b} F \quad (6.58)$$

b) for full discontinuity regions $\left(b > \frac{H}{2}\right)$, see Figure 6.25 b:

$$T = \frac{1}{4} \left(1 - 0,7 \frac{a}{h}\right) F \quad (6.59)$$

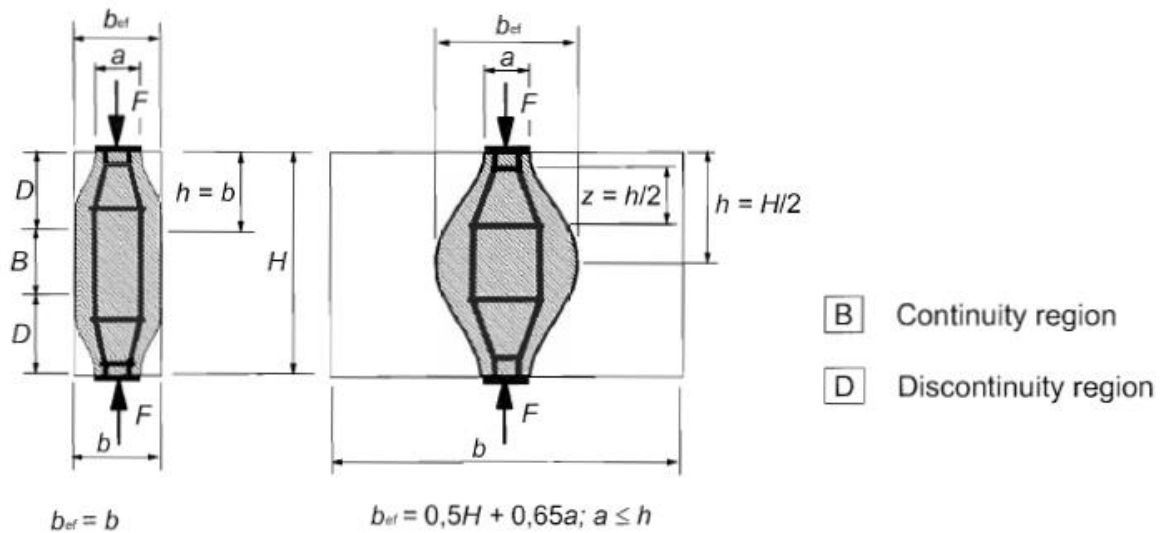


Figure 6.25: Parameters for the determination of transverse tensile forces in a compression field with smeared reinforcement

Figure 10 - Strut and tie-models of partial and full discontinuity (taken from Eurocode 2)

According to the Eurocode eccentric loading, overlapping loads and not uniformly distributed loads needs to be taken into account.

To give a guide to the Eurocode, several books have been published in the “Eurocode designer’s guide” series. The partially loaded areas in concrete are featured in the book “Designers’ guide to EN 1992-2”²³. The design guide gives detailed information on different methods to fulfil Eurocodes demands as well as some of the theory the formulas are based upon.

The formula for F_{Rdu} is derived with respect to the surrounding concrete of the core as it provides a passive lateral confinement to the core with perimeter b_2 and d_2 . The reason is that the surrounding concrete has some tension capacity and therefore the surrounding concrete will behave as a “tension ring”, up to the loading were capacity is reached and spalling occurs. Due to the tension ring the core establishes a triaxial stress state which leads

²³ “Designers guide to EN-1992-2, Eurocode 2: Design of concrete structures, Part 2: Concrete bridges” - C. R. Hendy and D. A. Smith

to the enhanced compressive strength. The confining reinforcement can also give restraints. Other effect that helps resist splitting is the shear stress at surface A_{c1} and the traction forces between the loading plate and the specimen at A_{c0} .

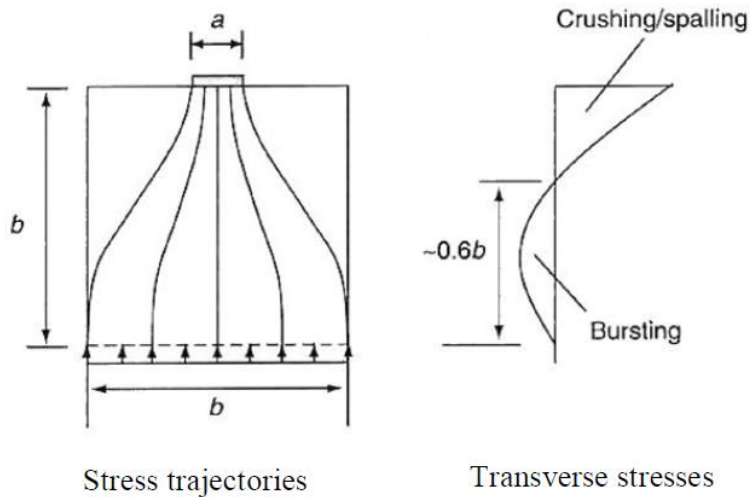


Figure 11 - Stress field under concentrated load according to linear analysis²⁴

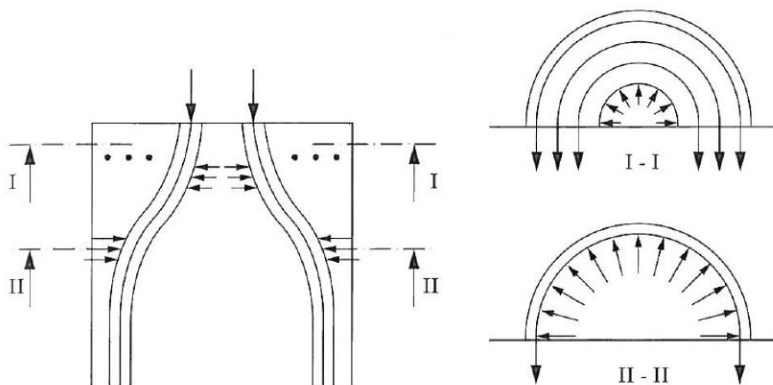


Figure 12 - Transverse stresses including splitting forces²⁵

As the figures show, the upper part, section I-I, is not necessarily the most critical one, as it has more surrounding concrete which gives a stronger tension ring. Section II-II on the other hand has much less surrounding concrete which gives a weaker tension ring. Therefore, the stresses in the transverse reinforcement is likely to develop first in the bursting zone in section II-II.

The Eurocode does not consider cases where the loaded area is smaller than the loaded specimen in only one direction, as seen below. In circumstances like this the tension ring does not seem to be able to develop, and it seems like the partial effect vanishes. The code

²⁴ Taken from "Designers guide to EN-1992-2" – Hendy, S. R. & Smith, D. A.

²⁵ Taken from "Designers guide to EN-1992-2" – Hendy, S. R. & Smith, D. A.

however, does not indicate whether the formula for F_{Rdu} is valid or not for this case. Though, it should have been stated more clearly in the Eurocode.

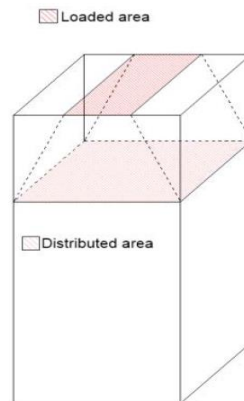


Figure 13 - Loaded area smaller in only one direction, taken from Furnes and Hauges Thesis

2.4.2.2 NS 3473 & DNV-OS-C502 (offshore concrete structures)

On the subject of partially loaded areas these two design codes is basically the same, as the DNV²⁶ code is based on NS 3473²⁷. These codes are a bit more complementary than the Eurocode.

Where the Eurocode only have one formula, NS 3473 & DNV-OS-C502 have complementary text and two formulas, one for normal situations and one if the ratio between the larger and smaller dimension (the ratio between a_1 and b_1 , please see figure below) is smaller than two, and A_2 (distributed area) is assumed to be geometrically identical to A_1 (loaded area).

Formulas:

Normal situations:

$$F_{cd} = A_1 * f_{cd} * \sqrt[3]{A_2/A_1}$$

Ratio less than two:

$$F_{Rdu} = A_1 * f_{cd} * \sqrt{A_2/A_1} \leq 3,0 * A_{c0} * f_{cd}$$

²⁶ "Offshore standard DNV-OS-C502 Offshore concrete structures" – Det Norske Veritas

²⁷ "Concrete structures - Design and detailing rules" – Standard Norge

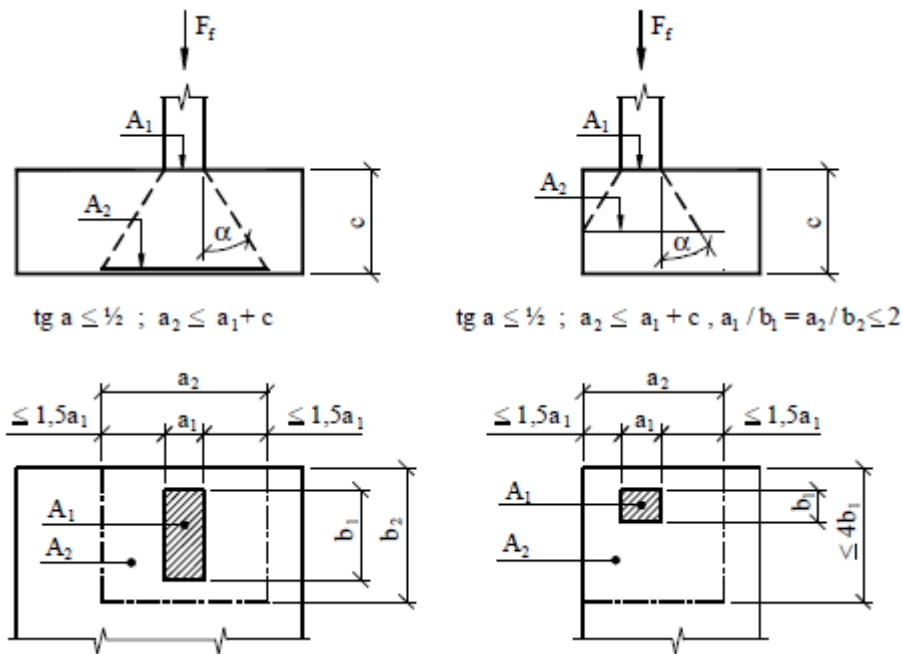


Figure 14 - Geometrical limitations for partial loaded areas, taken from DNV-OS-C502

In difference from Eurocode these two codes have an own formula to find appropriate reinforcement for the transverse tensile forces. In the two principal directions perpendicular to the compressive force, appropriate reinforcement for the tension forces is given by:

$$0.25F_f(1 - a_1/a_2) \text{ and } 0.25F_f(1 - b_1/b_2)$$

Unlike the Eurocode these two codes gives specific instructions for the placement of the transverse tension reinforcement. The codes states that the reinforcement should be placed such that its centre of gravity is placed at a distance from the loaded area equal half the length of the side of the distribution area in the same direction²⁸, however not greater than the distance to the distribution area. The reinforcement bars could be distributed over a width equal to the length of the distributed area side normal to the bars, and over a height that equal half the side of the distributed area parallel to the bars.

The codes also remarks when calculating required transverse tension reinforcement, expansion of soft supports, fluid pressure and similar have to be taken into account.

²⁸ Taken from DNV-OS-C502

2.4.2.3 Model code 2010

In Model Code 2010 partially loaded areas are featured in Volume 2 part 7.2.3.1.7. The rules, and their theoretical background, are basically equal to the rules in the Eurocode, where an increased capacity is allowed under certain circumstances.

7.2.3.1.7 Partially loaded areas

For a uniform distribution of load on an area A_{c0} (Figure 7.2-14) the concentrated resistance force may be determined as follows:

$$F_{Rdu} = A_{c0} f_{cd} \sqrt{A_{c1} / A_{c0}} \leq 3.0 f_{cd} A_{c0} \quad (7.2-22)$$

where:

A_{c0} is the loaded area;

A_{c1} is the maximum design distribution area with a similar shape to A_{c0} .

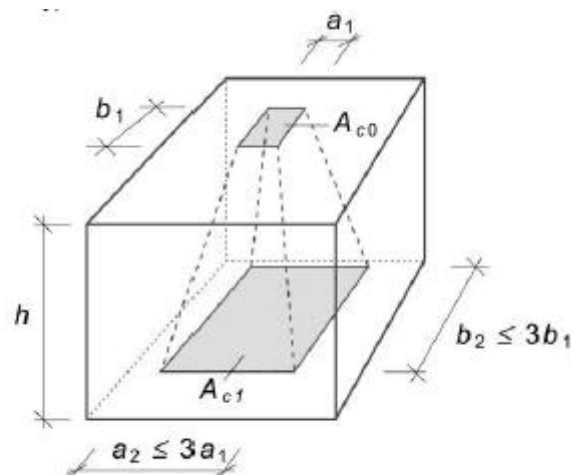


Figure 7.2-14: Load distribution for partially loaded areas

To fulfil these circumstances some requirements must be met. The dispersion of concentrated forces causes biaxial or triaxial compression immediately under the load, whereas it produces transverse tension forces. These forces have to be taken by transverse reinforcement. As for the Eurocode, no specifications on the reinforcement or its position is mentioned. In addition, if there is more than one compression force action on the concrete, the designed distribution areas should not overlap.

2.4.3 Partially loaded areas exposed to fatigue

Partially loaded areas exposed to fatigue are not mentioned in any design code. The problem with this is the issue of validity of the codes for this particular design problem. As it is not much previous test results or literature on the subject other than Furnes and Hauges thesis, it would be vague to draw final conclusions.

Furnes and Hauges results indicated that the formula for increased F_{Rd} for the partially loaded area is adequate with the existing design code formulas for fatigue of dry concrete. Furnes and Hauge even suggest that the C1-factor in the fatigue formulas in DNV-OS-C502 can be increased when the partially loaded area with splitting reinforcement is taken into account. They however emphasizes that further testing is required, especially the impact of humidity on the specimen with regard to the design codes.

3. Materials, Test Specimens and Instrumentation

3.1 Introduction

The materials, test specimens and instrumentation will be described in this section. The section will contain a description of specimen size, concrete mix, curing conditions, preparation and instrumentation.

3.2 Materials and concrete mix

3.2.1 Casting frame

The casting frame for the 18 specimens was divided into 3 batteries with 6 specimens each. The batteries consist of 432 drilled holes and 216 threaded bars. Reinforcement with instrumentation was inserted into the frame.

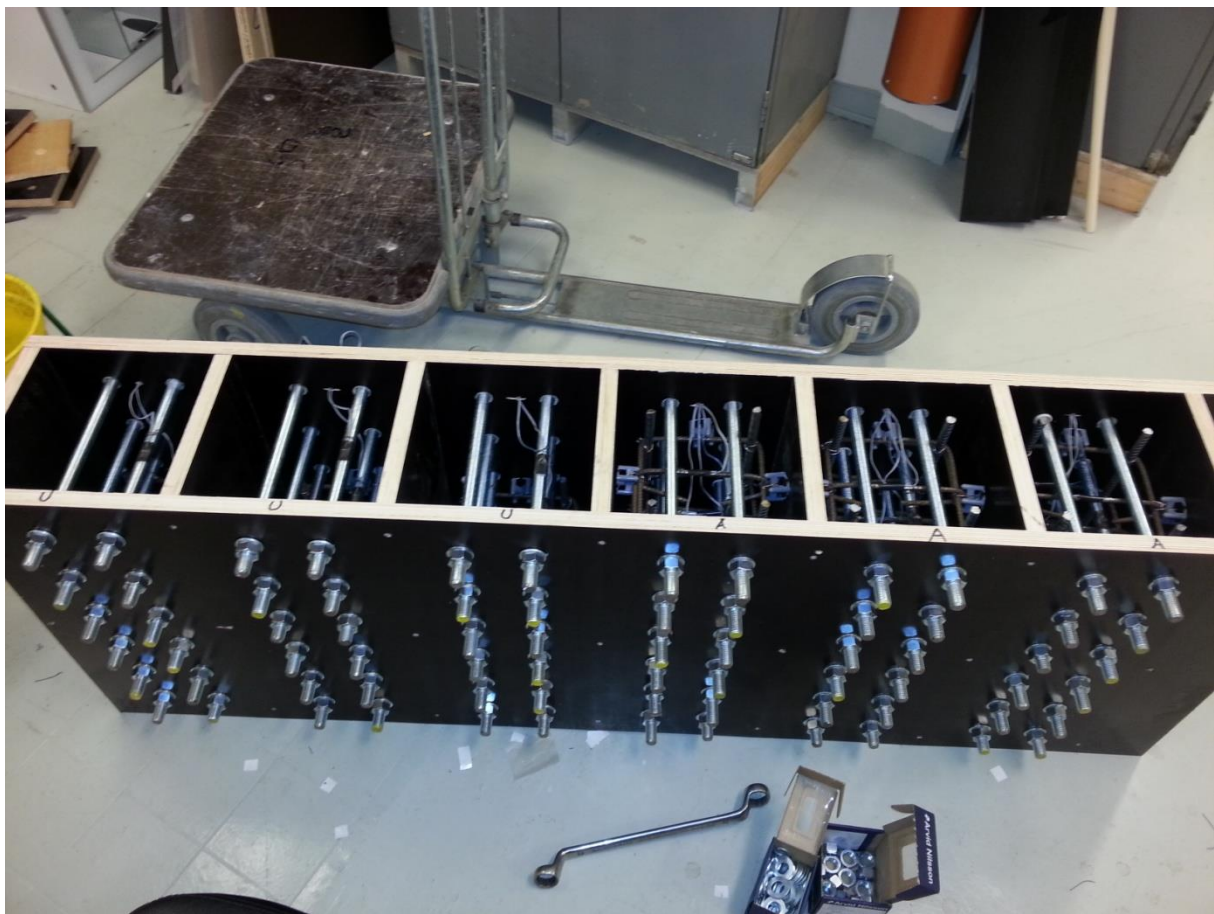


Figure 15 - Casting frame

3.2.2 Concrete mix

Due to the laboratory equipment at the DNV laboratory the compressive strength of the concrete could not be too high. The concrete was aimed to have a compressive cube strength of 25 MPa. Test casting was considered unnecessary. The concrete recipe is as follows:

Concrete mix	
Mixing Volume	517 liter
Date	31.01.2014
Done by	Ove Loraas, Vegard Vee, Tor Magne Sølvørød Mo, Erlend Bognøy

Materials:	Recipe[kg/m ³]	Amount[kg]	Humidity[%]	Correction[kg]	Weight[kg]	
Norcem Standard FA	288,0	148,9	-	-	148,9	
Silica	-	-	-	-	-	
Fly ash	-	-	-	-	-	
Free water	187,2	96,8	-	-12,9	84,0	90,5
Absorbed water	12,5	6,5	-	-	6,5	
Årdal 0/8 mm nat.vask	1103,7	570,6	1,9	10,8	581,4	
Årdal 8/16 mm	738,0	381,5	0,5	1,9	383,5	
RMC 420	0,3	0,2	82	-	0,171	
Fresh concrete						
Slump Measure	160 mm					
Air	2,4					
Density	2,365					

3.2.3 Reinforcement

The reinforcement²⁹ chosen were equal to the one in the master thesis of Furnes and Hauge³⁰. Control of their calculations were made, based on NS-EN-1992-1-1³¹. In total, there were casted nine specimens with splitting reinforcement and 9 specimens without splitting reinforcement.

According to their calculations six $\phi 6$ splitting bars were needed. Also four $\phi 10$ vertical bars were used to support the stirrups ($\phi 6$). In the specimens with splitting reinforcement there were used six stirrups and in the specimens without there were used four stirrups in the lower part of the specimens. The stirrups were placed with 80 mm centre distance in both types of specimens.

²⁹ See sketches of the reinforcement in attachment A3 and A4, and calculation in attachment A1 and A2

³⁰ "Fatigue capacity of partially loaded areas in concrete structures" - Alexander Furnes and Ole Martin Hauge

³¹ See section 2.4.2.1 "NS-EN-1992-1-1"

In the two top layers in the specimens with splitting reinforcement, the stirrup running perpendicular to the load direction will act as splitting reinforcement. Therefore, only two more splitting bars had to be added.

The $\phi 6$ reinforcement has a yield strength of 500MPa, with corresponding strains at approximately $2500\mu\text{m/m}$. It is also assumed a modulus of elasticity equal to 200 000MPa.

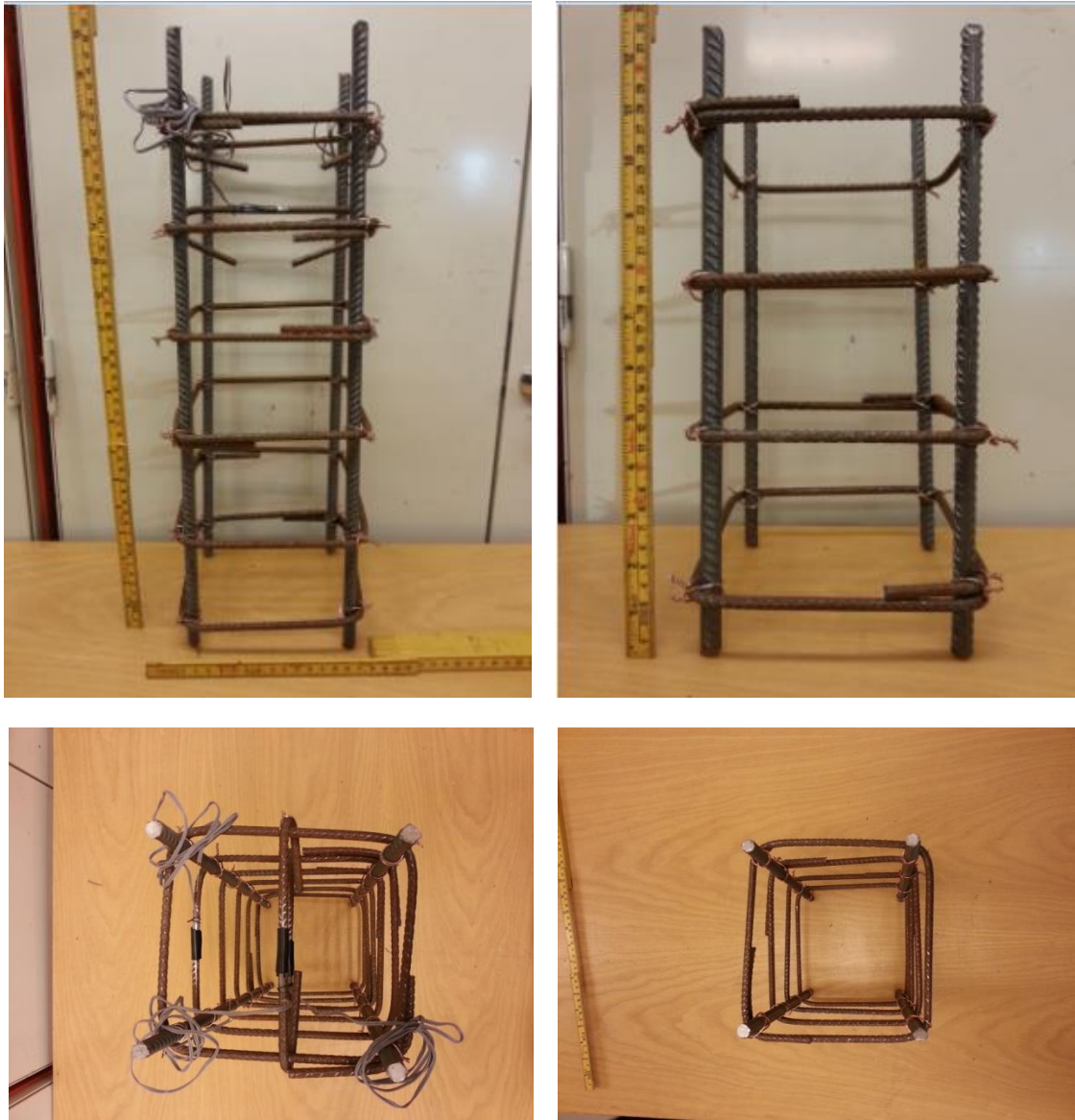


Figure 16 - With and without splitting reinforcement

3.2.4 Threaded bars

To prevent the specimens from deforming parallel to the line-load, there were two options, an end plate on each side, or threaded bars. The threaded bars were chosen to prevent any traction forces to occur from the end plates. The alternative would have been a traction free plate on each side. The water penetration conditions is not the same for threaded bars and traction free end plates. The threaded bars will allow more water penetrating, due to the waters direct access to the cracks. As water is incompressible pore pressure will occur in

compression. However on a “real life” structure, the structure is submerged in water for several years and then the pores in the concrete will be filled with water regardless. Therefore the threaded bars is a fairly good simplification of the wind turbine foundation.

All the specimens were installed with 12 bars each, and cast as the concrete was poured. After the casting frame was dismantled, the threaded bars were restrained with plates and bolts.



Figure 17 - Threaded bars

Threaded bars

Property class	Yield strength (MPa)	Ultimate limit strength (MPa)	Minimum tensile strength (kN)	Diameter(mm)	Length(mm)
8.8	640	800	125	16	330

3.2.5 Test specimens

There were 18 test specimens and 54 test-cubes created. All of the specimen have measurements: 210x210x525 mm. The test-cubes have measurements 100x100x100 mm.

Specimen	Reinforced	Testing	Number of strain gauges
1-3	No	Static	2
4-6	Yes	Static	4
7-12	No	Dynamic	2
13-18	Yes	Dynamic	4

3.2.5.1 Size of specimens

Size of the specimens was 210x210x525 mm, to represent a part of the wind turbine foundation. This is the same measurements as in Furnes and Hauges thesis.

3.2.5.2 Casting

The concrete was poured into the casting frames at once after mixing. To remove air from the forms, a vibrator was used. Slump measure, air content and density were also measured³²

3.2.5.3 Instrumentation

The specimens with splitting reinforcement were installed with four strain gauges. The gauges were placed on the stirrup in the 2nd layer from the top, on the two splitting reinforcement bars and on one of the threaded bars in the 2nd layer from the top.

The specimens without splitting reinforcement were installed with two strain gauges. The gauges were placed on one of the threaded bars in the 1st and the 2nd layer from the top.



Figure 18 - Strain gauges mounted on reinforcement

The strain gauges are of the type FLA-3-11-3L, and are delivered by Tokyo Sokki Kenkyujo CO., Ltd³³. The properties of the strain gauges are shown in the table below.

Type	Gauge length (mm)	Gauge width (mm)	Backing length (mm)	Backing width (mm)	Resistance (Ω)	Lead wire pre-attached	Type name of lead wire preattached
FLA-3-11 FLA-3-17 FLA-3-23	3	1.7	8.8	3.5	120	Paralleled 1m Paralleled 3m Paralleled 5m 3-wire 3m 3-wire 5m	-1L -3L -5L -3LT -5LT
Applicable specimen	Metal, Glass, Ceramics			Backing	Epoxy		
Operational temperature(° C)	-20~+80° C			Element	Cu-Ni		
Temperature compensation range(° C)	+10~+80° C			Strain limit	5% (50000 × 10 ⁻⁶ strain)		
Bonding adhesive	CN, P-2, EB-2			Fatigue life at room temperature	1 × 10 ⁶ (± 1500 × 10 ⁻⁶ strain)		

³² See section 3.2.2 “Concrete mix” for details

³³ Tokyo Sokki Kenkyujo CO., Ltd, URL: <http://www.tml.jp/e/>

3.2.5.4 Storage and curing

Since water content in the specimens and the test-cubes should be equal, the specimens had to be wrapped with soaked burlap sacks inside. This insured the loss of humidity to be a minimum, and a constant humidity at around 90-95%.

The test-cubes were stored in water at NTNU with temperature at approximately 20 degrees Celsius.



Figure 19 - Soaked burlap sacks, plastic wrapped shipment

4. Testing

4.1 Introduction

Both static and dynamic testing of the specimens was performed at DNV GL's laboratory at Høvik in Oslo. The reference cubes were simultaneously tested in NTNU's laboratory in Trondheim by the laboratory staff. All the specimens should be tested until failure, both static and dynamic. Tests were performed in a period from 6st of March until 2nd of April.

In difference from Furnes and Hauges, thesis the specimens were tested submerged in a water-container, which provides the specimens to be fully covered in water. This to be able to see how the water affects the concrete when exposed to dynamic loading.

The static tests consist of 6 specimens in total, 3 reinforced and 3 without reinforcement. The dynamic tests consist of 12 tests in total, 6 reinforced (3 short term and 3 long term) and 6 without reinforcement (3 short term and 3 long term).

Specimen	Test Type	Reinforced	Short/Long term	Date [dd.mm.yy]	Load range / rate [mm/min] / [P _{max} ,P _{min}]
1	Static	No	-	06.03.14	0,4
2	Static	No	-	07.03.14	0,4
3	Static	No	-	07.03.14	0,4
4	Static	Yes	-	07.03.14	0,4
5	Static	Yes	-	07.03.14	0,4
6	Static	Yes	-	10.03.14	0,4
7	Dynamic	No	Short	19.03.14	379,4/50,6 kN
8	Dynamic	No	Short	20.03.14	379,4/50,6 kN
9	Dynamic	No	Short	21.03.14	379,4/50,6 kN
10	Dynamic	No	Long	25.03.14	328,8/50,6 kN
11	Dynamic	No	Long	27.03.14	328,8/50,6 kN
12	Dynamic	No	Long	27.03.14	328,8/50,6 kN
13	Dynamic	Yes	Short	11.03.14	625,5/73,6 kN
14	Dynamic	Yes	Short	14.03.14	551,9/73,6 kN
15	Dynamic	Yes	Short	18.03.14	551,9/73,6 kN
16	Dynamic	Yes	Long	28.03.14	478,9/73,7 kN
17	Dynamic	Yes	Long	31.03.14	478,9/73,7 kN
18	Dynamic	Yes	Long	01.04.14	478,9/73,7 kN

4.2 Testing equipment

To perform the tests a hydraulic jack with static capacity of 1000 kN, and dynamic capacity of 800 kN was used. The jack was of type MTS (MTS, 2011) with an Instron 8500 (INSTRON, 2011) controller.



Figure 20 - Hydraulic jack "MTS", Instron 8500 controller, Spider8 logger and a computer

The logger Spider8 and had 8 channels. On the static tests all the data could be logged by one logger, the dynamic tests however had need of 2 more channels due to the LVDT's. Therefore two loggers were daisy chained on the dynamic test to have enough channels.

Logger setup for the static tests:

Channel	Measurement	Sampling rate [Hz]
1	Time [s]	5
2	Load [kN]	5
3	Stroke [mm]	5
4	Strain 1 [$\mu\text{m}/\text{m}$]	5
5	Strain 2 [$\mu\text{m}/\text{m}$]	5
6	Strain 3 [$\mu\text{m}/\text{m}$]	5
7	Strain 4 [$\mu\text{m}/\text{m}$]	5

Logger setup for the dynamic tests:

Channel	Measurement
1	Time [s]
2	Load [kN]
3	Stroke[mm]
4	Strain 1 [$\mu\text{m}/\text{m}$]
5	Strain 2 [$\mu\text{m}/\text{m}$]
6	Strain 3 [$\mu\text{m}/\text{m}$]
7	Strain 4 [$\mu\text{m}/\text{m}$]
8	LVDT 1 [mm]
9	LVDT 2 [mm]

*Different sampling rate for each test depending on computer capacity and duration of test

Reinforced tests	Placement of strain gauge	Unreinforced tests	Placement of strain gauge
Strain 1	the stirrup in the 2 nd layer from the top	Strain 1	one of the threaded bars in the 2 nd layer from the top
Strain 2	splitting reinforcement in the 2 nd layer from the top	Strain 2	one of the threaded bars in the 1 st layer from the top
Strain 3	splitting reinforcement in the 1 st layer from the top	Strain 3	---
Strain 4	one of the threaded bars in the 2 nd layer from the top	Strain 4	---

The two LVDT's were placed in the corners diagonal to each other. The LVDT's were used to find the deformation of the concrete, by averaging the results from the two LVDT's. This will probably be more accurate than the stroke measurement on the jack, as it will be some error depending on applied load.

As mentioned there might be some error in the stroke measurements directly from the jack. To find out how big this error is a test with only a steel plate between the jacks pistons were performed. The results give the opportunity to take these errors into account³⁴.

³⁴ See section 5.2.3.1 "Force deformation relation in reinforced specimens" for further details.

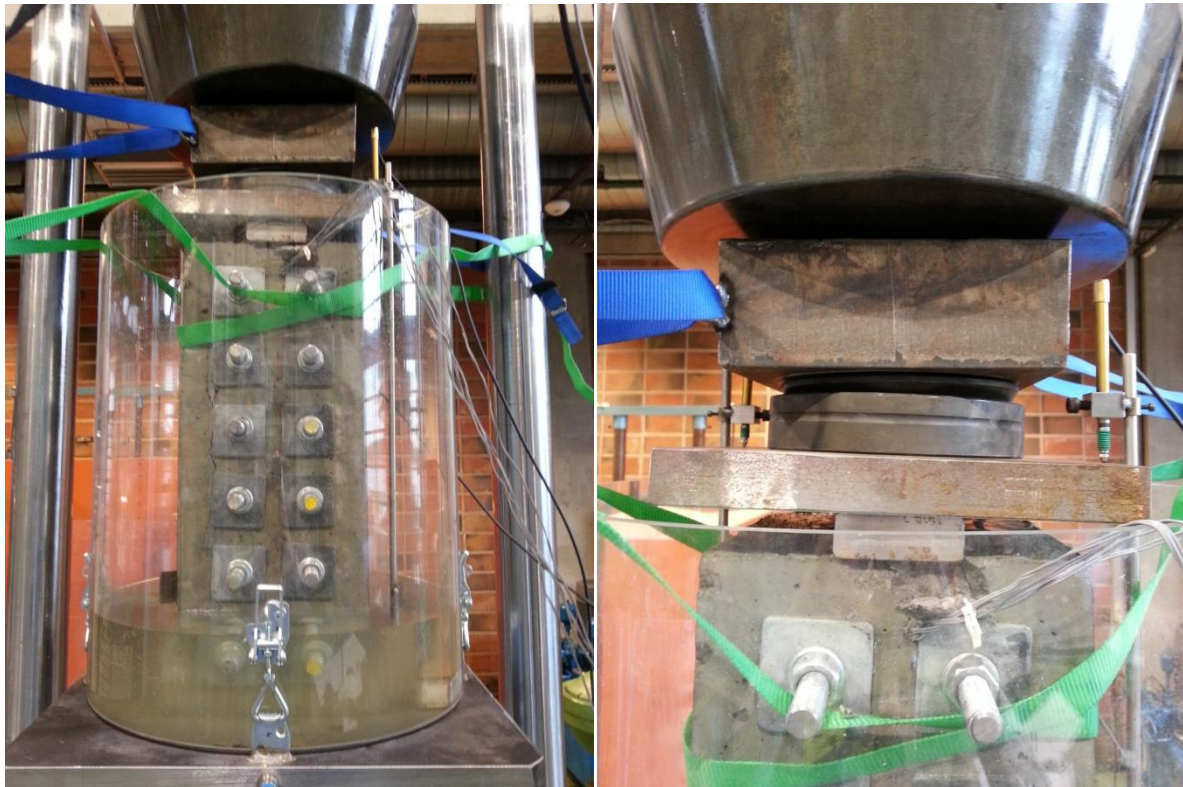


Figure 21 - Rigging of the LVDT's, load transferring plates and spherical bearing

Other equipment used was different steel plates to transfer the load and a spherical bearing. Straps were used as a safety precaution in case the specimens would overturn and fall, as this could have a destructive effect on the hydraulic hoses and other expensive equipment.

4.3 Test cubes

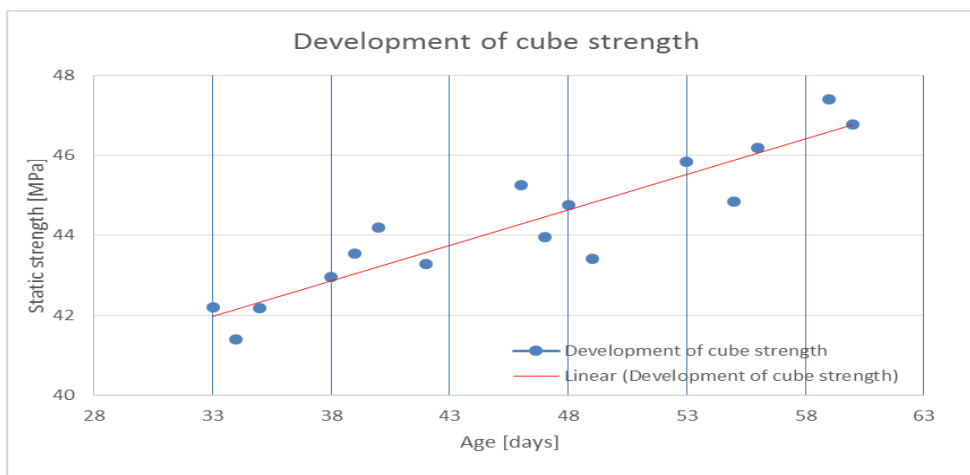


Figure 22 - Development of cube strength

As the concrete will continue to cure and the strength develops, also after 28 days, reference tests were performed before each test. To find the concrete strength at specimen test start three test-cubes were tested and averaged to find approximate concrete strength.

The planned compressive cube strength of the concrete mix was 25 MPa. The cube test³⁵ however, showed a higher strength than planned and was approximately 42 MPa.

4.4. Problems due to higher cube strength than expected

Since the concrete strength was much higher than expected, problems with the reinforcement occurred. The reinforcement was supposed to take care of the transverse tension forces that appear, by this securing a compression failure in the concrete. The reinforcement³⁶ was calculated based on a compressive cube strength of 25 MPa, which require 6 reinforcement bars. Calculations based on 42 MPa however, require 10 reinforcement bars. With this concrete quality, the reinforcement was not sufficient to withstand the transverse tension forces. Since the reinforcement was not able to take care of all the transverse tension forces, the specimen could fail in tension instead of compression. This means that the compressive strength of the concrete might not be fully utilized. The consequence of this was a lower static strength of the specimens than expected from a cube strength of 42MPa.

The capacity of the hydraulic testing machine originally required a cube strength lower than 30 MPa. This is not fulfilled, but will not be a problem due to the insufficient reinforcement.

4.5 Static testing

The first six tests performed were static compression tests, three without reinforcement and three with reinforcement. All the specimens were tested until failure. Failure is defined as the point where the load starts to decrease while the deformation continues to increase.

The load rate for all the static test was 0,4 mm/min, which mean that the hydraulic jack compresses the specimen with 0,4 mm per minute. The data from the tests were sampled with a rate of 5 Hz on all the static tests, which means that the computer logs 5 times per second.

4.6 Dynamic testing

4.6.1 Introduction

A total of 12 specimens were to be tested dynamically, six without reinforcement and three with reinforcement. All the specimens were tested until failure. In the dynamic test, the failure criteria are set as an upper limit of the stroke in the hydraulic jack. At this upper limit, the deformations will increase rapidly and the specimens will not be able to support the load level any more. In practice, the specimens collapses. The maximum and minimum loads to be used in the dynamic testing were calculated from the results of the static testing.

³⁵ Appendix A5

³⁶ Appendix A1

4.6.2 Preliminary calculations

4.6.2.1 Load levels

As the test program should simulate the behavior of a wind turbine fundament, the specimen should constantly be under compression. To simulate the wind loading to the wind turbine fundament a sinusoidal load were applied on the dynamic testes. To be able to plot the results in a Wöhler-curve, a minimum of two load levels is needed. Therefore the specimens are tested both in short term and long term. In short term a higher percentage of the averaged static load capacity is used and therefore a shorter fatigue life expected. The long term is then the opposite, lower level of static capacity and therefore most likely longer fatigue life. In both short term and long term the minimum load level were set to 10% of average static capacity to ensure that the specimens were exposed to constant compression.

Worth mentioning in context of the load levels is the cube-strength development between the static tests and each individual dynamic test. As the dynamic specimens will have an increased static strength compared to the static tests the “actual” load level will be a bit lower than calculated. In this thesis the load levels are set from the static capacity, for practical reasons.

4.6.2.2 Calculation of load levels

Which percentage of the averaged static load capacity to set as the maximum load level were calculated according to different design codes³⁷ and with experiences from Furnes and Hauges thesis. The aim were to get an appropriate amount of cycles for both short term and long term.

4.6.2.3 Short term reinforced

For the short term a maximum and a minimum load level for the testing where selected. The maximum load level was first set to 0.85 on the short term testing of the first reinforced specimen. This because design calculations combined with previous testing (Furnes & Hauge) would imply an appropriate amount of cycles until failure. However the first reinforced test failed at just 231 cycles. In the second test the maximum load level was set to 0.75. This gave a much longer fatigue life and was used on the remaining two reinforced specimens that were short term tested.

Since the first test were totally crushed by the jack when it failed, a stroke limit was set from start on the remaining dynamic tests. The limit was set to 10 mm at first, but later downscaled on the remaining test as the results indicated that a lower limit could be set. Besides the stoke limit a maximum and minimum load limit were set. These limits were respectively approximately 25kN above maximum load and 25kN below minimum load. This to prevent for instance when the specimen yields that the hydraulic jack stops when a load below the minimum limit occurs.

³⁷ See appendix A6 & A7 for the calculations of amount of cycles at different load levels

According to the DNV design code a sinusoidal load with maximum load on 85% and minimum load on 10% of static strength should give 46 cycles until failure. Aas-Jacobsen’s formula proposed 317 cycles, but it’s not applicable for load ratios above 80% of static strength. Holmen’s formula gave an estimate of 112 cycles. As seen the test result gave a bit higher amount of cycles than the valid formulas. This because the design codes should be on the conservative side, so a result that indicates this is good. Worth to mention is that the DNV formula is the only which takes water into account³⁸.

According to the DNV design code a sinusoidal load with maximum load on 75% and minimum load on 10% of static strength should give 599 cycles until failure. Aas-Jacobsen’s formula suggested 15000 cycles, and Holmen’s formula estimated 2630 cycles.

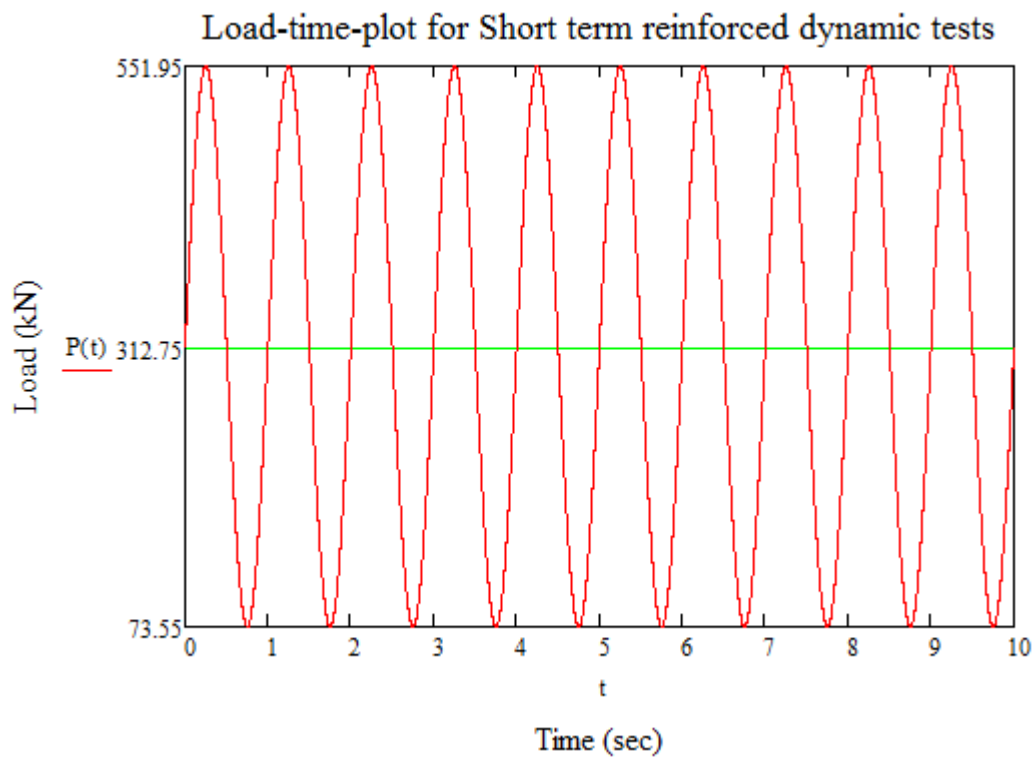


Figure 23 - The sinusoidal load for short term reinforced tests with a maximum load level of 75% for an excerpt of 10 seconds

³⁸ Section 2.2.2.2 “Environmental effect”

4.6.2.4 Short term unreinforced

For all the unreinforced specimens there were no previous results which could indicate appropriate load level. Therefore the load level was set to the same as for the reinforced specimens, 75% of static strength as maximum and 10% as minimum.

The stroke limit were first set to 7mm but later downscaled to 5mm. The maximum and minimum load limit were set to 25kN above maximum load and 25kN below minimum load

According to the formulas the number of cycles until failure should be the same for the concrete in short term reinforced and short term unreinforced, as the fatigue life of concrete and reinforcement should be calculated independently of each other.

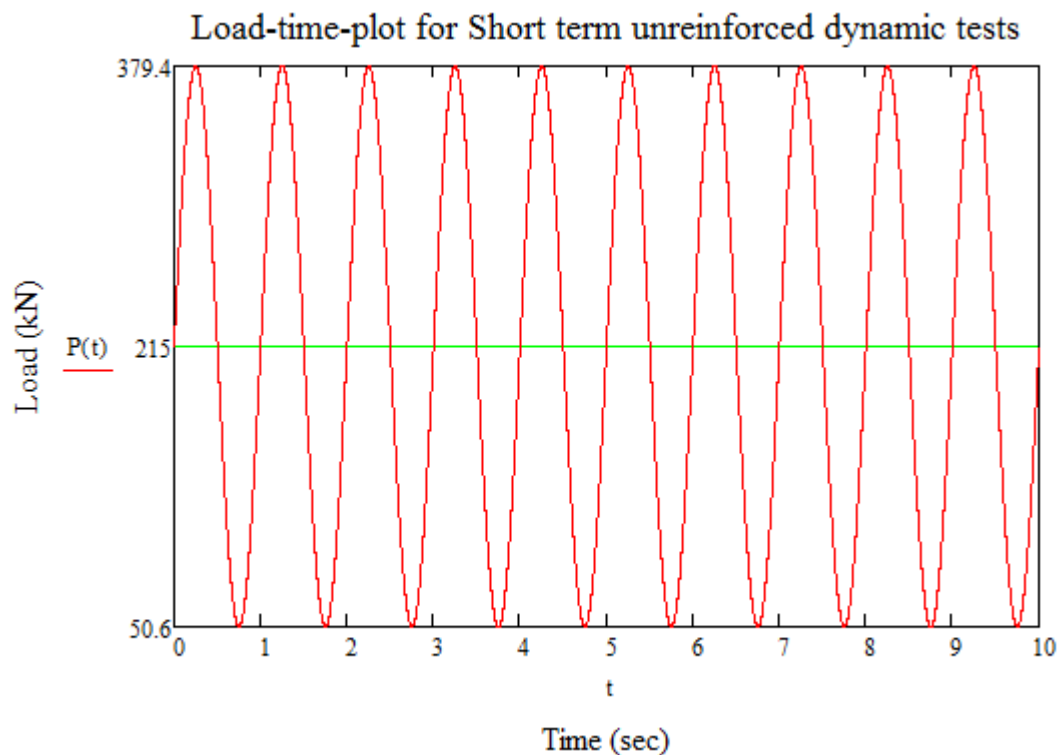


Figure 24 - The sinusoidal load for short term unreinforced tests with a maximum load level of 75% for an excerpt of 10 seconds.

4.6.2.5 Long term reinforced

To get a longer fatigue life than for the short term, the maximum load was set to 65% of static strength. The stroke and max/min limits were set to be the same as in the short term tests.

According to the DNV design code a sinusoidal load with maximum load on 75% and minimum load on 10% of static strength suggested 7735 cycles until failure. Aas-Jacobsen's formula approximated 690000 cycles, and Holmen's formula gave an estimate of 61380 cycles.

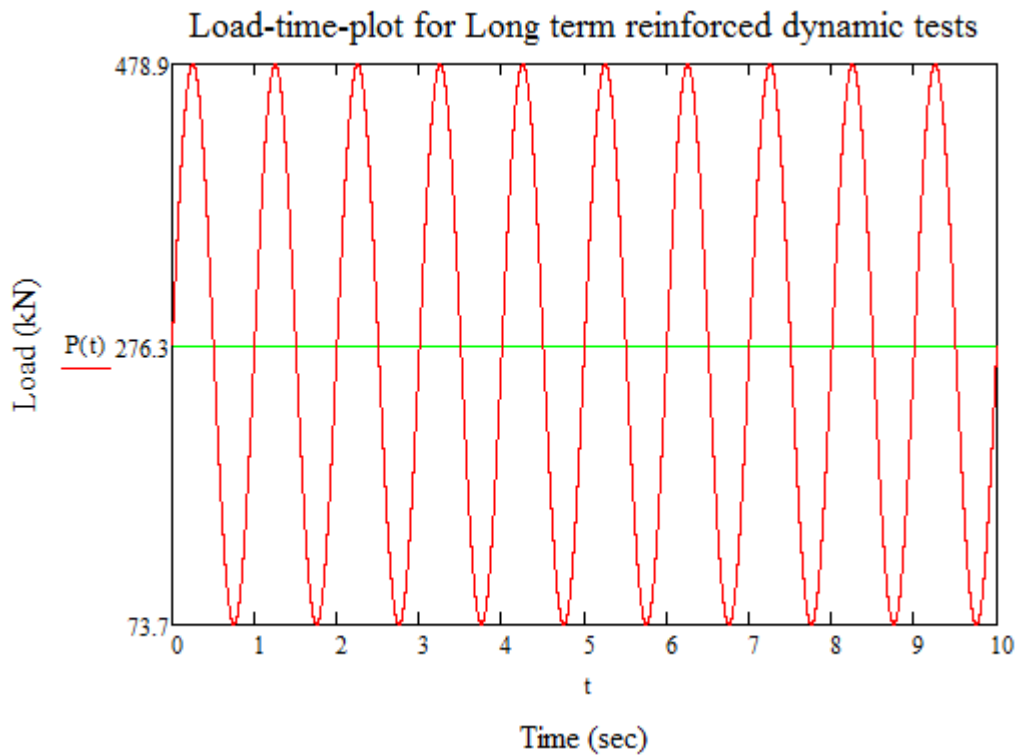


Figure 25 - The sinusoidal load for short term reinforced tests with a maximum load level of 65% for an excerpt of 10 seconds.

4.6.2.6 Long term unreinforced

The maximum and minimum loads were set to respectively 65 and 10% of static strength, and the limits were set to be the same as for the short term unreinforced.

As for the short term tests the number of cycles until failure should be the same as for the reinforced long term tested specimens.

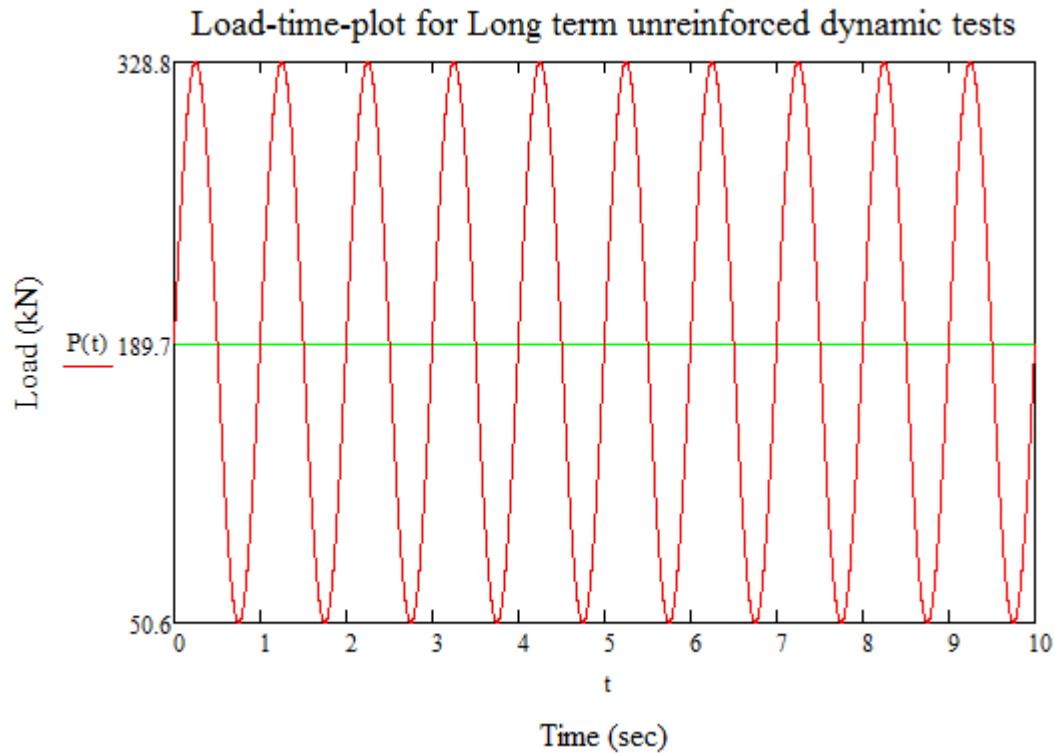


Figure 26 - The sinusoidal load for short term reinforced tests with a maximum load level of 65% for an excerpt of 10 seconds.

4.6.2.7 Pre-cyclic routine

Before the dynamic test there was performed a “dummy” where the specimen was loaded up to P_{max} , stroke data was logged, and then unloaded. This was done so that a reasonable stroke limit could be set for each individual specimen for safety precautions.

After the “dummy” the specimens were loaded up to the middle load (green line in the sinusoidal figures above). This because the hydraulic jack used this as a starting point for the cycles, then varying up to P_{max} (maximum load) and down to P_{min} (minimum load) with a programmed set amplitude.

5. Static test results

5.1 Introduction

The results from the statically tested specimens are presented below.

5.2 Results

5.2.1 Maximal static load at fracture

Maximum static load						
Specimens without splitting reinforcement (specimen number)	Load rate [mm/min]	Maximum load [P_{fail}]	Test duration (to max load)	Test date	Sampling rate (time)	
1	0,4	552,72	11 min 17,4 sec	06.03.14	5 Hz	
2	0,4	460,64	7 min 52 sec	07.03.14	5 Hz	
3	0,4	504,04	8 min 29,2 sec	07.03.14	5 Hz	
Specimens with splitting reinforcement						
4	0,4	753,28	15 min 49,4 sec	07.03.14	5 Hz	
5	0,4	743,36	15 min 42 sec	07.03.14	5 Hz	
6	0,4	713,44	14 min 19 sec	10.03.14	5 Hz	

Without reinforcement, the average static capacity was: 505,8 kN (standard deviation 37,6 kN)

With reinforcement, the average static capacity was: 736,7 kN (standard deviation 16,9 kN)

5.2.2 Capacity of partially loaded areas

NS-EN 1992-1-1 allows an increase in compressive strength due to partially loaded areas. In this situation, the formulations³⁹ allows the compressive strength to be increased by an

amplification factor equal to $\sqrt{\frac{A_{c1}}{A_{c0}}} = \sqrt{\frac{44100}{14700}} = 1.73$

DNV-OS-C502 also takes this partial effect into account in the formulations⁴⁰. However, the allowed increase in this situation is a bit more conservative than the Eurocode, with a

amplification factor equal to $\sqrt[3]{\frac{A_2}{A_1}} = \sqrt[3]{\frac{44100}{14700}} = 1.44$

³⁹ Section 2.4.2.1 "NS-EN-1992-1-1"

⁴⁰ Section 2.4.2.2 " NS 3473 & DNV-OS-C502 (Offshore concrete structures)

Test	Test cubes f_{cm} $= f_{cm,cube}$ $* 0,8$	Compressive strength $F_c = f_{cm} * A_{c0}$	Test result	Factor	Average factor	Comment
1	33,11	486,7 kN	552,72 kN	1,14		Not reinforced
2	33,74	496,0 kN	460,64 kN	0,93	1,03	Not reinforced
3	33,74	496,0 kN	504,04 kN	1,02		Not reinforced
4	33,74	496,0 kN	753,28 kN	1,52		Reinforced
5	33,74	496,0 kN	743,36 kN	1,50	1,48	Reinforced
6	34,36	505,1 kN	713,44 kN	1,41		Reinforced

However, the formulations in both codes require that the transverse tension forces in the top of the specimen are distributed into the reinforcement.

6.7 Partially loaded areas

(1)P For partially loaded areas, local crushing (see below) and transverse tension forces (see 6.5) shall be considered.

This requirement was not satisfied for the three specimens without reinforcement. As expected, these specimens did not show an increase of compressive capacity, with an average factor of 1,03. These unreinforced tests can therefore be seen as a confirmation of the rules in the code.

In the three specimens with reinforcement the transverse tension forces are supposed to be taken care of by the reinforcement. These specimens showed an increased capacity of 1,48 in average. According to DNV design code the allowed increase is 1,44. Even though one of the test dropped a bit below that factor, the partial effect in the DNV design code is documented.

However, the Eurocode allows a amplification factor of 1,73. As seen, our results were way below that factor. The tension reinforcement in our specimens have a lower capacity than the compression capacity of the concrete⁴¹. That means that the transverse tension forces in the top are not fully taken care of, and the specimens breaches before the compression capacity of the concrete was reached.

The theoretical basis for the increase in capacity for partially loaded areas is an effect called tension ring⁴². A tension ring develops in the surrounding concrete and helps keeping the concrete together. A precondition is that the loaded area are surrounded by concrete in all directions, such that the tension ring is not broken. In our case, the loaded area is only surrounded by concrete in two directions. Thereby the tension ring is broken and this part of the code does not seem to be applicable.

⁴¹ See section 4.4 "Problems due to higher cube strength than expected"

⁴² See section 2.4 "Partially loaded areas in concrete"

However, the increased capacity seen in our results indicates a certain partial effect. In 2011 Furnes and Hauge⁴³ conducted similar tests, though not submerged in water, where they concluded that the partial effect in fact was present. Their results showed without any doubt a partial effect higher than NS-EN-1992-1-1 allowed. Compared to their results it is reasonable to assume that this study would get the same results if the reinforcement would have been satisfactory.

By this, one can imagine that the reinforcement somehow creates an effect similar to the tension ring. The stirrups keeps the concrete together the same way as the surrounding concrete were supposed to, creating the partial effect.

5.2.3 Force deformation relation

The stroke data shows the relation between the force and the vertical deformation. Simply explained, the relation shows how much the machine was pressed together as the load increased.

5.2.3.1 Force deformation relation in reinforced specimens

The plot from the 3 static tests with splitting reinforcement is shown below. The stroke (deformation) is here plotted against the load

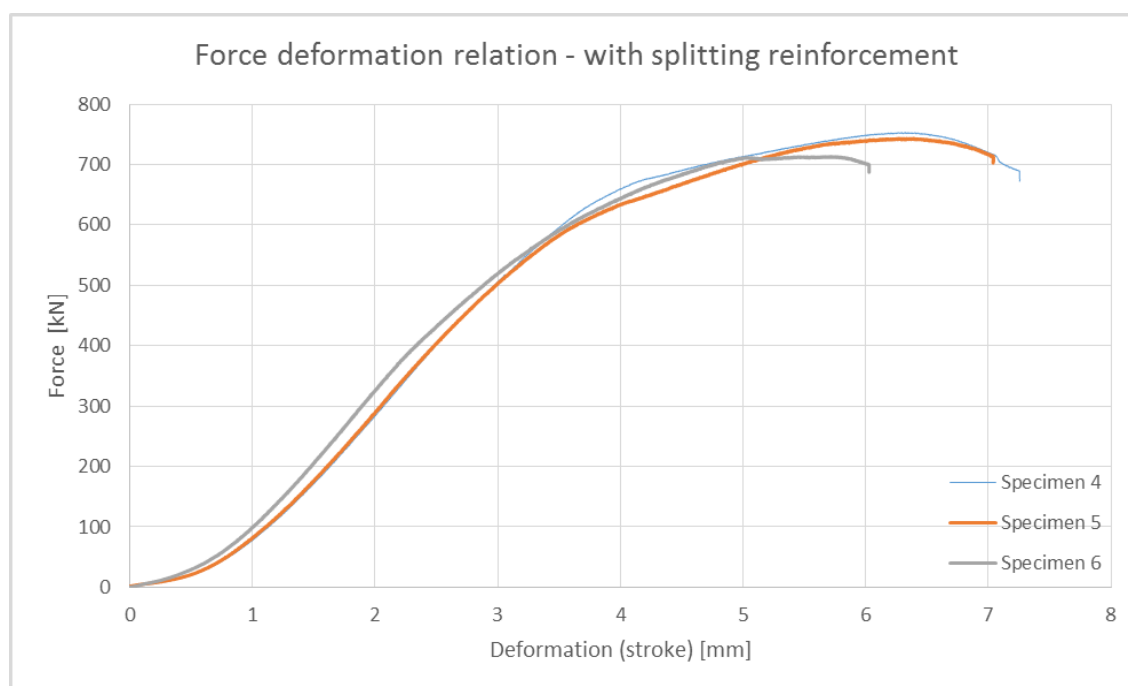


Figure 27 - Force deformation relation - with splitting reinforcement

The three specimens with splitting reinforcement nearly shows the same behaviour. The lifetime of the specimens seems to be divided into three phases. First phase shows a rapid deformation rate up to roughly 100 kN, the second phase up to 600 kN have a slower rate, while deformation rate is rapid in the third and final phase.

⁴³ "Fatigue capacity of partially loaded areas in concrete structures" - Alexander Furnes and Ole Martin Hauge

When the tests were performed the resulting graphs contained the stroke from the machine and the equipment. That means that the force deformation relation is not exactly correct. To find the exact force deformation relation the stroke from the machine and equipment had to be taken into account.

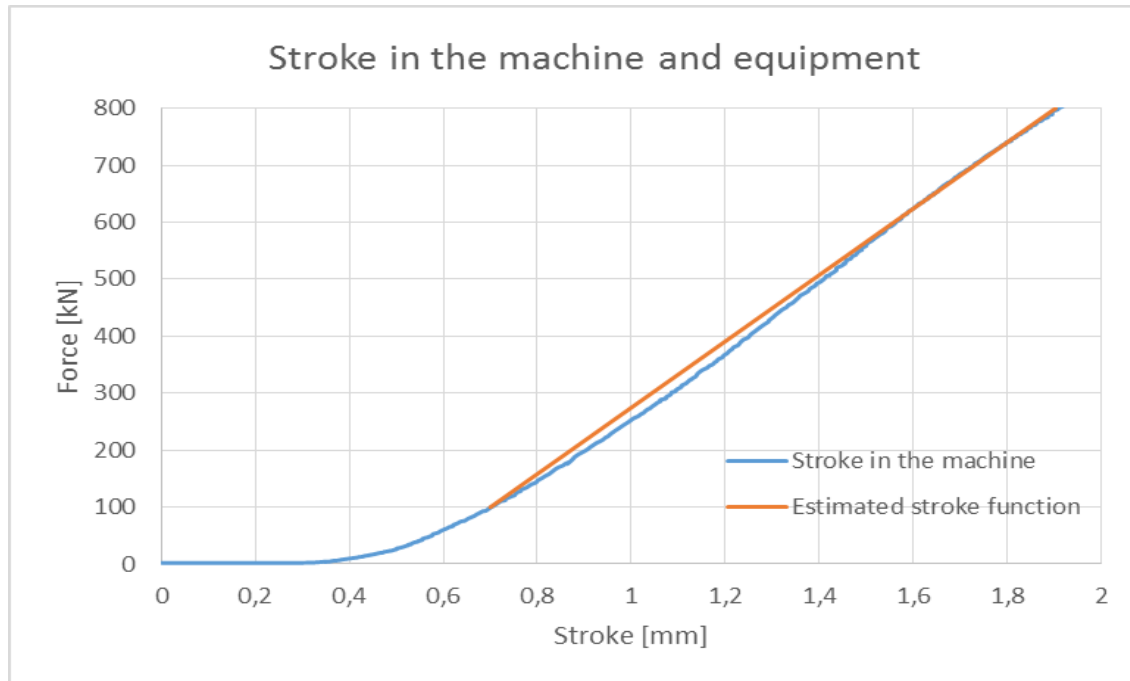


Figure 28 - Stroke in the machine and equipment

A test of the stroke in the machine and equipment was therefore performed. A steel plate was placed in the machine, and a load range from 0 kN to 800 kN was applied. The plot above show the result from this test. As seen, the graph is close to linear from 100 kN up to 800 kN. The orange line is an estimated linear stroke function, which simplified the calculations of the modified stroke plot.

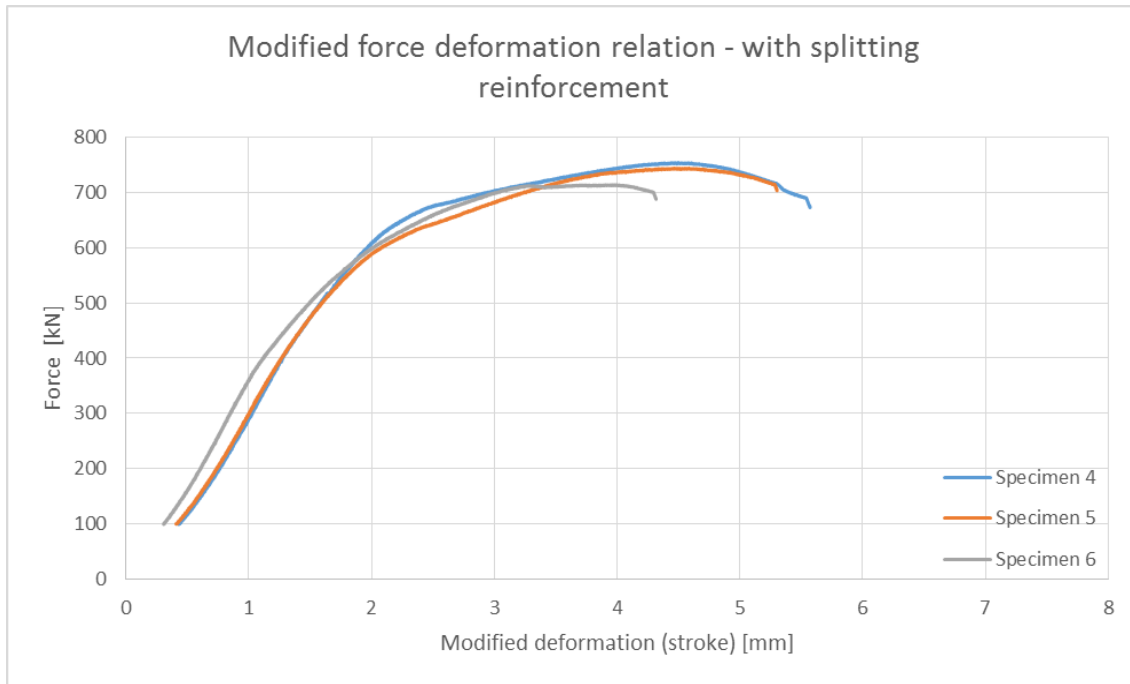


Figure 29 - Modified force deformation relation - with splitting reinforcement

The graph above shows the modified stroke plot of the reinforced specimens. The values from the stroke of the machine was subtracted from the original stroke curve to create the modified stroke. The linear part of the machine stroke started at 100 kN. Because of that the modified force deformation relation is only applicable at values above 100 kN.

5.2.3.2 Force deformation relation in unreinforced specimens

The plot from the 3 static tests without splitting reinforcement is shown below.

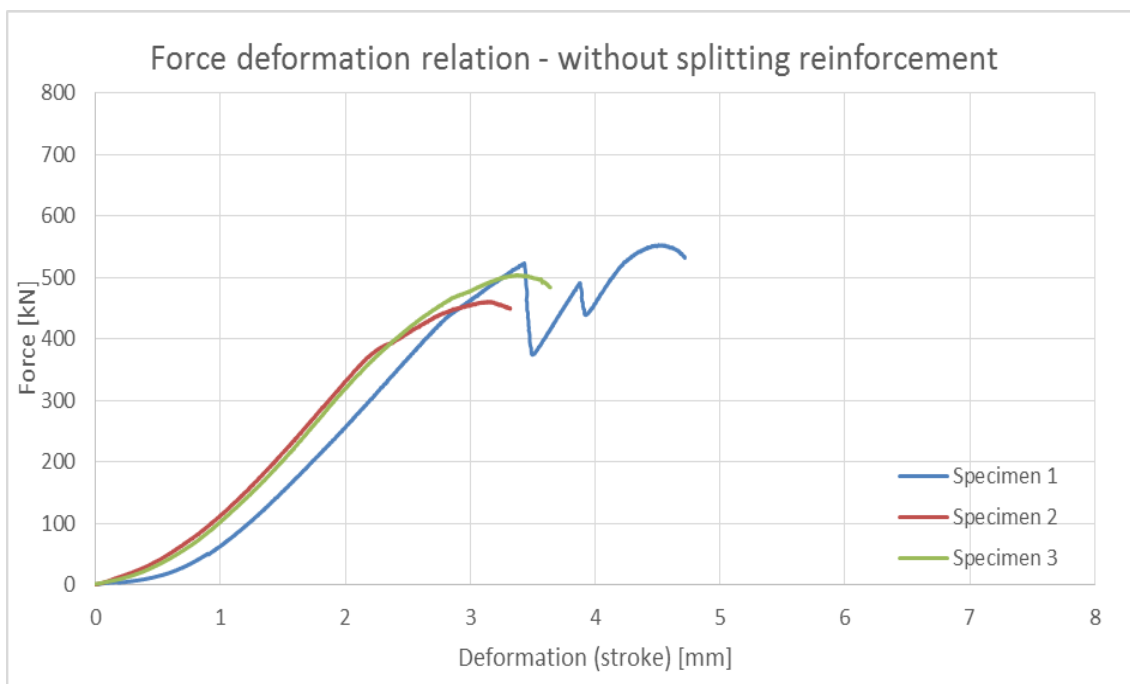


Figure 30 - Force deformation relation - without splitting reinforcement

The three specimens without splitting reinforcement also show some of the same behaviour, but also some differences. The unreinforced specimens have a three-phased life, like the reinforced specimens. The first phase is rapid, the second is slow, while the third have a rapid deformation. The difference from the reinforced specimens is the duration of the second and third phase, which is much shorter. Specimen 1 stood out because it experienced a “load dump” in the final phase.

While comparing the results from the reinforced and the unreinforced specimens, one can see that the splitting reinforcement obviously improves the strength, but also the ductility of the specimen.

As for the specimens with splitting reinforcement, the force deformation relation had to be modified. The plot below shows the modified deformation relation for the specimens without splitting reinforcement.

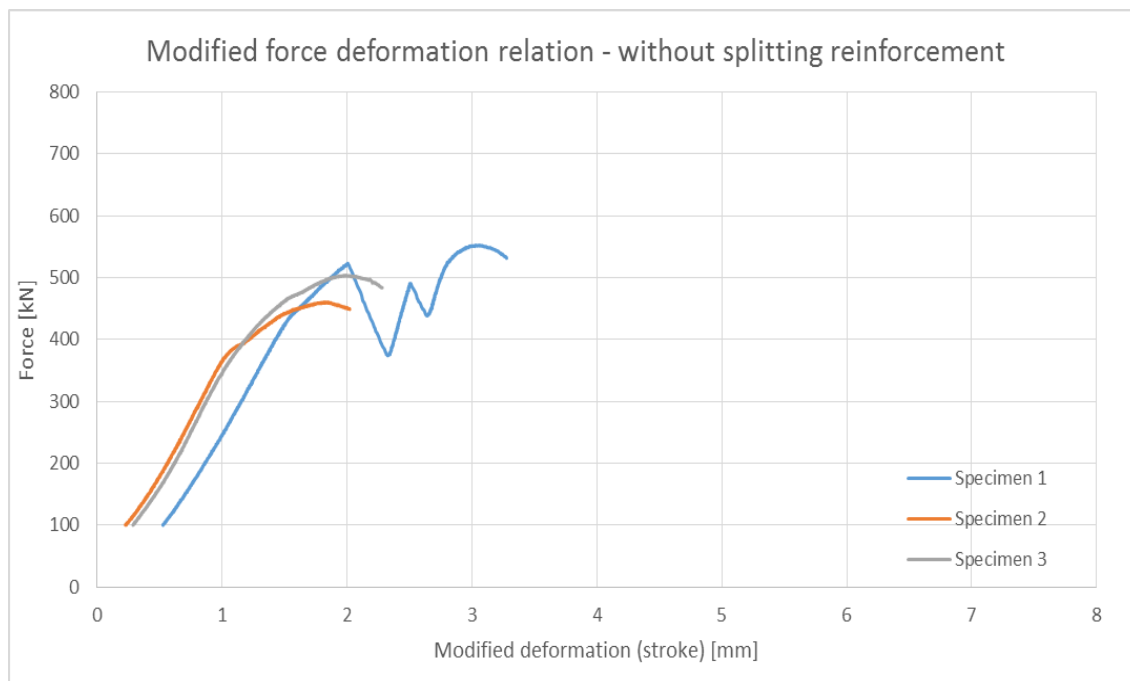


Figure 31 - Modified force deformation relation - without splitting reinforcement

5.2.4 Force strain relation in concrete

Based on the modified stroke plot, it was possible to calculate the vertical strain in the concrete specimens. As for the force deformation plots, the graph starts at 100 kN and ends short after the load peak. The vertical strain in the specimens with splitting reinforcement is plotted below. The strain is given as $[\mu\text{m}/\text{m}]$ for practical purposes.

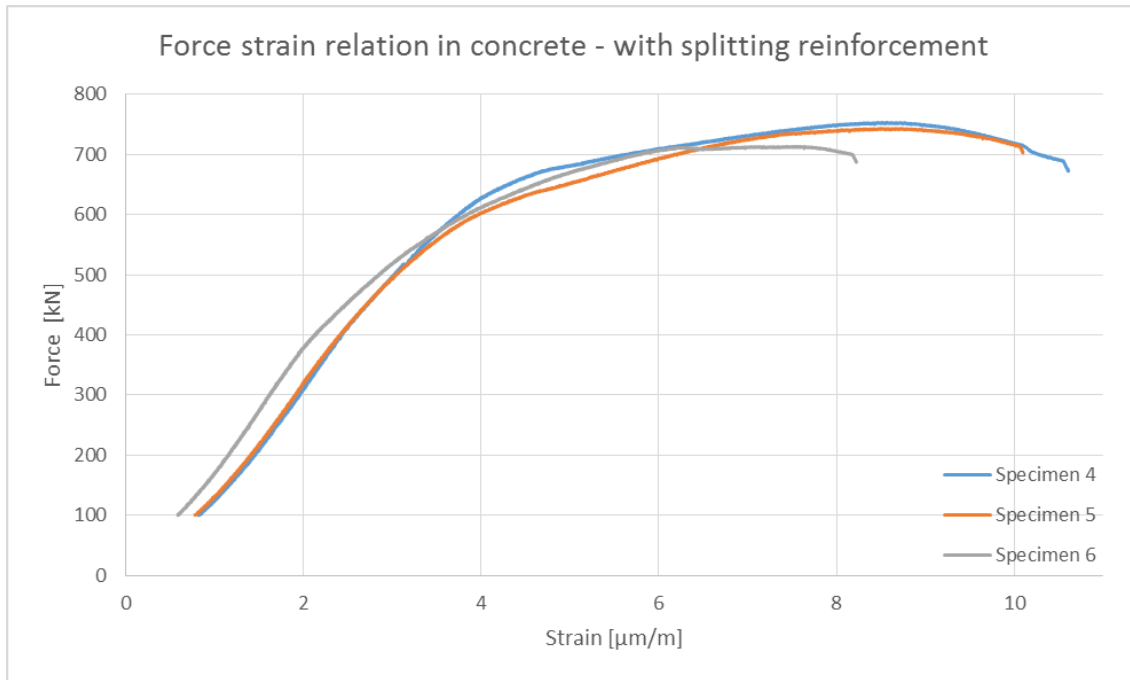


Figure 32 - Force strain relation in concrete - with splitting reinforcement

All three graphs above show similar behaviour with increasing strain rate after 600 kN. Specimen 6 differs from the two other tests with a lower strain at failure. At the end, the strain in the concrete is very high, and the reinforcement carries most of the load.

The vertical strain in the specimens without splitting reinforcement is plotted below.

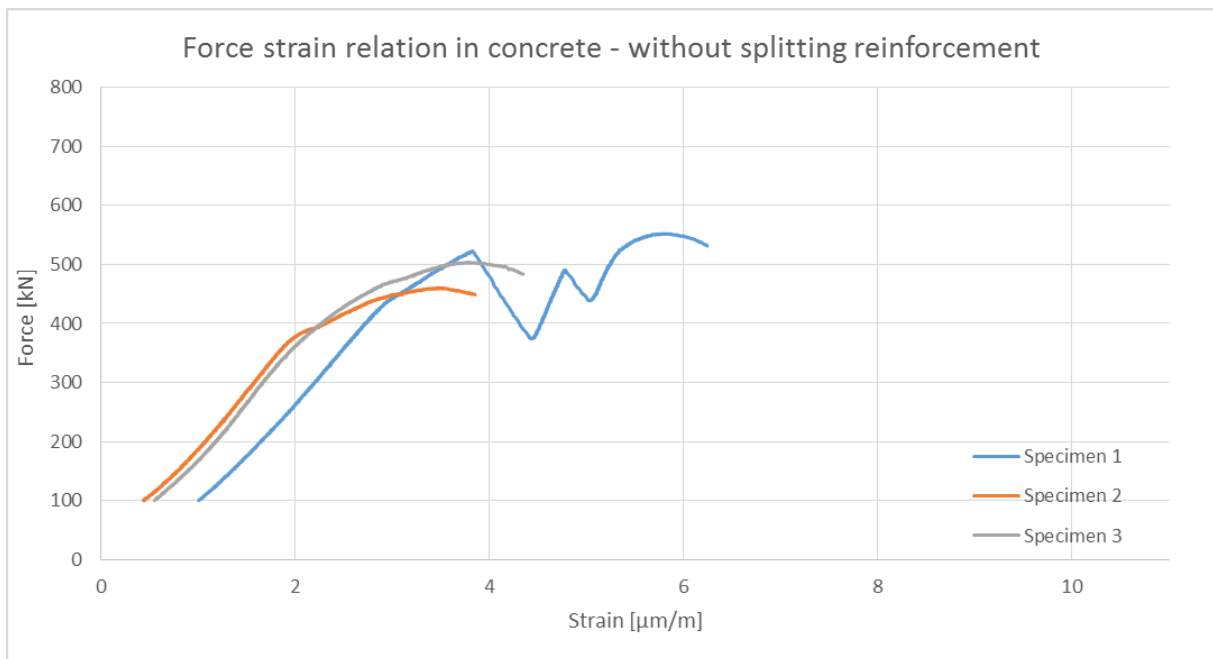


Figure 33 - Force strain relation in concrete - without splitting reinforcement

As for the reinforced specimens, the three graphs show similar behaviour. Specimen 1 differs at the end because of the load lump it experienced. Up to around 500 kN the 3 specimens

are similar to the reinforced specimens. But while the unreinforced specimens are failing, the reinforced specimens experience an increasing load and increasing strain, due to reinforcement carrying most of the load.

5.2.5 Strain in reinforced tests

As seen in the graphs below, the strain in the reinforcement was fairly constant until a load of around 380 kN, which is 78% of the capacity for the unreinforced specimens. After this, the reinforcement was activated. The load was further carried by the reinforcement until the yielding capacity of the steel was reached. The steel in the upper split yielded at around 2500 $\mu\text{m}/\text{m}$. Specimen 6 differed from the two others by yielding earlier at 1500 $\mu\text{m}/\text{m}$. By assuming the modulus of elasticity in the reinforcement to be 200 000MPa, the theoretical yield strain was calculated as 2500 $\mu\text{m}/\text{m}$ while the yield stress was 500MPa.

Strain 1 at the lower stirrup showed three different behaviours. Specimen 6 acted as expected and specimen 5 did not experience much strain, while specimen 4 had a behaviour somewhere between the others. Strain 1 do not give any unambiguous conclusions, due to the big variances between the three specimens. Strain 2 at the lower split showed similar behaviour in the 3 specimens. However, it is worth mentioning that specimen 4 experienced lower strains than the other two. Strain 3 at the upper split experienced almost the exact same behaviour in the three specimens. A constant increase in strains from around 380 kN until yielding.

The threaded bars were installed to secure zero horizontal deformation in the direction parallel to the line-load. The load was expected to spread in the perpendicular direction. As seen, the strains in the threaded bars were not zero, which means that the specimen was not fully restraint in that direction. However, the strains were lower than the yield strain, giving a confining effect. Specimen number 4 differed from the two others, but ended up at roughly the same strain. The strain at the end was between 1100 and 1700 $\mu\text{m}/\text{m}$.

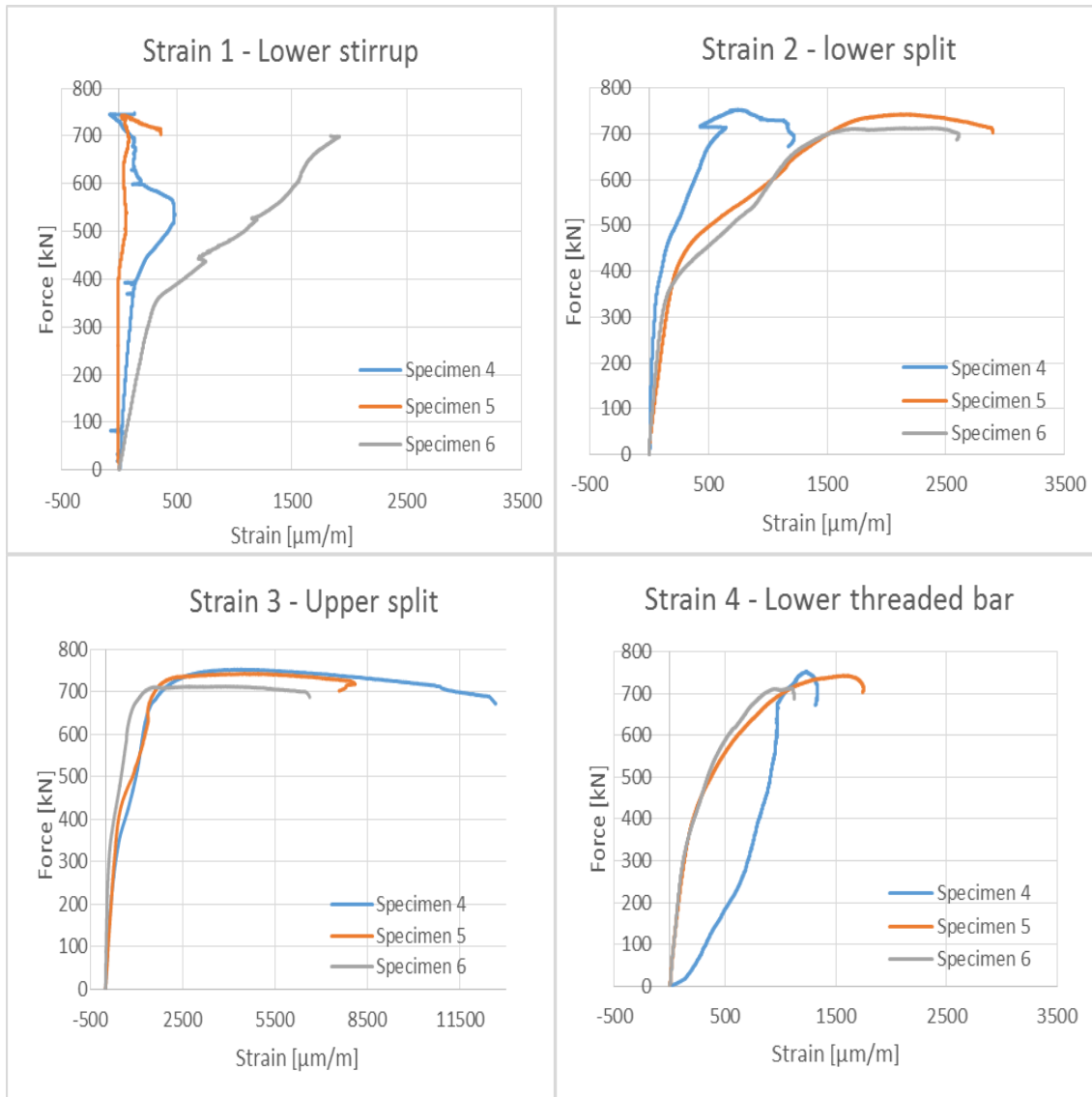


Figure 34 - Strain in reinforcement (NB! Strain 3 illustrated using larger strain values)

As seen below, the strains in the lower layer were activated earlier than the strains in the upper split. This was expected, due to the theory of stress fields under concentrated loads, as mentioned earlier⁴⁴. The distribution of transverse stresses shows compressive stresses close to the top, while tensile bursting stresses in lower part.

As for strain vs force, strain 1 do not give any certain tendency. Each of strain 2-4 have the same tendency in the 3 specimens. Slow strain rate in the start, then a sudden change to rapid strain rate.

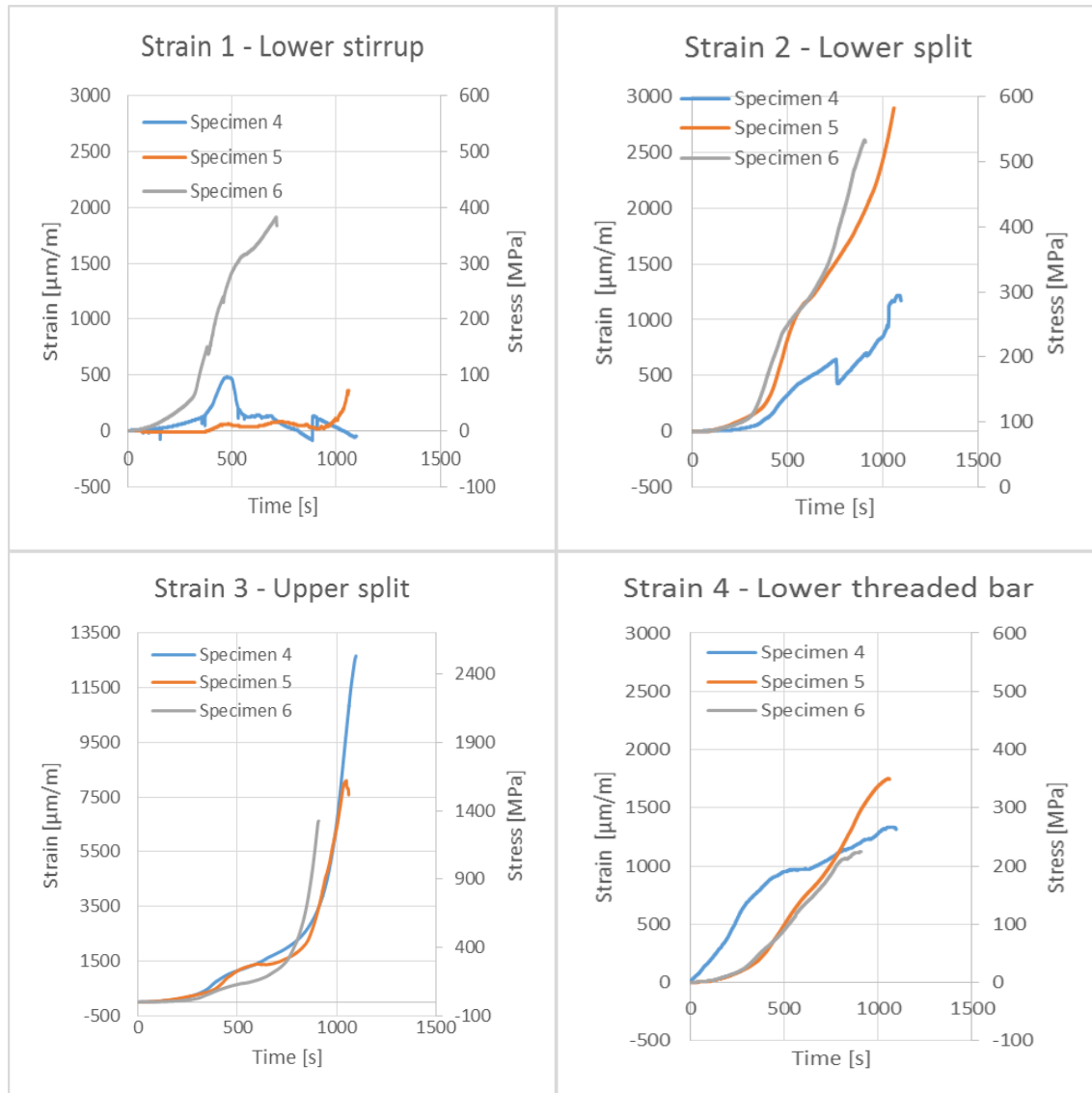


Figure 35 - Strain in reinforcement vs time (NB! Strain 3 illustrated using larger strain values)

⁴⁴ See section 2.4.2.1 “NS-EN-1992-1-1”

5.2.6 Strain in unreinforced tests

In the unreinforced tests, there were only strain gauges at two of the threaded bars. These were used to control horizontal deformation parallel to the line-load. As illustrated below, the strain in both lower and upper threaded bar are fairly low. It is therefore reasonable to assume that the threaded bars worked to its purpose.

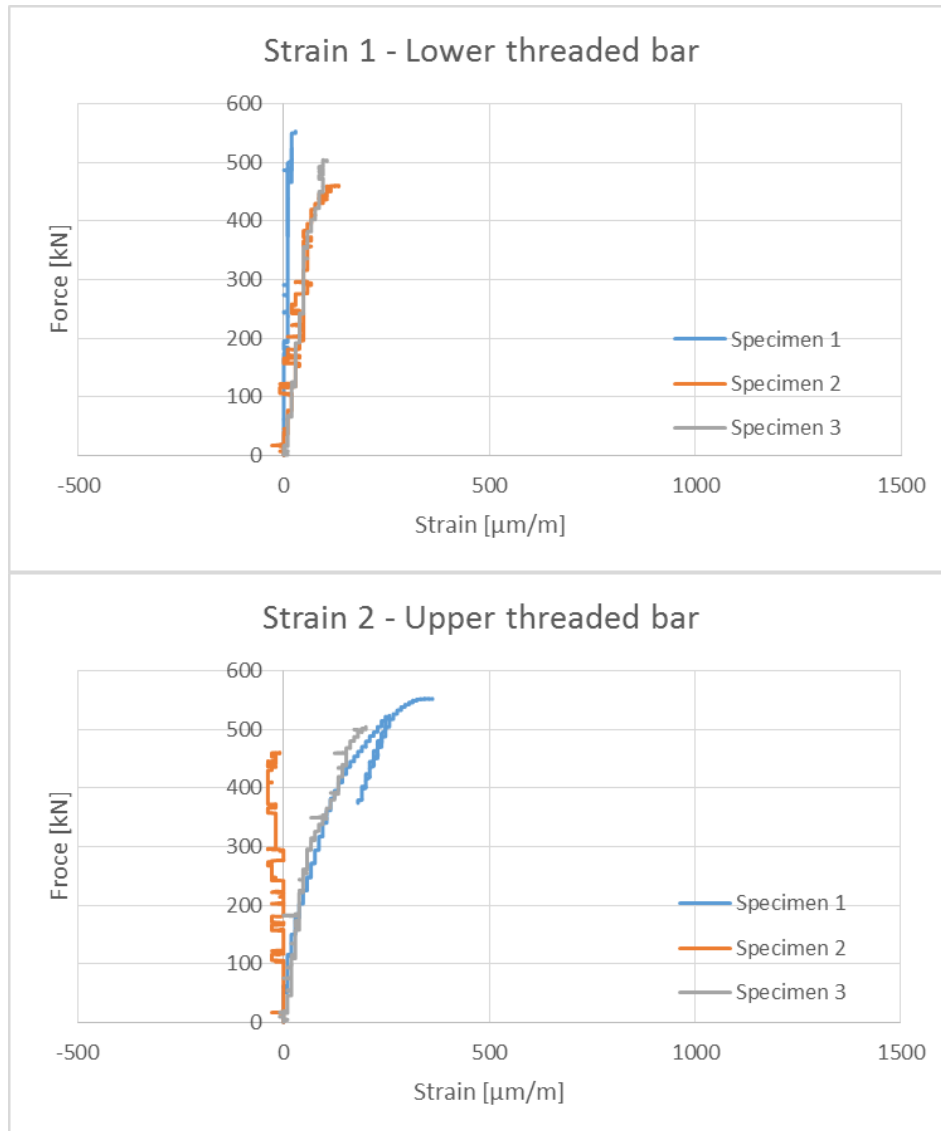


Figure 36 - Strain in threaded bars in unreinforced specimens

5.2.7 Crack patterns in static tests

The six static test showed the same tendency in crack propagation. All of the specimens had a first phase with local crushing at the top, due to uneven surface. Next, parts of the cover concrete at the edge of the load area started to fall off, as showed below.



Figure 37 – Spalling of cover concrete

The first real cracks started to develop around the second layer of threaded bars at approximately 70% of failure load, as vertical cracks. For partially loaded specimens, the area for the load distribution increases below the loaded surface. This means that the horizontal tension forces increases from the top and down. The fact that the cracks started in a distance from the top can therefore be seen as logical.



Figure 38 - First critical cracks

After the first cracks started to develop, the crack propagation increased. The initial cracks became longer and wider, while new vertical cracks occurred in the middle of the specimen. At the end, the initial cracks had developed, in an angle, to the corner of the loaded plate at the top and to the side below the initiation. The width of the crack differed in each test. That was due to when the test was manually stopped. The test was practically finished when the applied load decreased while deformation continued increasing, but some of the tests were not stopped exactly at the peak load. After the peak load, the crack width grew faster, hence the variation.

Even though the reinforced and unreinforced specimens had similar tendency and behaviour, there were one main difference. Below one can see a reinforced specimen on the left and an unreinforced specimen on the right. The reinforced specimens have its main crack outside of the threaded bars and outside of the reinforcement. In the unreinforced specimens the crack was allowed to develop in the middle of the specimen, and inside of the two top layers of threaded bars. At the third layer the cracks went outwards because the unreinforced specimens had stirrups in that area. The reinforcement held the specimen together and secured no crucial crack development inside the reinforced area.

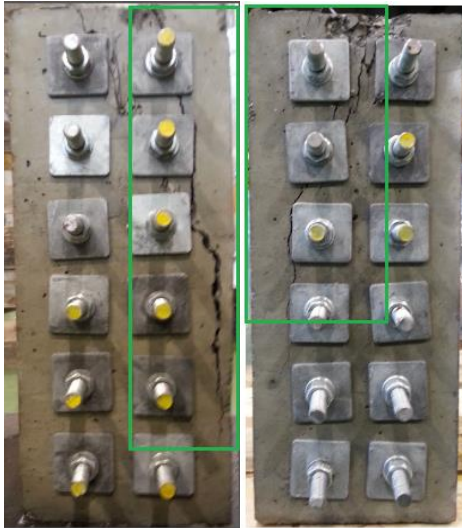


Figure 39 - Critical cracks in reinforced (left) and unreinforced (right) specimens

At the top of the specimens the loaded plate was pushed a couple of millimeters into the concrete, by crushing the top.



Figure 40 - Crushing of the top in static specimens

The crack patterns at failure for each individual test are illustrated in the appendix⁴⁵

⁴⁵ See appendix A10

6. Dynamic test results

6.1 Introduction

In this section the dynamic test results will be presented, analysed and discussed. A total of 12 dynamic tests were conducted, 6 with reinforcement and 6 without. In both cases long and short term tests were performed.

6.2 Results

Dynamic test results							
Specimen	Max dynamic load [kN]	Min dynamic load [kN]	Cycles until failure	Stroke [mm]	LVDT [mm]	Load level	Average cylinder strength [N/mm ²]
7	379,4	50,6	2872	3,7	2,4	0,75/0,10	35,2
8	379,4	50,6	7099	3,2	2,4	0,75/0,10	35,8
9	379,4	50,6	2595	3,3	2,5	0,75/0,10	34,7
10	328,8	50,6	21675	3,5	-	0,65/0,10	36,7
11	328,8	50,6	7821	4,7	3,2	0,65/0,10	35,9
12	328,8	50,6	46407	3,7	2,9	0,65/0,10	35,9
13	625,5	73,6	231	5,8	-	0,85/0,10	34,8
14	551,9	73,6	4749	4,0	4,0	0,75/0,10	34,6
15	551,9	73,6	5023	7,6	6,0	0,75/0,10	36,2
16	478,9	73,6	40523	5,7	-	0,65/0,10	37,0
17	478,9	73,6	26040	7,7	6,7	0,65/0,10	37,9
18	478,9	73,6	61854	7,5	6,4	0,65/0,10	37,4

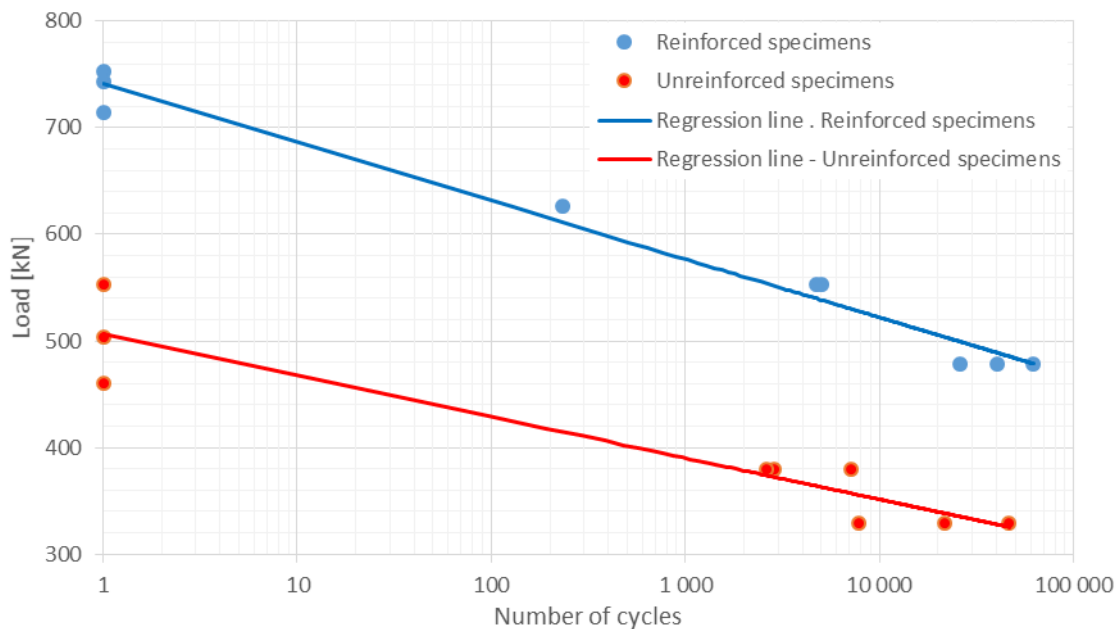


Figure 41 - Load vs number or cycles

Type of specimen	Average amount of cycles	Standard deviation	Average stroke [mm]	Standard deviation
Reinforced short-term	4886 *	137*	5,80*	1,800*
Reinforced long-term	42806	14710	6,97	0,899
Unreinforced short-term	4189	2061	3,40	0,216
Unreinforced long-term	25301	15960	3,97	0,525

*only specimens tested at load level at 75 %, not the one at 85 %.

As shown in the tables above the reinforced short term tests had similar results. Though the average and the standard deviation only is taken from the two specimens tested at 75% of static capacity. Two specimens is nevertheless too few to be able to give a good statistical basis. If more specimens had been tested the possibility of a more scattered results is present, causing a higher standard deviation. To have a sufficient statistical basis a minimum of three reinforced short-term specimens should have been tested, preferably even more. Unfortunately this was not possible as the load rate on specimen 13 was set to high.

Both on the reinforced long term and the unreinforced long term tests the result were more scattered than on the short term. This was as expected as previous research has indicated that low load levels gives a bigger scatter⁴⁶, and has its logical explanation in that for each added cycle the uncertainty rises.

The unreinforced reinforced short-term test gave very deviating results. Two of the specimens had very similar results, but one of the specimens deviated with almost three times as many cycles as the two other (2872 and 2595 vs. 7099). This results underlines the big uncertainty in predicting fatigue life.

Since some of the LVDT results were not properly logged, the statistics regarding deformation in the table above are based on the stroke results.

As mentioned only two specimen were tested on reinforced short-term at a load level of 75% (specimen 14 & 15). The average stroke on the reinforced short term tests should of the same reason as for the cycles had one or more specimens tested to have a good statistical basis. An additional factor which also interrupt the average stroke and the standard deviation on the reinforced short-term is the fact that the pre-cyclic dummy preformed before each test were not properly logged. The outcome of this were that specimen 14 have an artificial low deformation. If the dummy had been properly logged the total stroke on the specimen would have been higher, causing the average stroke to increase and the standard deviation to decrease.

From the results the differences between the reinforced and unreinforced specimen can be seen. The reinforced specimens allows more deformation than the unreinforced. Less deformation allowed will contribute to have a low standard deviation as the more deformation the bigger the uncertainty becomes. Another observation is that it seems that

⁴⁶ Please see section 2.2.2.1 "Historical perspective"

the deformation at failure is independent of amount of cycles and load level for the two types of specimen.

6.2.1 Wöhler-diagram

The regression line analysis in this chapter were performed using logarithmic trend lines in Excel.

6.2.1.1 Results compared to DNV design code

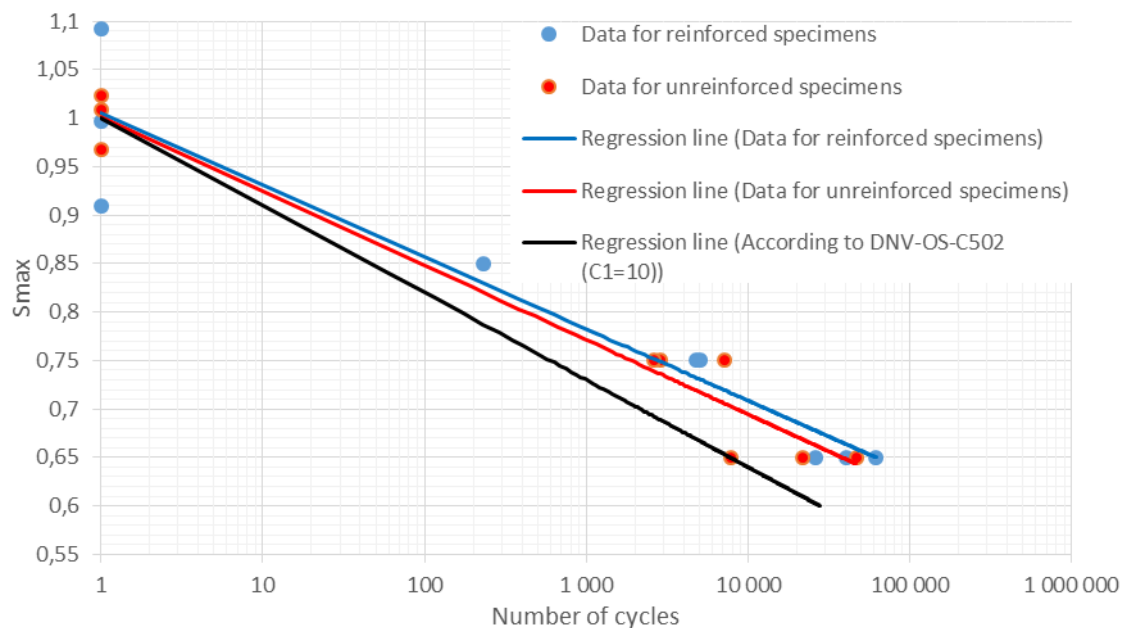


Figure 42 – Results compared to DNV-OS-C502

The Wöhler diagram above shows a comparison between our test results and the theoretical values according to DNV design code, presented with respect to maximum load levels. The black line represent the regression line achieved according to DNV-OS-C502, with C1 equal to 10. The formulations are presented below.

$$\log_{10} N = C_1 \frac{\left(1 - \frac{\sigma_{max}}{C_s \cdot f_{rd}}\right)}{\left(1 - \frac{\sigma_{min}}{C_s \cdot f_{rd}}\right)}$$

The factor C₁ shall be taken as:

- 12.0 for structures in air
- 10.0 for structures in water for those stress-blocks having stress variation in the compression-compression range
- 8.0 for structures in water for those stress-blocks having stress variation in the compression-tension range.

The blue data points shows the results for reinforced specimens, with a corresponding logarithmic line. The red data points show test results for unreinforced specimens, with its corresponding logarithmic line.

As illustrated, if the regression lines are considered the DNV design code is generally conservative enough. Both the reinforced and the unreinforced specimens endured more cycles than the calculated number in the design code. Nevertheless, one data point from an unreinforced test (specimen 11) challenges the DNV design code, as it is really close to the

code (only 86 cycles over the code). Despite specimen 11, the results indicate that the factor C1=10 is conservative enough for fatigue in concrete submerged in water. However, with these results, it might be useful to do further testing to get more statistically satisfactory results.

The difference in fatigue life between reinforced and unreinforced specimen is relatively small, but it is notable. For the same load level, the reinforced specimens seems to endure a few extra cycles compared to the unreinforced specimens. The reason for the extra strength might be the confining effect from the reinforcement, which gives the concrete some extra cycles before failure. However, as further explained in section 6.4, the crack pattern occurred outside the reinforcement. Thus the reinforcement was not activated and did not fully contribute in the fatigue life of reinforced specimens.

6.2.1.2 C1-factor

Generally, the results showed that the rules in DNV-OS-C503 are rather conservative. All tests, but one, gave much better results than the code would estimate with the C1-factor equal to 10. The exception was specimen 11, which was fairly close to the estimate from DNV, based on the formulation below.

$$\log_{10} N = C_1 \left(\frac{1 - \frac{\sigma_{max}}{C_s \cdot f_{rd}}}{1 - \frac{\sigma_{min}}{C_s \cdot f_{rd}}} \right)$$

The factor C₁ shall be taken as:
 12.0 for structures in air
 10.0 for structures in water for those stress-blocks having stress variation in the compression-compression range
 8.0 for structures in water for those stress-blocks having stress variation in the compression-tension range.

An interesting aspect was to see if it is possible to suggest an increase of the C1 factor for structures in water based on this study.

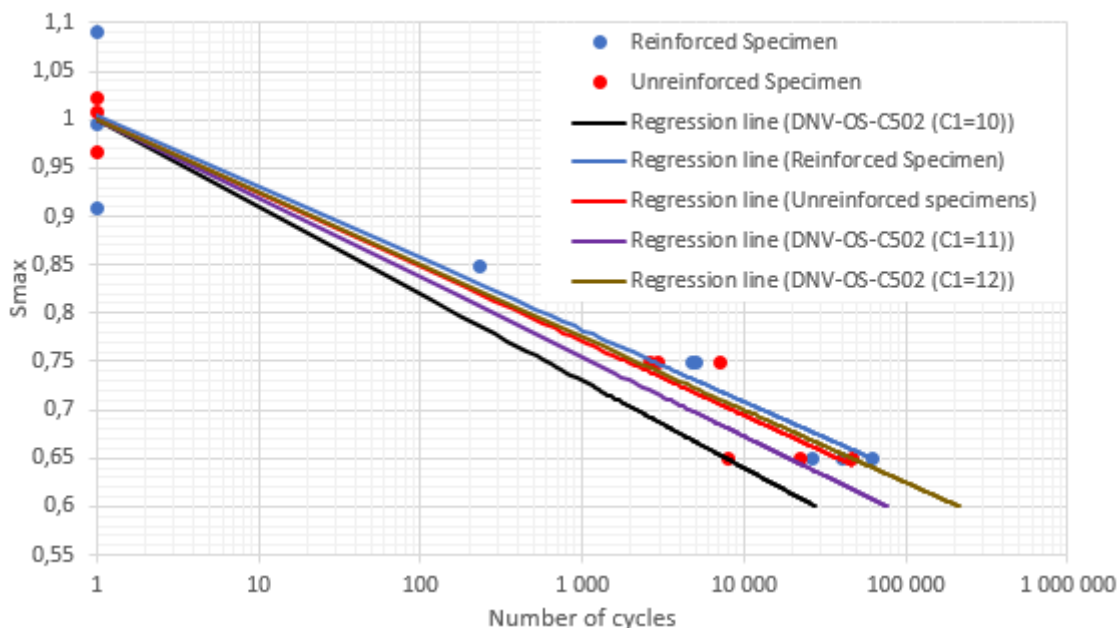


Figure 43 - Results compared to DNV-OS-C502 with different C1-factors

In the graph above the results from the reinforced tests and unreinforced tests are plotted as blue and red lines, respectively. The last three lines are DNV estimates with C1 equal to 10, 11 and 12. As seen, the black line which represents the existing design rules with C1=10, is conservative enough for all the results. The design rules are challenged by specimen 11, but is still conservative.

The brown line represents a proposed C1=12. This gives a line that better fits the regression lines for the experimental results, but in general C1=12 must be seen as too liberal. Several of the results drops below the brown line. A proposed C1= 11 is plotted as the purple line, which is adequate for all but one result. This could in many ways be considered as an appropriate C1. In design codes however, the rules must be conservative enough such that no single result will challenge the rules, in which specimen 11 does.

Because of that an increased C1 does not seem to be possible for concrete specimens submerged in water. However, with one specimen deviating from the rest, it might be useful to do further testing to get more statistically satisfactory results.

6.2.1.3 Wet/dry comparison

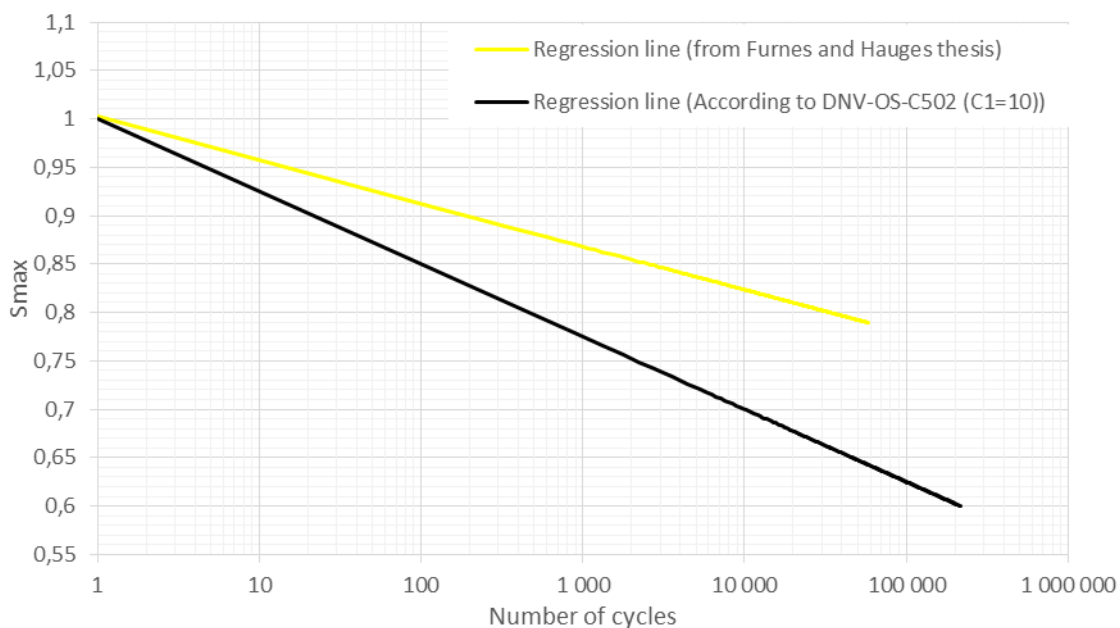


Figure 44 - Results from Furnes and Hauges thesis compared to DNV-OS-C502 (C1=10)

In 2011 Furnes and Hauge performed fatigue testing on dry specimens exposed to air. The graph shown above is a comparison between the data achieved by Hauge and Furnes, and the data points calculated according to DNV-OS-C502, fatigue of concrete in air. The results from Furnes and Hauges thesis indicates conservatism in DNV-OS-C502's fatigue calculations. Based on their test results, with two run outs, it is reasonable to assume that the shown curve is too steep, and that the design code is even more conservative than it

appears in the graph above. Based on their results, Hauge and Furnes proposed a new multiplication factor, $C1=16$.

The results achieved from testing in water are not that far from the DNV-OS-C502. It is therefore reasonable to assume that the $C1$ for fatigue of concrete in air is more conservative than $C1$ for fatigue in water.

6.2.1.4 Results compared to other formulas and design codes

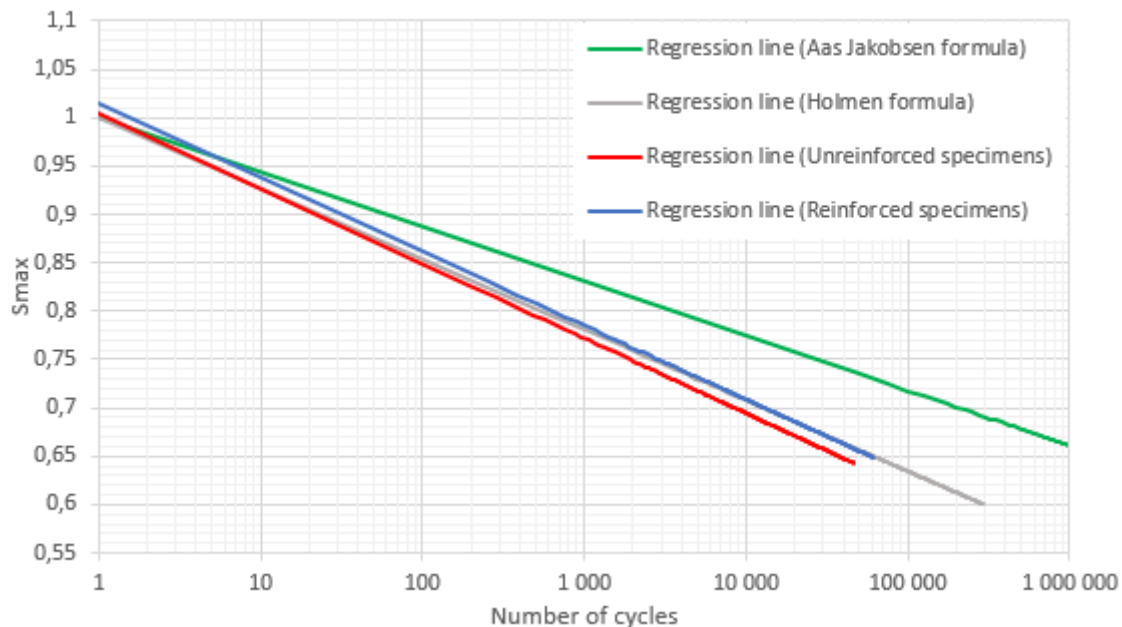


Figure 45 - Results compared to other formulas

The graph shows a comparison between formulas, codes and test results relevant to our thesis. All formulas and codes are based on a logarithmic calculation, where the load levels are the most determining factor.

The green line represent the most liberal formula, the Aas Jakobsen⁴⁷ formula for fatigue life. The Aas Jakobsen formula is based on a material constant, β , a very determining factor. It should also be taken into account that the formula is not applicable for load levels $> 0,8$ and cycles $> 10^6$.

The Holmen⁴⁸ regression line is very similar to the regression line derived from the reinforced specimen in this study. As mentioned earlier, the regression line from reinforced specimens matches the DNV prediction with $C1=12$ quite well. Hence, the constants used in the Holmen formula seems to be equivalent to the $C1$ factor used in DNV. On the other hand, the only fatigue life calculation taking water as an environmental effect into

⁴⁷ See Aas Jakobsen formula in section 2.2.3 "Calculating fatigue life"

⁴⁸ See Holmens formula in section 2.2.3 "Calculating fatigue life"

consideration, is the DNV formula. Even if the regression line from Holmen and our test results seem to match, it may be a coincidence.

In this part it would be practical to compare the results with the formulations used in Model Code 2010 and the Eurocode. However, Model Code 2010⁴⁹ does not consider the effect of the reinforcement which means that the static strength in the code will only depend on the concrete. This means that the applied loading in our tests will be larger than the capacity from the Model Code 2010 and the calculated cycles to failure is less than one. This is also a problem with the Eurocode⁵⁰. The Eurocode does also have a different method of considering fatigue problems. The code does not calculate the number of cycles before failure, as DNV-OS-C502 and Model Code 10 do. Instead, the Eurocode verify that the concrete can withstand a given number of cycles. In addition, neither of Model Code 2010 or Eurocode take the environmental effect into account, which is proven to have a great effect on fatigue life.

6.2.1.5 Effect of concrete strength development

From day one of testing to the last day of testing the cylinder strength of the test cubes⁵¹ had increased from 33,76 to 37,42 N/mm², roughly 10%. However, the static strength of the specimens were tested only the first few days. This static strength was later used while calculating the load levels for dynamic testing, which means that the load levels were not based on the static strength at that particular test day. The result of this was that the applied load level was always lower than the planned load level. For instance, in specimen 18 the actual load level was 0,59 when 0,65 was planned. This is a negative effect, which means that the results are too liberal.

Finding the exact static strength at any given time is not possible, but somehow an estimation was needed. In chapter 5⁵² the theoretical static strength were compared with the static strength results. By using the same factor, it was possible to roughly estimate the static strength at any given time. In the table below, this effect has been taken into account.

⁴⁹ See the formulations in section 2.2.3.3 «Calculating fatigue life according to Model Code 2010»

⁵⁰ See the formulations in section 2.2.3.2 “Calculating fatigue life according to NS-EN-1992-1-1”

⁵¹ See attachment A5

⁵² See section 5.2.2 “Capacity of partially loaded areas” and appendix A9 for the calculations

Dynamic test results

Specimen	Max dynamic load [kN]	Min dynamic load [kN]	Cycles until failure	Theoretical max load level	Planned load level	Average cylinder strength [N/mm ²]
7	379,4	50,6	2872	0,72	0,75/0,10	35,2
8	379,4	50,6	7099	0,707	0,75/0,10	35,8
9	379,4	50,6	2595	0,728	0,75/0,10	34,7
10	328,8	50,6	21675	0,598	0,65/0,10	36,7
11	328,8	50,6	7821	0,611	0,65/0,10	35,9
12	328,8	50,6	46407	0,611	0,65/0,10	35,9
13	625,5	73,6	231	0,827	0,85/0,10	34,8
14	551,9	73,6	4749	0,734	0,75/0,10	34,6
15	551,9	73,6	5023	0,702	0,75/0,10	36,2
16	478,9	73,6	40523	0,597	0,65/0,10	37,0
17	478,9	73,6	26040	0,582	0,65/0,10	37,9
18	478,9	73,6	61854	0,59	0,65/0,10	37,4

The consequences are that the regression line for both reinforced and unreinforced specimens are lowered, meaning that the capacities are lowered. The two curves will now be closer to the curve specified in the DNV-rules. Three of the data point obtained from testing even drops below that curve. This indicates that the rules are not conservative enough.

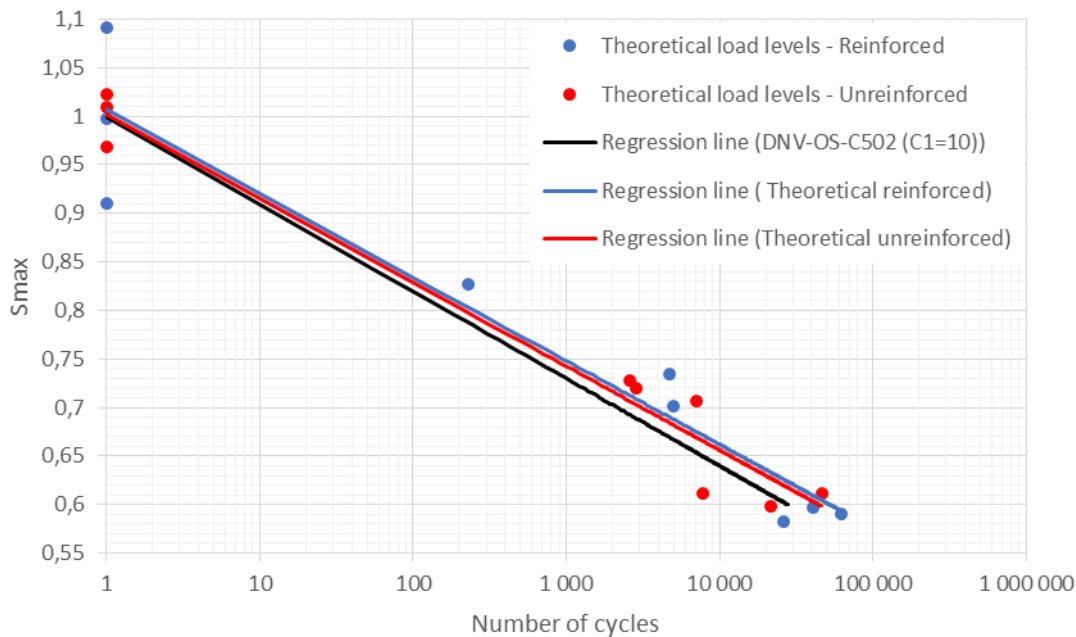


Figure 46 - Effect of concrete strength development

On the other hand, there is one mitigating effect as well. The cylinder strength is based on test cubes in water. The test specimens however, were soaked in water and sealed in high humidity. The strength development of the cubes in water are expected to be higher than

for the sealed specimens, which means the test cubes had a higher strength than the specimens did. This means that the load levels will most likely be a bit higher than the calculated theoretical load levels.

6.2.1.5.1 Partial factor for fatigue

The DNV design code does not cover the topic of partially loaded areas exposed to fatigue⁵³. However, Paula Mayorca and DNV-GL are conducting a study to find appropriate rules on the topic. As of now, their suggestion is to use an amplification factor of 1,3 for design situations in fatigue, which means that the compressive strength of the concrete can be amplified with a factor of 1,3 due to partially loaded areas. This amplification factor is of course only applicable for concrete where the transverse tension forces is accounted for by reinforcement. For unreinforced specimen the amplification is 1,0.

In comparison, the reinforced specimens in this study showed a static amplification factor of 1,48. The unreinforced specimens achieved 1,03. By use of these amplification factors for dynamic capacity as well, some of the results in the study challenged the fatigue formulations in the DNV design code. This was in particular a problem when the effect of concrete strength development⁵⁴ was taken into account. The code was not conservative for all the results.

Dynamic test results

Specimen	Max dynamic load [kN]	Min dynamic load [kN]	Cycles until failure	Planned load level	Max load level design situation (partial factor =1,3)	Theoretical max load level (partial factor =1,3)	Average cylinder strength [N/mm ²]
7	379,4	50,6	2872	0,75/0,10	0,765	0,734	35,2
8	379,4	50,6	7099	0,75/0,10	0,765	0,721	35,8
9	379,4	50,6	2595	0,75/0,10	0,765	0,743	34,7
10	328,8	50,6	21675	0,65/0,10	0,663	0,61	36,7
11	328,8	50,6	7821	0,65/0,10	0,663	0,623	35,9
12	328,8	50,6	46407	0,65/0,10	0,663	0,623	35,9
13	625,5	73,6	231	0,85/0,10	0,97	0,94	34,8
14	551,9	73,6	4749	0,75/0,10	0,855	0,834	34,6
15	551,9	73,6	5023	0,75/0,10	0,855	0,797	36,2
16	478,9	73,6	40523	0,65/0,10	0,742	0,678	37,0
17	478,9	73,6	26040	0,65/0,10	0,742	0,661	37,9
18	478,9	73,6	61854	0,65/0,10	0,742	0,67	37,4

It was therefore an interesting aspect to check how the results compared to the code when the new proposed partial amplification factors for fatigue were used. By reducing the

⁵³ 2.4.3 "Partially loaded areas exposed to fatigue"

⁵⁴ 6.2.1.5 "Effect of concrete strength development"

amplification factors, the applied load levels increased and the code was more conservative. This can be seen in the plot below, with the reinforced and unreinforced specimens as blue and red dots respectively. All 12 results are now on the safe side of the code. The one unreinforced specimen that originally challenged the design code is now a bit further above the design code.

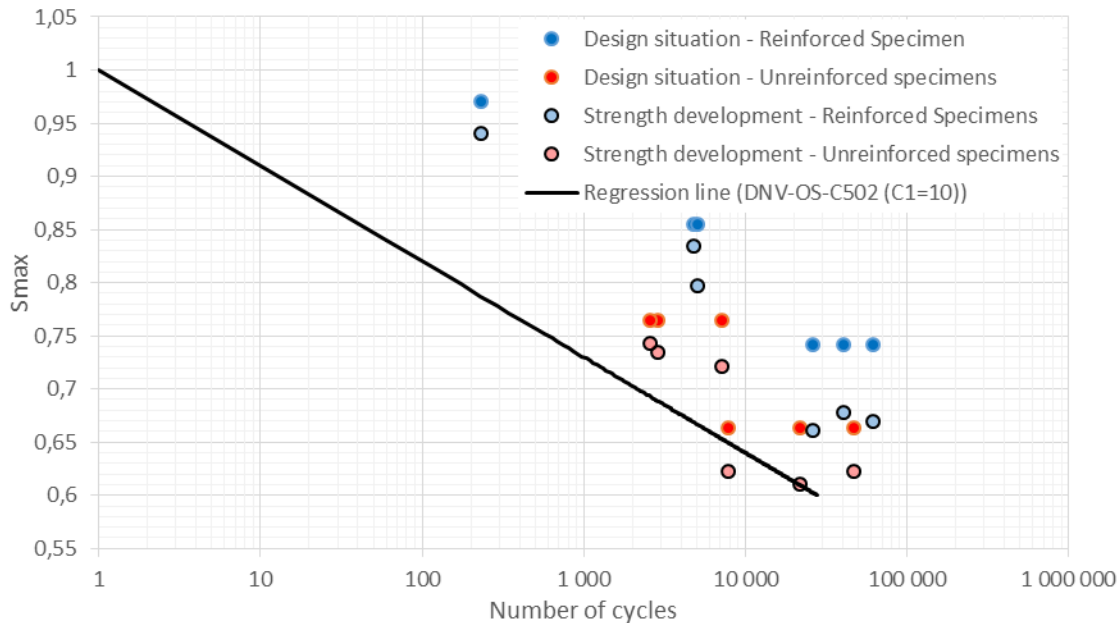


Figure 47 - Results in design situation compared to DNV-OS-C502

As for section 6.2.5.1 the effect of concrete strength development had to be taken into account as well. A new plot with the new partial amplification factors and the effect from concrete strength development is seen above, with reinforced and unreinforced specimens as blue and red dots with black borderline respectively. These dots are directly below the corresponding dots where the effect of concrete strength development is not taken into account. With both effects accounted for, one of the unreinforced specimens drops below the DNV design code and one is fairly close. However, all the reinforced specimens have satisfactory results compared to the design code.

The proposed partial amplification factor of 1,3 for fatigue seems to be adequate for the reinforced specimens. However, the unreinforced specimens with amplification factor 1,0 is still unsatisfactory. For the fatigue rules in DNV-OS-C502 to be conservative for all situations a requirement of reinforcement must be implemented. If this requirement can not be implemented, the unreinforced results indicate that a reduction of C1 must be made. C1 equal to 9 would be sufficient.

6.2.1.6 General tendency of data points

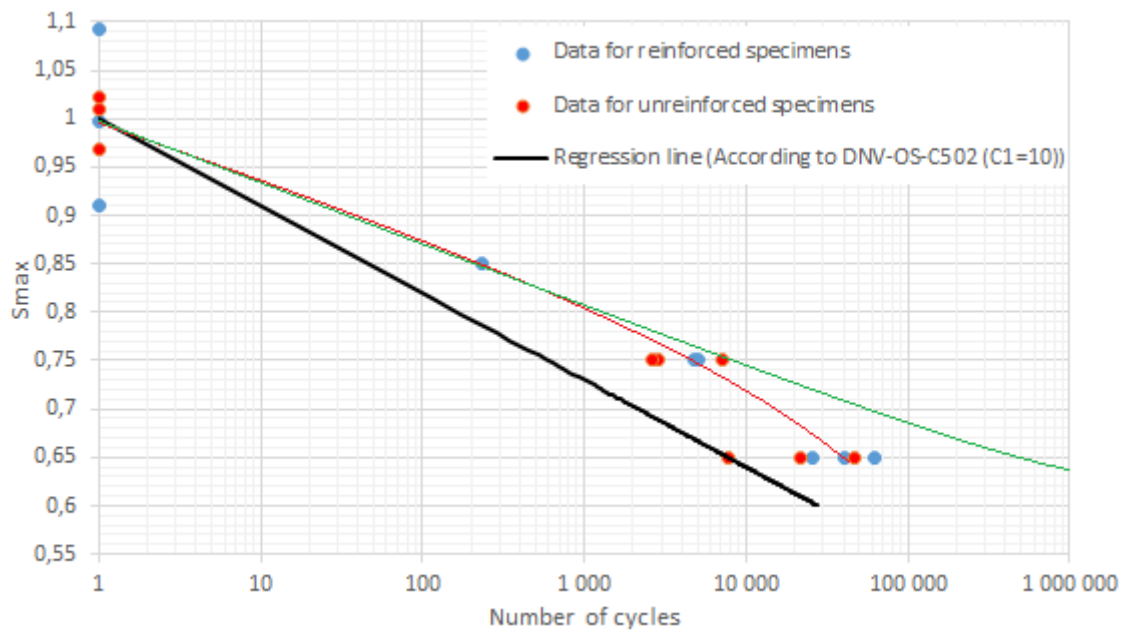


Figure 48 – General tendency of data points

Some materials have an endurance limit⁵⁵, where the fatigue life converges towards infinity at lower load levels. The data points achieved in this study show a dipping tendency in fatigue life for submerged specimens, illustrated by the red line above. This fatigue life development might confirm that concrete submerged in water does not have an endurance limit. However, the fatigue life of concrete is expected to converge towards a great number of cycles at lower load levels. This tendency is illustrated by the green line.

Nevertheless, the dipping curve may indicate that tests on lower load levels can not endure, or at least come closer to, the number of cycles predicted in DNV-OS-C502. This indicates that the DNV design code is more conservative for short term dynamic loading than for long term, with regard to concrete submerged in water. If this is the actual trend, it may be reasonable to question the applicability of logarithmic calculation of fatigue in concrete submerged in water. This might be due to the significant effect of water.

However, this study only included load levels of 0,85 to 0,65. To get a better understanding of the behaviour of concrete submerged in water, tests at lower load levels <0,65, should be conducted.

⁵⁵ See section 2.2.1 “Fatigue in general”

6.2.2 Life cycle development

6.2.2.1 Reinforced specimens

6.2.2.1.1 Stroke development

The development throughout the fatigue lifetime of the specimens can be described by three phases, as earlier research⁵⁶ also conclude with. In the first phase the deformation rate is rapid, but after a while decreases, before it starts on the second phase where the stroke development is more or less constant with regard to time/cycles. The third phase indicates the end of the fatigue life, where the stroke development again starts to increase. In the beginning of the third phase the stroke increases slowly, but with time/cycles it accelerates more and more until it finally goes to failure. If the stroke development is plotted with regard to N/N_f (percentage of total fatigue life) it will appear with a non-linear first phase, linear second phase and non-linear third phase. The six reinforced specimens are plotted below, to present the stroke development with regard to fatigue life, three short term and three long term.

Some of the reason to the steep stroke development in the first phase is crushing of the concrete knobs from the casting under the loading plate. Some of the most knobbed specimens were grinded to be able to stabilize the loading plate. Settlement of the specimens are also a factor. The second phase and linear phase starts when the specimens have settled and lasts until the deformation and cracks have become too great and the third phase starts.

Short term:

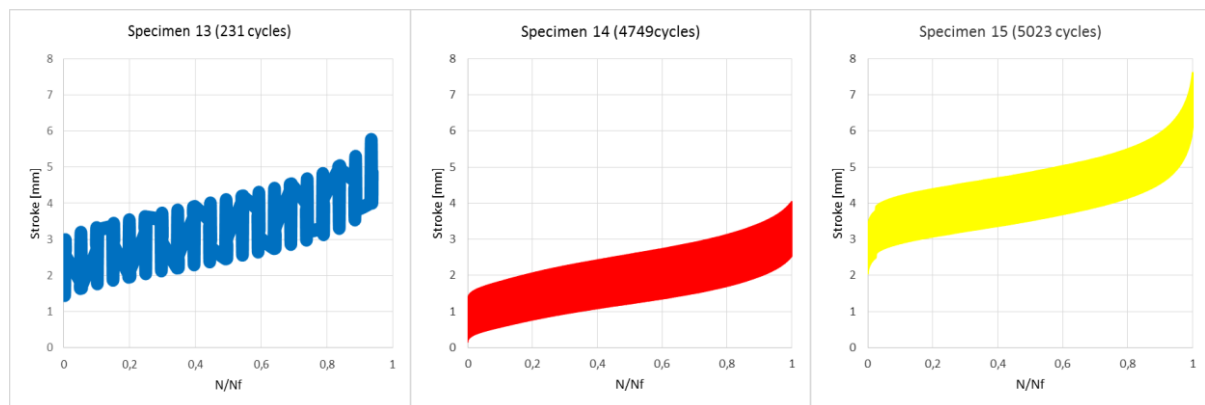


Figure 49 - Stroke development for short term reinforced

As seen on the plot for specimen 13 it is very jagged. This is because it was the first test to be performed and a periodic logging (logged every 10 seconds) were applied, due to expectations of a longer fatigue life. However it failed after only 231 cycles at 1 Hz, causing few data point in the graph.

⁵⁶ 2.2.1 "Fatigue in general"

During test of specimen 13 and 14, no proper logging of pre-test dummy were performed. This is illustrated in the first phase of stroke development, in both 13 and 14. Both test starts lower than they probably should, compared to the 2 mm on specimen 15. Specimen 13 and 14 would most likely have started at about the same level as specimen 15 if the pre-test dummy had been logged properly.

The maximum load in the pre-test dummy (mean load during testing) was 351kN for specimen 13 and 314kN for specimen 14 and 15. These loads caused the initial deformations shown above. The logging of specimen 14 started at 80kN. Specimen 15 had about 1mm deformation at the same load. This leads to assume that an increase of at least 1mm is reasonable.

The test on specimen 14 were stopped a bit too early. If the third phase on specimen 14 and 15 are compared one can see that specimen 15 have a very much steeper increase of the stroke towards the end of the fatigue life. From the plots one can see that specimen 14 have about 5 % left of its fatigue life when the test was stopped. By adding the remaining 5 % specimen 14 would have gone to failure at roughly 5000 cycles.

By accounting the sources of error above the total deformation will not be too scattered between the three short term specimens. The slope of the 2nd phase is more or less the same on specimen 14 and 15.

Long term:

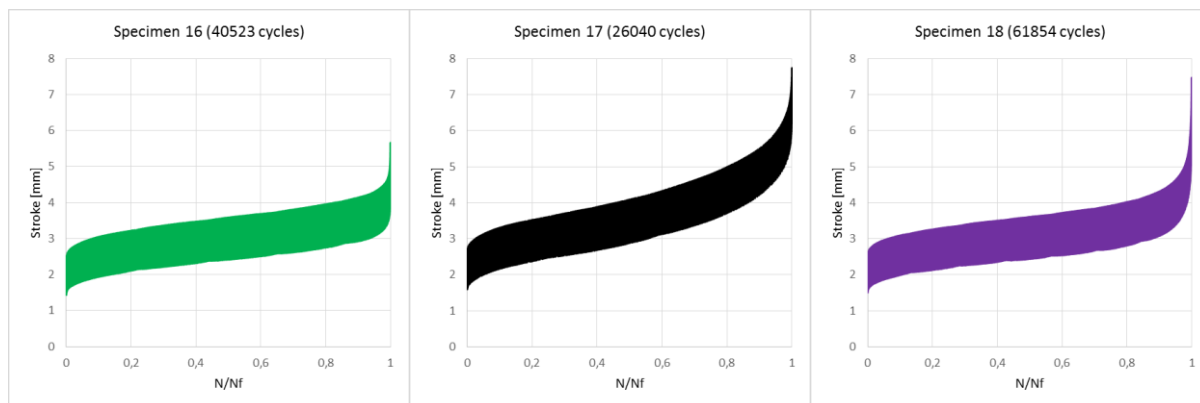


Figure 50 - Stroke development for long term reinforced

The maximum load during the pre-test of long term reinforced specimens, was 486kN. This caused an initial deformation of about 2mm, as shown above.

Specimen 17 separates from the two other by having much higher ductility, even though it failed at fewer cycles. During the test big cracks occurred at a low amount of cycles, but

somehow the specimen kept on deforming without failing. A possible reason can be that the bond between concrete and reinforcement in this specimen were particularly strong⁵⁷.

The 2nd phase on the long term test seems a bit flatter than on the short term test, which means that the stroke develops faster with higher load level.

Note the difference in the duration of the 3rd phase between the short and long term specimens. As the 3rd phase in the short term tests make up between 10 and 15 % the long term 3rd phase only make up around 5 %. The stroke development graphs from Furnes and Hauges thesis also indicates this observation.

6.2.2.1.2 LVDT development

As for the stroke development the LVDT development measures the deformation of the specimens over the fatigue lifetime. While the stroke have some errors in the measurements the LVDT's have no similar error source. An accurate LVDT measurement is therefore likely to be more realistic than the results directly from the stroke. However both stroke and LVDT should have the same form and indicate the three phases the same way. Though, the stroke will have a bit higher deformation at P_{max} , as the stroke error is highest at P_{max} and almost none at P_{min} . This can also be seen from that the deformation at P_{min} is practically identical for both stroke and LVDT. At P_{max} stroke is however higher depending on the value of P_{max} . The size of the error at P_{max} on stroke, compared to LVDT, fits the results from the machine stroke test⁵⁸.

Short term:

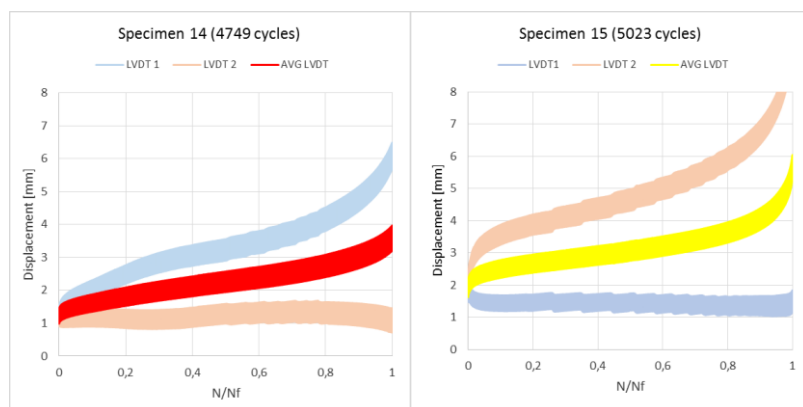


Figure 51 - LVDT development for short term reinforced

⁵⁷ For more on this see section 6.4 "Cracks"

⁵⁸ 5.2.3.1 "Force deformation relation in reinforced specimens"

Long term:

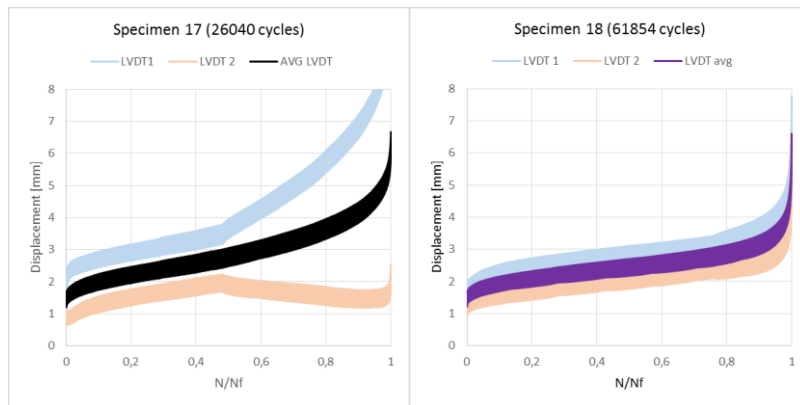


Figure 52 - LVDT development for long term reinforced

The LVDT result from specimen 13 was not properly logged, and therefore excluded from this report. In addition, the LVDT logging failed during test of specimen 16. Therefore, LVDT data from this tests is not available.

By comparing LVDT 1 with LVDT 2 on the different tests, the trend is they often start with the same deformation development in the first phase. As deformation develops, the two LVDT's starts to differ from each other. Typically, one LVDT have very little development after the first phase, while the other increases more and more. This is illustrated on the picture below.



Figure 53 - Deformation under the loading area on specimen 17

There can be several reason to why this occur. The imperfections of the concrete surface from the casting made it hard to make the loading area 100% horizontal. This initial inclining may have escalated during the test. Another reason can be local weaknesses in the concrete

which will deform easier causing sloping to occur. The sloping does not seem to have an effect on the crack development in the rest of the specimen, as the photo above shows. The main cracks in this specimen is on the opposite side of the LVDT with most deflection. This is also the case for some of the other specimens as well. It is difficult to say if the water effected the sloping development.

6.2.2.1.3 Superimposing of stroke development

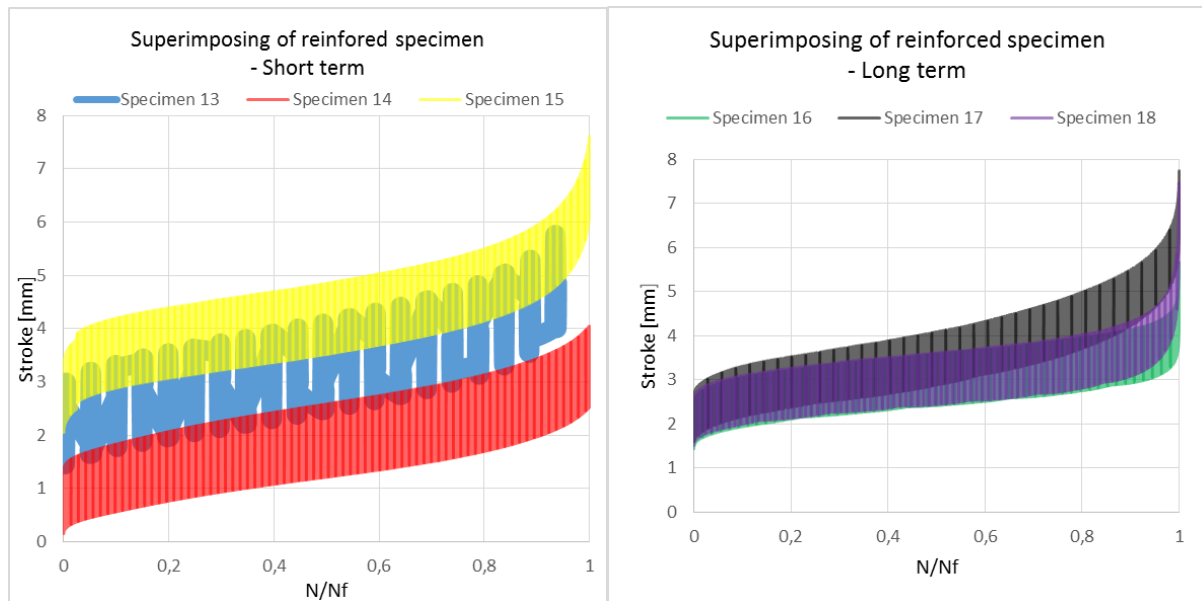


Figure 54 - Superimposing of short term (left) and long term (right) reinforced

Superimposing of the stroke results is an easy way to compare the results from same type of specimens with the same load level. The reinforced short term tests had some issues with logging of the dummy, and periodic logging on specimen 13. However the shape is very identical. It is also important to comprehend that specimen 13 had a higher load.

In the long term test specimen 16 and 18 had similar shape, while specimen 17 had a bit steeper slope, as explained earlier.

6.2.2.2 Unreinforced specimens

6.2.2.2.1 Stroke development

The stroke in unreinforced specimens, both short and long term, is relatively small before failure. The deformation rate of the stroke during the 2nd phase is quite low.

The 1st phase is only approximately 5 % of the total fatigue life because of the relatively low P_{max} , which leads to less local crushing under the loading plate. This is also confirmed by the LVDT measurements where the difference between LVDT 1 and LVDT 2 is fairly small⁵⁹.

⁵⁹ 6.2.2.2.2 "LVDT development"

The 3rd phase is critical. The stroke development during the 2nd phase is almost constant until failure, therefore the 3rd phase is almost non-existent. This was also noticed while observing the tests. Failure occurred much earlier than expected with regard to deformation rate. The cracks were small, and could have been of constant size during many cycles, but a sudden failure occurred. This very rapid failure can be very critical in a real construction, as one do not observe the deformations before failure.

Short term:

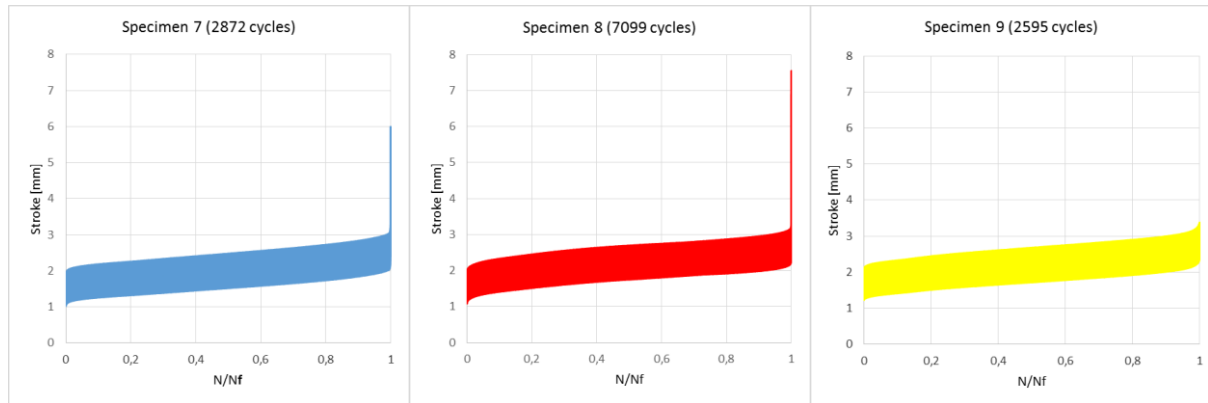


Figure 55 - Stroke development of short term unreinforced

The maximum load during pre-test for specimen 7,8 and 9 was about 390kN, causing an initial deformation as illustrated above.

Long term:

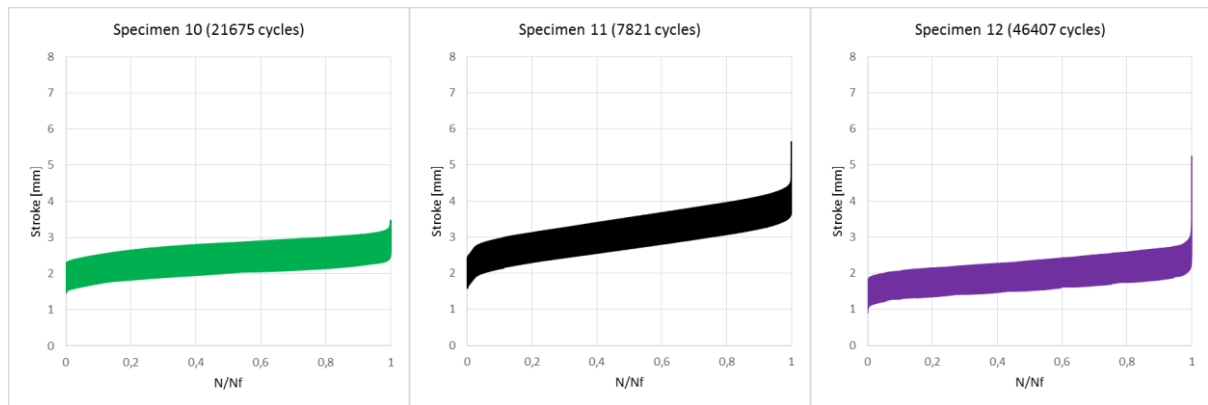


Figure 56 - Stroke development of long term unreinforced

The maximum load during pre-test for specimen 10, 11 and 12 was about 338kN, causing initial deformations shown above.

6.2.2.2.2 LVDT development

As mentioned earlier the deformation in unreinforced specimens are not especially large, as confirmed by the LVDT results. The LVDT results from the unreinforced specimens also indicates an error source in the stroke test.

Besides the stroke error in the machine on the stroke measurement, the stroke and average LVDT have near exactly the same shape. By comparing lower part of the plots (deformation at P_{min}) it is very similar. The only specimen with some deviation between the stroke and the LVDT measurements is the results from specimen 11. For some reason the stroke results have a bit steeper 2nd phase and the final deformation before failure is roughly 1 mm more on the stroke compared to the average LVDT at P_{min} .

The difference between LVDT 1 and LVDT 2 is relatively small. This is due to the relatively low loads on the unreinforced specimens. The lower loads leads to less local crushing under the loading plate, which results in smaller difference between LVDT 1 and LVDT 2.

Unfortunately the logger did not log the LVDT's on specimen 10.

Short term

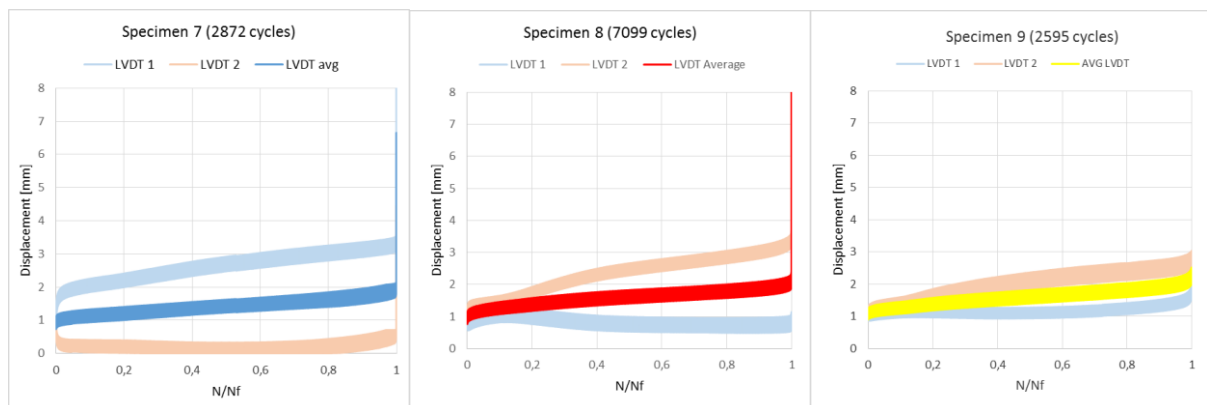


Figure 57 - LVDT development of short term unreinforced

Long term

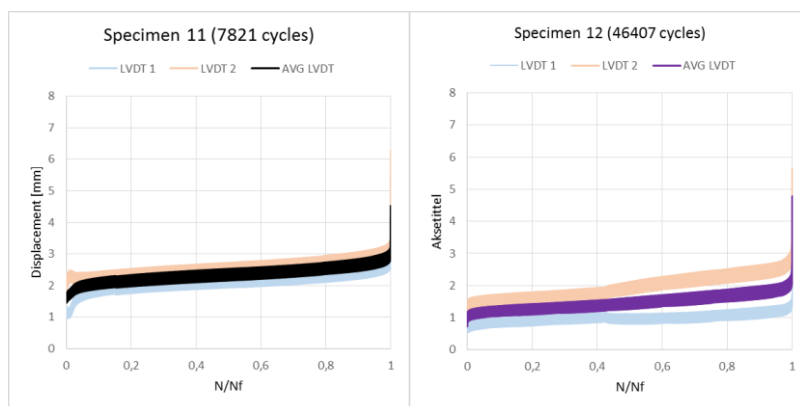


Figure 58 - LVDT development of long term unreinforced

6.2.2.2.3 Superimposing of stroke development

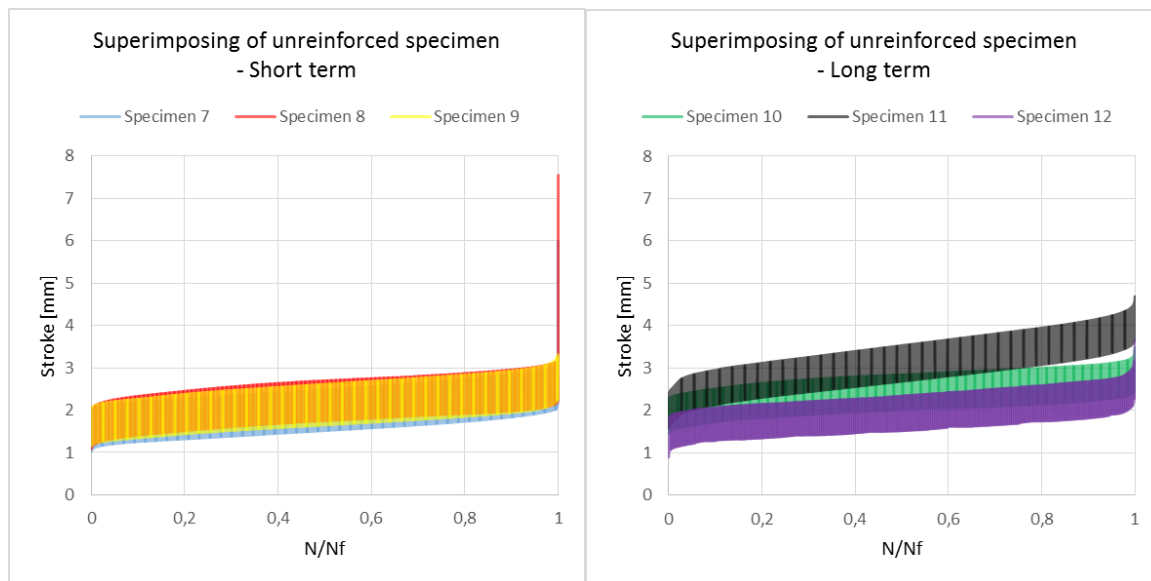


Figure 59 - Superimposing of short term (left) and long term (right) unreinforced

Superimposing of the results from the short term unreinforced specimens have more or less exactly the same shape. On the long term tests specimen 11 deviates a bit because of a bit steeper 2nd phase. Common for all of them is a very rapid 3rd phase before failure.

6.2.2.3 Comparison between reinforced and unreinforced specimens

The reinforcement clearly had a positive influence on the ductility, as the deformation is a lot higher before failure in the reinforced specimens. The specimens in this thesis had too little reinforcement compared to the concrete strength. It is reasonable to assume that more reinforcement allows more deformation. The effect of this is hard to predict because the critical cracks occurred outside the reinforcement⁶⁰.

The difference in deformation at P_{max} and P_{min} , both in the stroke and average LVDT, is much greater in the reinforced specimens than the unreinforced. This have its natural explanation in the applied load at P_{max} . The reinforced specimens had a much higher maximum load at the selected load levels, which naturally will give a much greater deformation at P_{max} .

The 2nd phase differs, as the unreinforced is much flatter compared to the reinforced. This is because the reinforced have larger P_{max} , as mentioned above, and therefore the stroke increases much faster than for the unreinforced. Anyhow, higher ductility allows this without failing at an earlier stage.

A very important observation is the difference between the 3rd phase of the reinforced and unreinforced specimens. While the reinforced specimens 3rd phase lasts approximately 10-15 %, the unreinforced specimens 3rd phase is almost non-existent. This is absolute worth

⁶⁰ See section 6.4.1 "Crack patterns»

taking notice of. In a real life structure the structure would then fail without any remarkable deformations without proper reinforcement.



Figure 60 – Short term specimen 9 unreinforced (left) and short term specimen 15 reinforced (right)

As shown in the pictures above there are less local crushing in the unreinforced specimen's compared to the reinforced specimens, as explained earlier due to lower P_{max} on the unreinforced specimens.

6.3 Strain gauges

6.3.1 Strain in reinforced specimens

Reinforced specimens	Placement of strain gauge
Strain 1	the stirrup in the 2 nd layer from the top
Strain 2	splitting reinforcement in the 2 nd layer from the top
Strain 3	splitting reinforcement in the 1 st layer from the top
Strain 4	one of the threaded bars in the 2 nd layer from the top

Some of the results from the strain gauges were not exactly as expected, as there were many individual differences. However some information of the behaviour throughout the fatigue life is possible to produce.

In general none of the reinforcement bars yielded where the strain gauge were installed.

By comparing the strain results from the statically tested specimens with the dynamically tested specimens one can draw some context between the two test types which explains why yielding does not occur. In the static results⁶¹ yielding in the reinforcement bars does not occur before it has reached a high load. The load level for the dynamic tests is below static yielding load. In general none of the reinforcement bars in the static tests yielded before the specimen were subjected to a load over 700 kN. The dynamic load level is below

⁶¹ Please see section 5 "Static test results"

this load and the critical cracks occurs on the outer side of the reinforcement. Hence, the strain in the reinforcement is lower than expected.

Cracks will expand the specimen in one or more directions⁶². If cracks occurs inside the reinforcement the reinforcement will try to prevent this expansion. This leads to tension in the reinforcement. Since the critical cracks occurs on the outer side of the reinforcement, the reinforcement is not activated as it would if the critical cracks occurred within the reinforcement. The reinforcement obviously prevents the cracks to occur within the reinforcement. This can be seen by comparing the cracked and failed reinforced and unreinforced specimens⁶³. The crack development is directed towards the weakest parts of the specimen. Therefore the cracks occur outside the reinforcement.

Another factor that influences the crack development is the threaded bars. The bars will work as crack assigners and might therefore have an indirect effect on the strain gauges.

A possibility regarding the reinforced specimens, is that cracks may reach critical stage faster due to pore pressure from the water, with failure as a result. Since the cracks occurs on the outer side of the concrete, the specimen would have failed without activating the reinforcement. However, if the cracks occurred within the reinforced area, water probably would have an increasing effect on the strain gauges due to the pore pressure. The magnitude or the influence of the pore pressure would most likely have a negative effect.

⁶² 2.2.2 "Fatigue in concrete"

⁶³ See section 6.4 "Cracks"

6.3.1.1 Strain 1 – stirrup in the 2nd layer from the top

Short term reinforced:

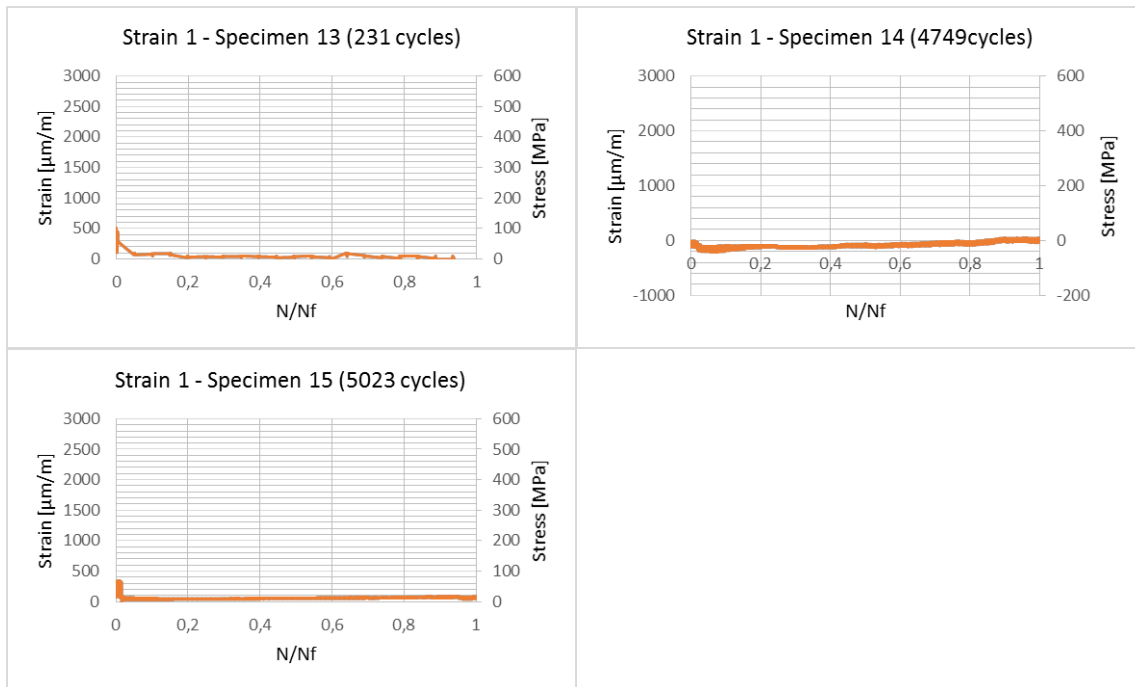


Figure 61 - Short term reinforced: strain 1

Reinforced long term:

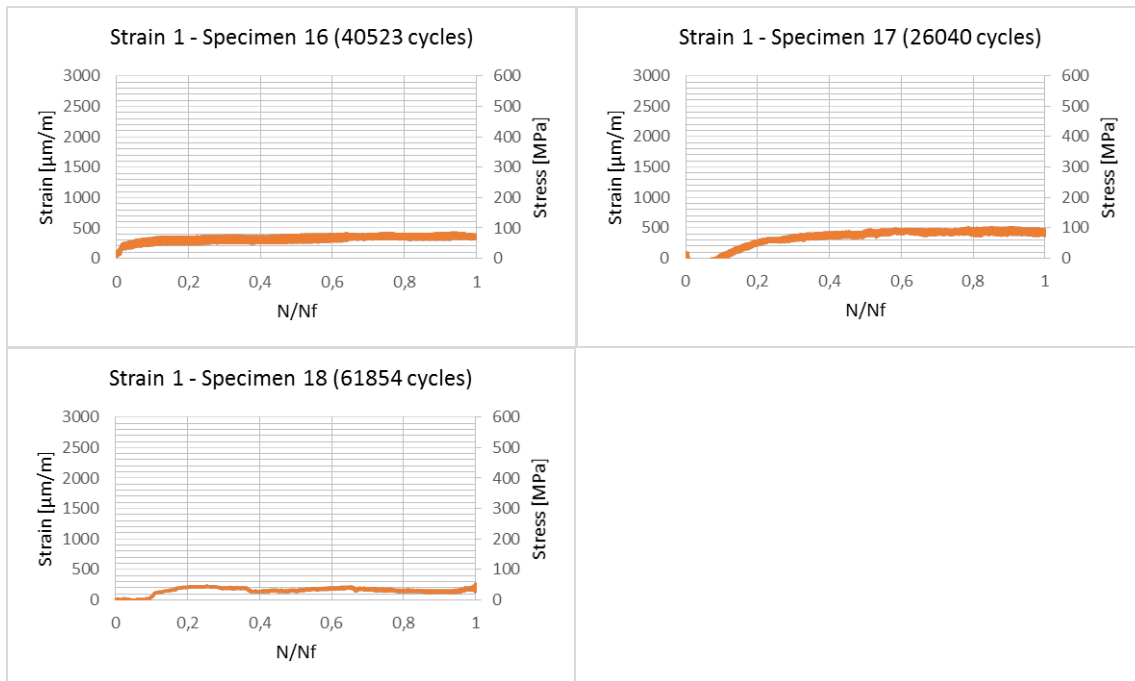


Figure 62 - Long term reinforced: strain 1

The short-term reinforced specimens all have very little impact on the strain gauges mounted on the stirrup in the 2nd layer from the top. As demonstrated in the graphs above, almost no strain were present. The reinforcement have a yield stress at 500 MPa (N/mm²), not causing any yielding in the reinforcement.

The long-term tests also have very little impact on the gauges though they in general have more impact than the short term tests. The reason why the strain is higher in the long-term tests is not known. Since the loads in the short-term tests were higher than in the long-term tests, it is reasonable to believe that strains in short term test should be higher.

In the calculations, the stirrups were seen as part of the splitting reinforcement. Before testing, higher strains in these gauges were expected. Furnes and Hauges thesis also indicates this, where most of the reinforcement yielded.

6.3.1.2 Strain 2 – splitting reinforcement in the 2nd layer from the top

Short term reinforced:

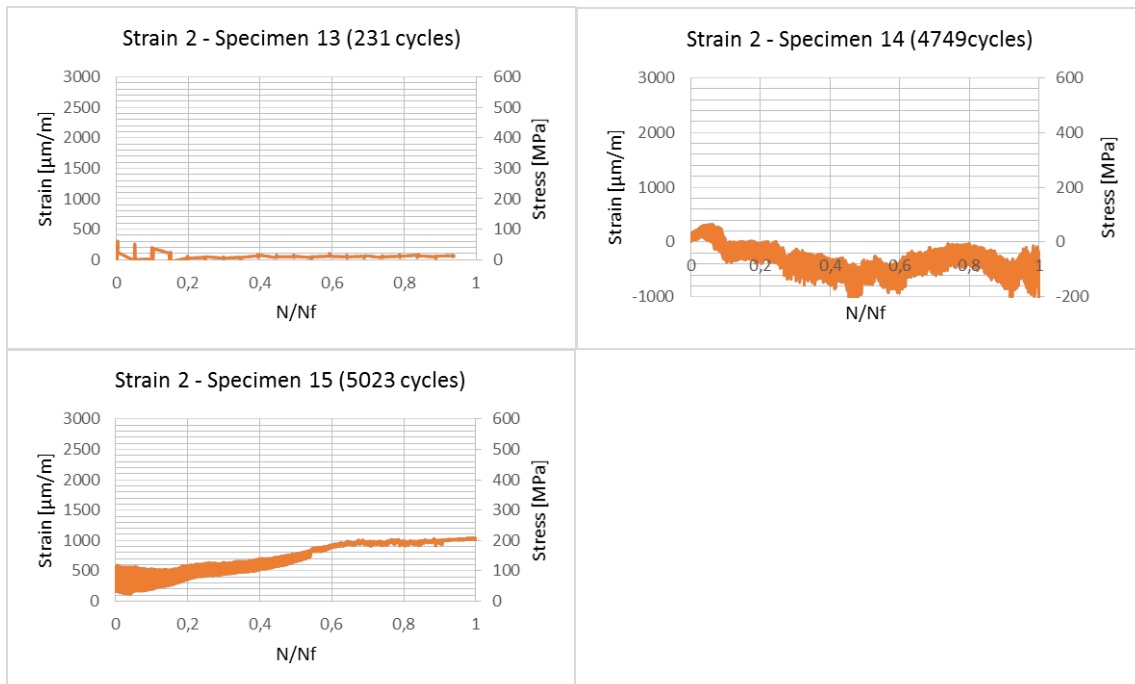


Figure 63 - Short term reinforced: strain 2

Long term reinforced:

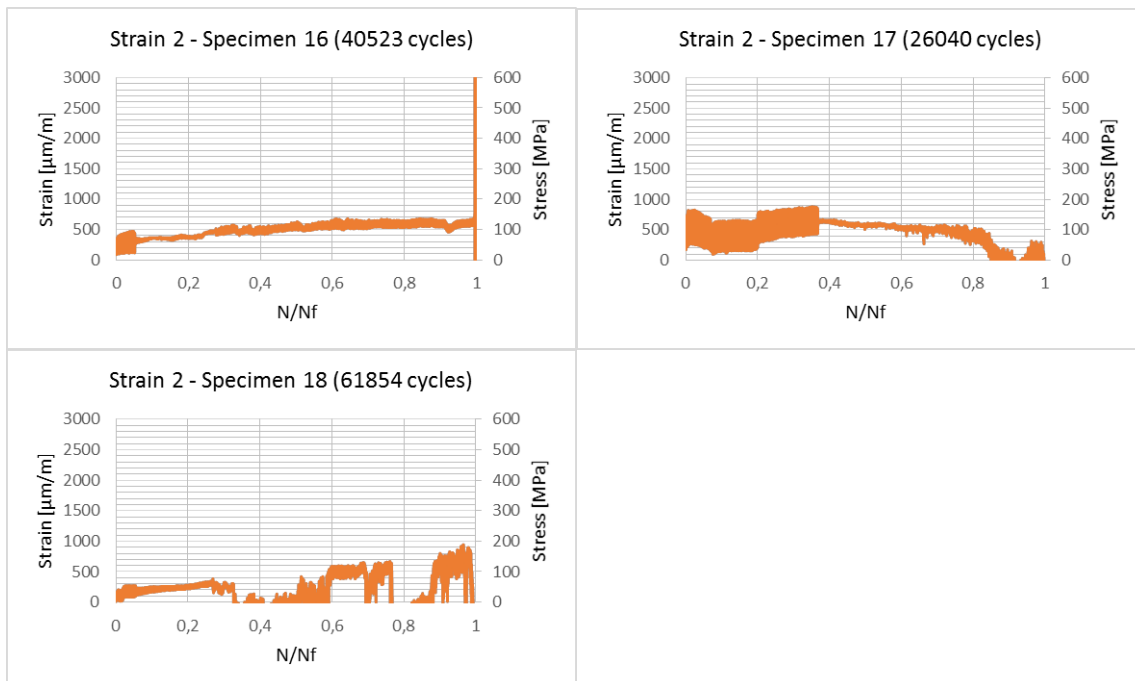


Figure 64 - Long term reinforced: strain 2

Theoretically, the splitting reinforcement in the 2nd layer from the top should have been the most impacted reinforcement bar. This is however not the case. As seen in the graphs above, the reinforcement bars in the different specimens, both short-term and long-term is nowhere near yielding.

The results from specimen 14 differs from the rest by having a negative strain. This indicates compression in the reinforcement bar. The result is unexpected since the rest of the specimens experienced tension forces in the same reinforcement bar.

6.3.1.3 Strain 3 – splitting reinforcement in the 1st layer from the top

Short term reinforced:

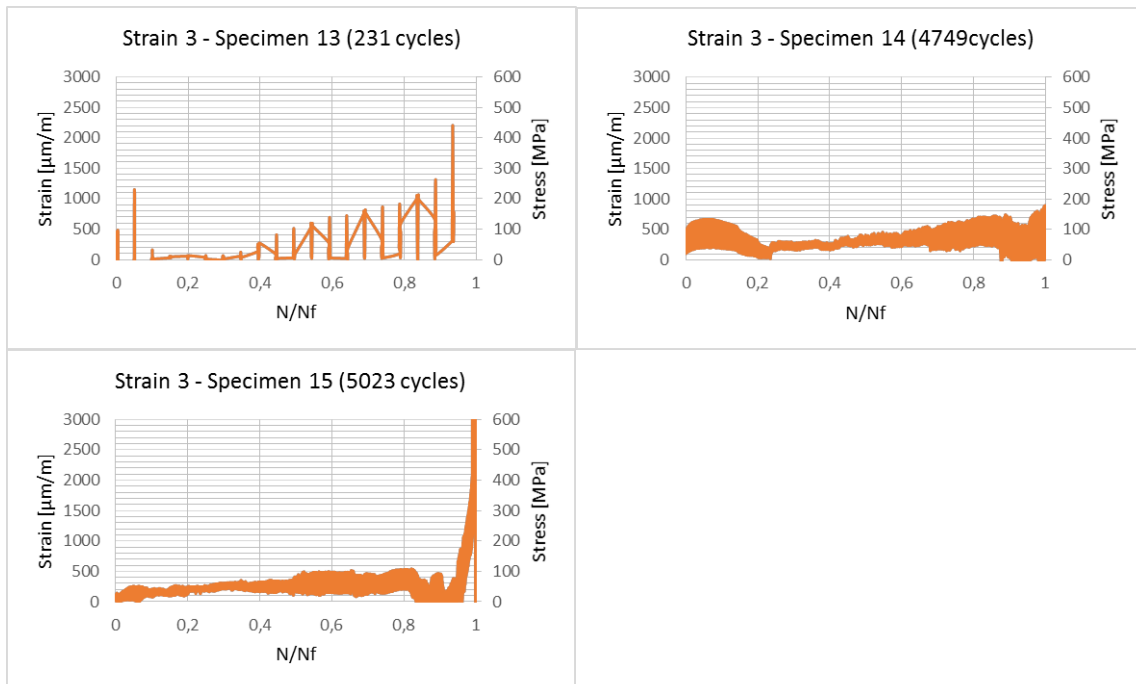


Figure 65 - Short term reinforced: strain 3

Long term reinforced:

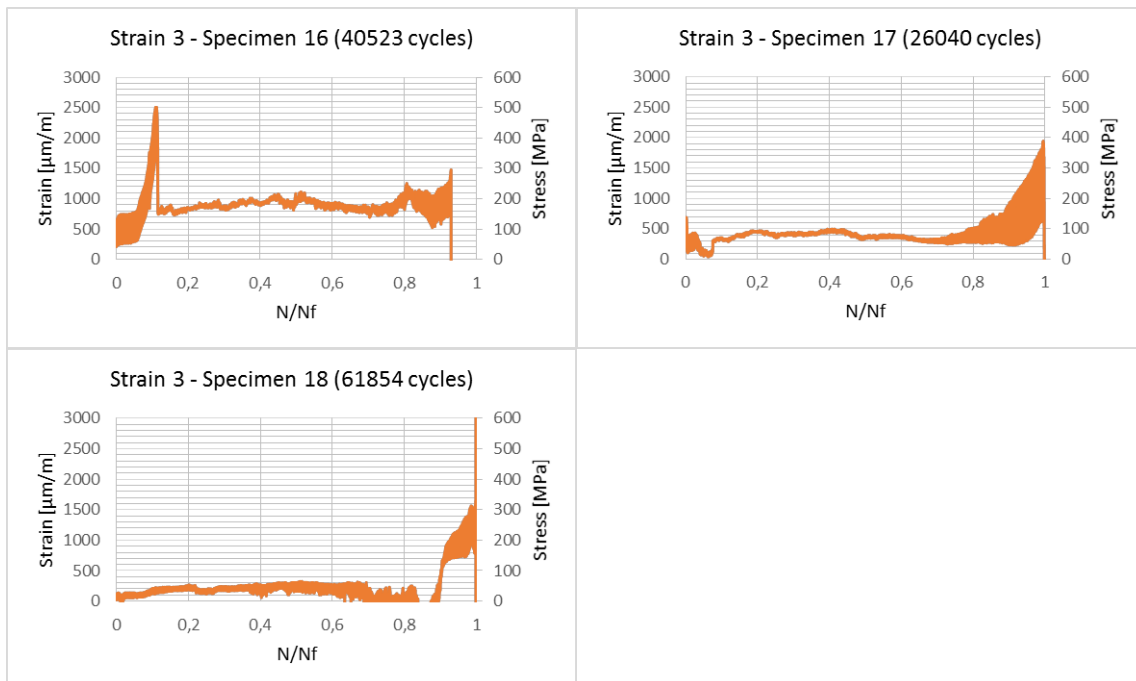


Figure 66 - Long term reinforced: strain 3

Strain 3 showed most impact of all gauges. A clear tendency from all the specimens, apart from specimen 14, was that the strain in the gauge on the splitting reinforcement in the 1st layer from the top increased significant the last 10 % of its lifetime.

The gauge on specimen 16 broke at about 90 % of its lifetime, but shows an indication that it would have increased, similar to the others.

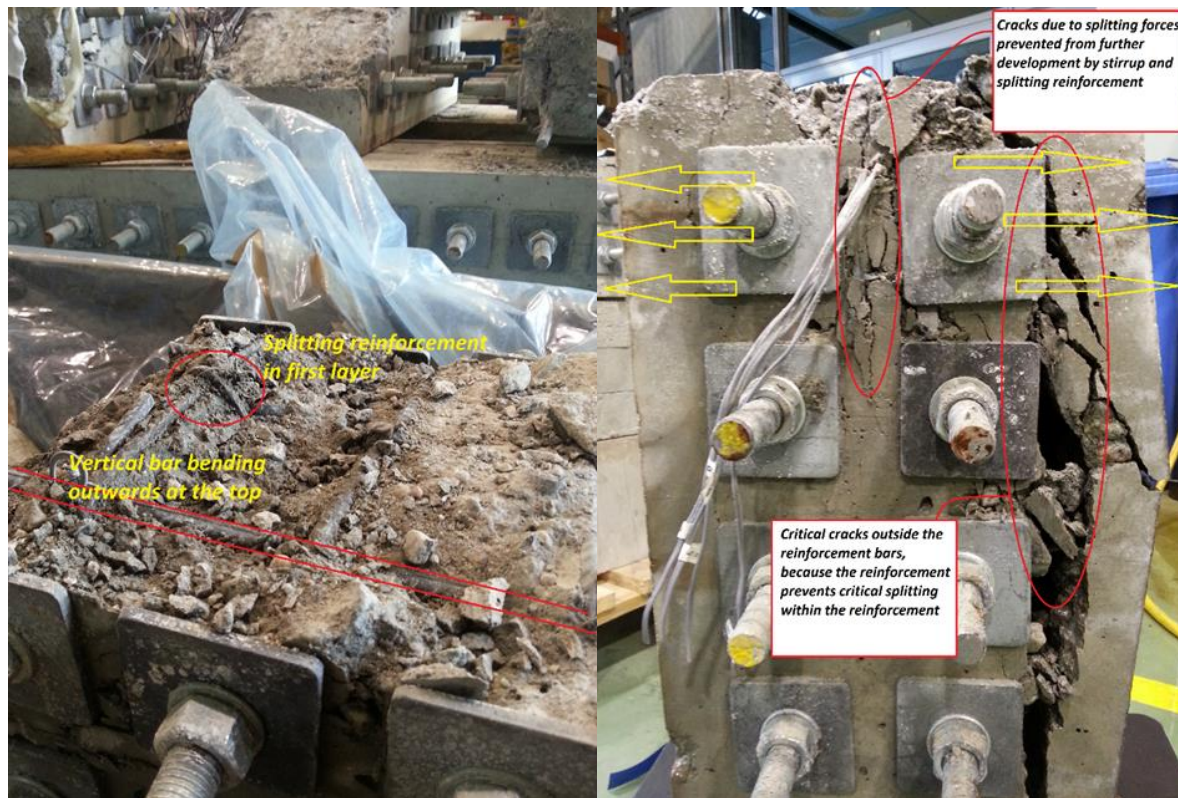


Figure 67 – Explanation of crack details

The graphs illustrates how no of the bars yielded, but the stress were relatively high at failure (approx. 350 – 450 MPa). Specimen 13 was the specimen with the highest strain. The high load level (0,85), probably made the reinforcement yield before the specimen failed. The graph illustrating this is incomplete due to the periodic logging.

When disassembling the tests, it was possible to see that the vertical bars were bent out at the top of the specimen. This observation corresponds well with the strain results, as the stirrup with splitting reinforcement will prevent critical crack development within the reinforcement due to transverse tension forces. As presented in section 6.4 Cracks⁶⁴, the critical cracks in the unreinforced specimens are more centered in the first and second layer of threaded bars, while the critical cracks in the reinforced specimens occurs on the outside of the reinforcement. This is because the stirrup and splitting reinforcement will prevent splitting due to transverse tension forces. As the cracks develops, especially towards the end

⁶⁴ See section 6.4 “Cracks” for more fulfilling details and pictures.

of the fatigue life, the reinforcement will be more and more affected. This theory seems to be compatible with the results.

6.3.1.4 Strain 4 – threaded bar in the 2nd layer from the top

Short term reinforced:

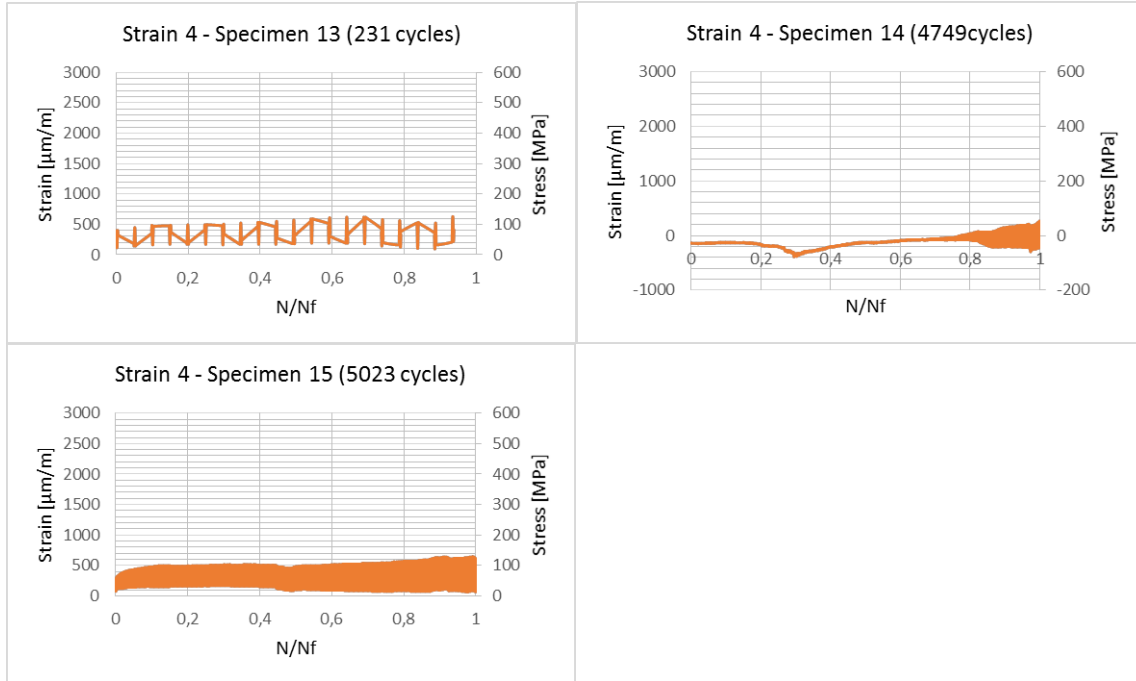


Figure 68 - Short term reinforced: strain 4

Long term reinforced:

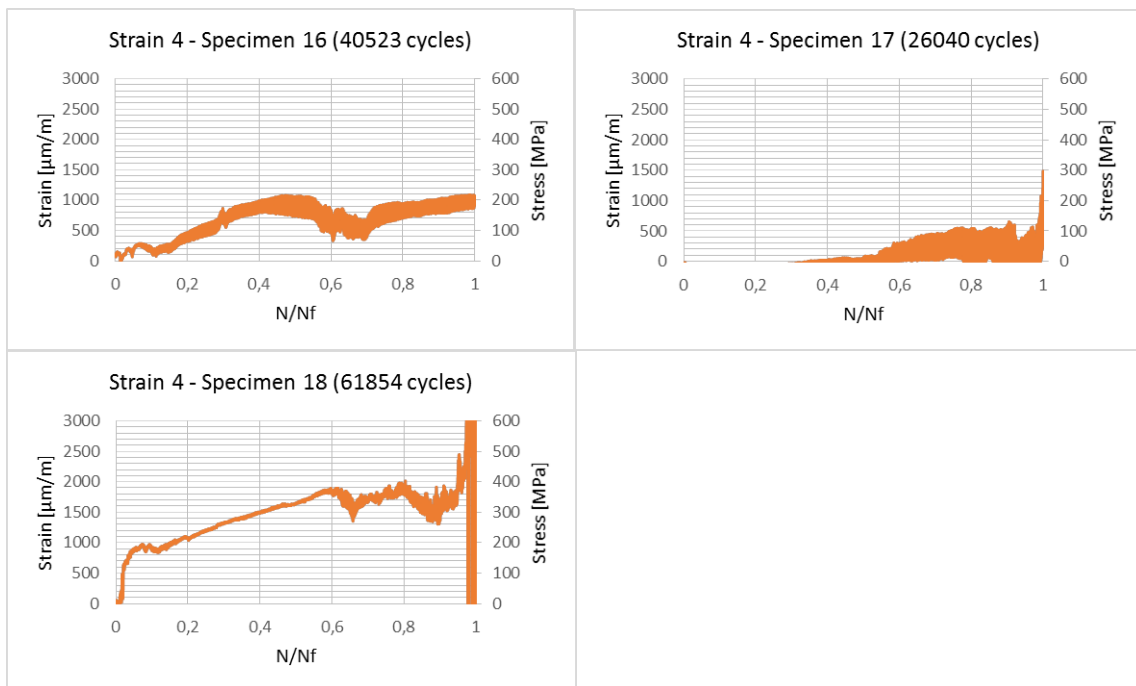


Figure 69 - Long term reinforced: strain 4

The gauge in strain 4 is placed on one of the threaded bars in the 2nd layer from the top. The purpose of the threaded bars were to prevent expansion of the specimen in the same direction as the bars and spread the load in the perpendicular direction. Therefore very small strains and stresses were expected in this gauge.

The results from the short term tests show very little impact on the gauge, as expected. The results from the long term test however shows a much larger impact, especially on specimen 18. On specimen 18 the strain develops quickly, and at the end it pushes yielding at almost 640 MPa.

The purpose of the threaded bars in most cases seems to be fulfilled, as the results in general shows low strains and stresses. This indicates that the expansion in the same direction as the bars is marginal.

6.3.2 Strain in unreinforced specimens

Short term:

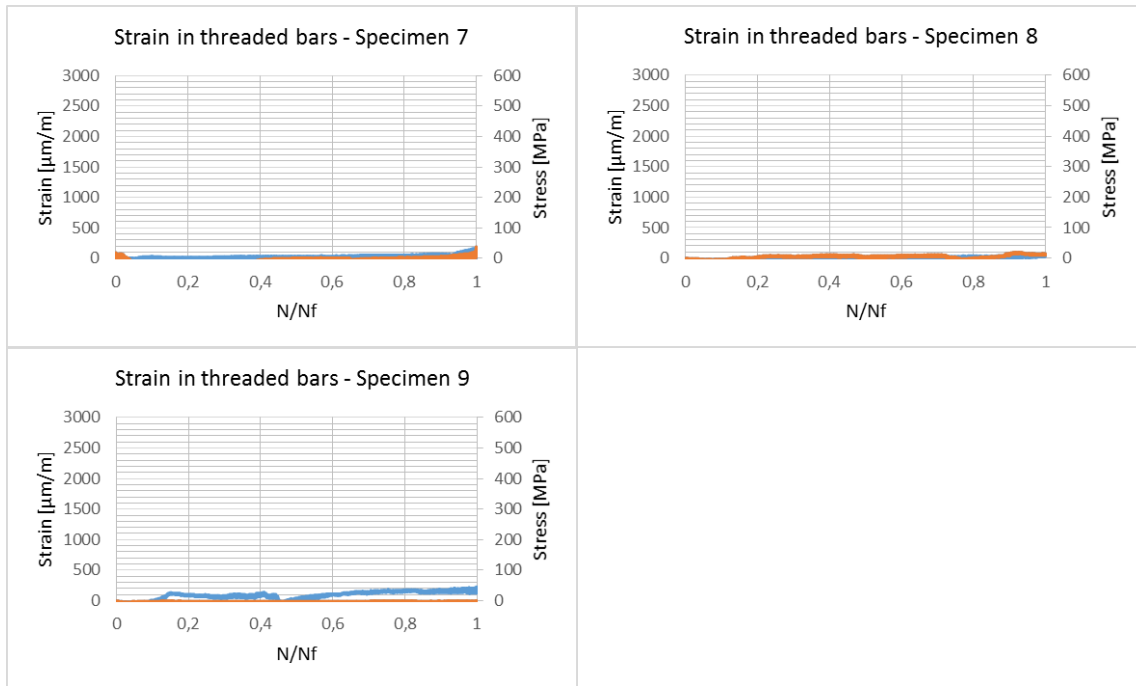


Figure 70 - Short term unreinforced: strain in threaded bars

Long term:

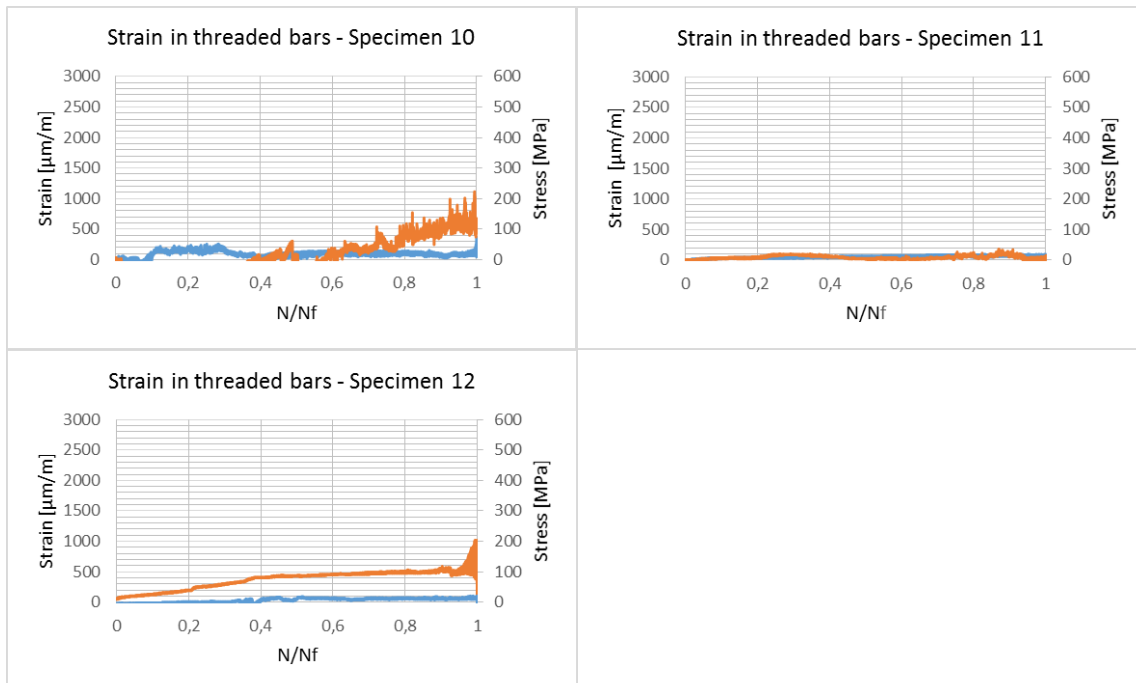


Figure 71 - Long term unreinforced: strain in threaded bars

Unreinforced specimens	Placement of strain gauge
Strain 1 (Red line)	one of the threaded bars in the 2 nd layer from the top
Strain 2 (Blue line)	one of the threaded bars in the 1 st layer from the top

As for the reinforced specimens the purpose of the threaded bars were to prevent expansion of the specimen in the same direction as the bars and spread the load in the perpendicular direction.

As expected the results showed very little strain in the gauges. None of the specimens had any particular impact in either strain 1 or strain 2. This indicates that the threaded bars have confined the specimen and prevented expansion in this direction. Worth mentioning is that a trend occurs as two of the long term test (Specimen 10 and 12) shows greater strains in strain 1. This might be caused by their lifetime which is about 3-7 times larger than the other unreinforced specimens.

6.4 Cracks

6.4.1 Crack patterns

The crack patterns in the dynamic tests roughly showed the same trend as the static tests. The main difference between specimens subjected to static and dynamic loading, was the amount of damage in the specimen. Specimens in dynamic loading were significantly more damaged, compared to the static tests. The main reason was how and when the tests were stopped. In the static tests the machine was manually stopped when deformation increased while applied load decreased. In the dynamic tests the machine stopped when it reached either the deformation limits or the pre-set load limit. Therefore the dynamic tests sometimes continued even after failure, causing more damage to the specimen.

Like the static tests, the first phase was local crushing at the top and cover concrete spalling at the edge of the load area, as shown below.



Figure 72 - Local crushing at the top

Next, cracks started to develop between the second and third layer of threaded bars. In the reinforced specimens these cracks developed at the end of the washer, while at the middle of the washer in the unreinforced specimens, as seen marked green below.

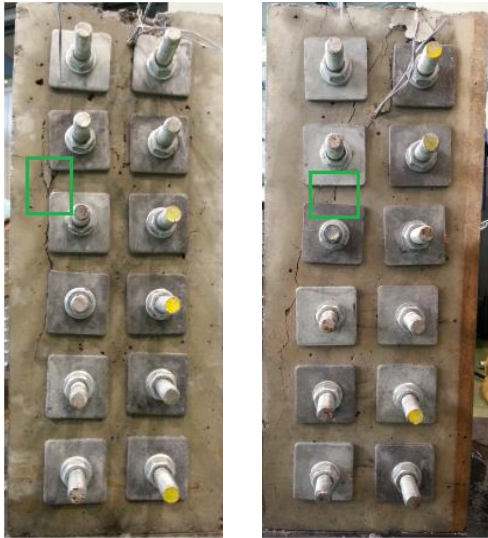


Figure 73 - Crack initiation in reinforced (left) and unreinforced (right) specimens

After the first crack initiation, the crack propagation increased. The cracks expanded and developed in length. However, the development differed between the reinforced and the unreinforced. As in the static tests, the reinforced specimens only had cracks at the outside of the threaded bars and reinforcement. The unreinforced specimens had cracks in the middle of the specimen. The cracks developed outwards at the third layer of threaded bars. In this area the unreinforced specimens had stirrups which prevented the cracks for propagating in the middle. The difference, which shows the effect of reinforcement, is illustrated below.



Figure 74 - Crack at failure in reinforced (left) and unreinforced (right) specimens

After the tests, the cracks were disassembled to get a better picture of where the cracks had developed, and the difference between the reinforced and the unreinforced specimens. The difference is shown below.



Figure 75 - Crack at failure (disassembled) in reinforced (left) and unreinforced (right) specimens

In the reinforced specimens the critical crack occurred at the edge between steel reinforcement and the concrete, as illustrated below. When the cracks were opened, it was possible to see that the failure occurred between the steel and the concrete, similar to a bond failure.



Figure 76 – Cracks appeared between steel and concrete

The crack patterns at failure for each test are illustrated in the appendix⁶⁵.

⁶⁵ See appendix A11 “Crack propagation in dynamic tests”

6.4.2 Crack initiation versus fatigue life

Early in the lifetime of the specimens, cracks in different forms appeared. Some appeared because of air pores or other imperfections in the specimens, with no further development. However, when the critical crack appeared, it was possible to follow its development. An interesting aspect was observing where in the lifetime of the specimen the first critical crack initiation appeared.

By comparing reinforced, unreinforced, short term and long term, it does not seem to be any clear differences on the number of cycles at first observed crack. However, high load levels seems to give shorter lifetime after initial crack, for both reinforced and unreinforced specimens. This trend is more significant for reinforced specimens than unreinforced specimens.

By looking at the percentages of lifetime after initial crack there appear to be no difference between reinforced and unreinforced specimens. A difference of only a couple percent can be seen. By disregarding this, about 85 % of the lifetime happens after the initial crack, which of course means that the initial cracks comes after 15 % of the lifetime. Specimen 7 and specimen 14, both short term, differed from the other tests. The two tests had only 32% and 37% of their lifetime after initial crack. Because they were both short term tests, it is possible to see a trend where short term tests have less percentage of their lifetime after initial cracks, compared to long term. Nevertheless, the data, with two tests showing deviation, is not good enough to conclude.

Specimen	First observed crack	Number of cycles at failure	Lifetime after crack (%)	Average (%)	Comments
7	1940	2870	32,40		Deviation from other results
8	450	7099	93,66	70,22	
9	400	2595	84,59		
10	1400	21675	93,54		
11	273	7821	96,51	95,56	Deviation from other results
12	1568	46404	96,62		No cracks at given cycles
13	1	231	99,59		Deviation from other results
14	3000	4749	36,83	77,47	
15	200	5023	96,02		
16	1000	40523	97,53		
17	600	26040	97,70	97,17	
18	2300	61854	96,28		No cracks at given cycles

By plotting the results, it is possible to see that the number of cycles at failure increases with increasing cycles before crack initiation, as seen below. This trend appears for both reinforced and unreinforced specimens.

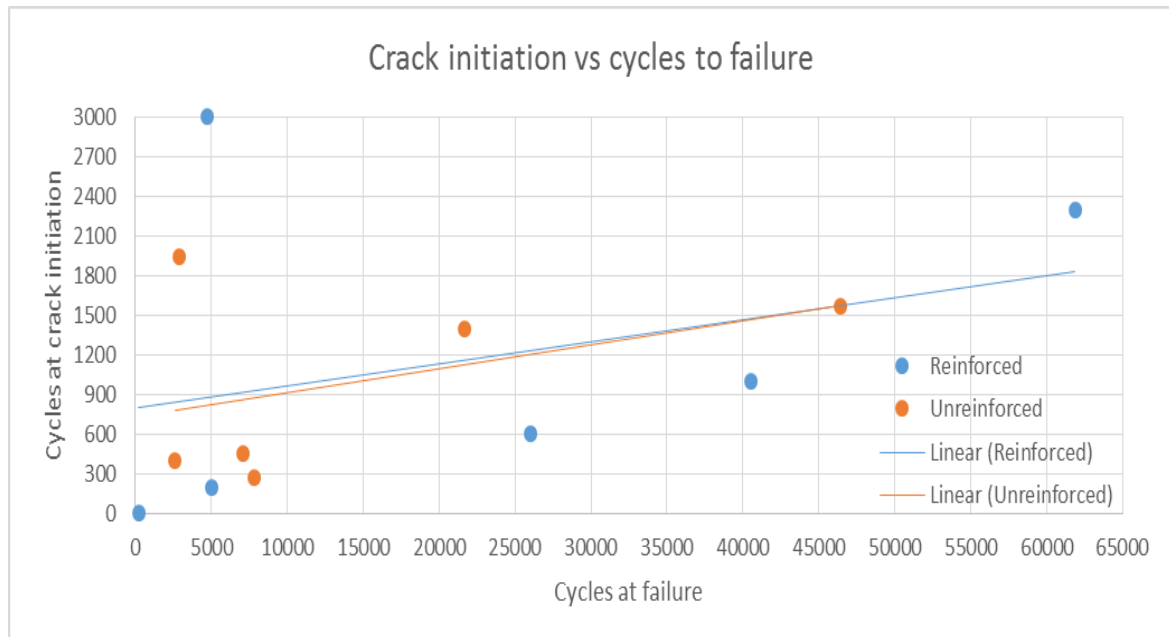


Figure 77 - Crack initiation vs cycles to failure

The fact that the number of cycles at first crack are not exact is of great importance. These are the first cracks observed with periodical observation. The numbers may vary with a couple of hundred cycles. Also, in specimen 12 and 18, there were no cracks at the given number of cycles. These tests were only observed until the given number, without observing any cracks. It is reasonable to assume that the crack appeared later, but this is not taken into account. In which case, the curve for both reinforced and unreinforced would be steeper. In addition, the size of the cracks when noted as initiated, were necessarily not the same. If this is an interesting aspect regarding the testing, it is advantageous to log the strain in concrete to achieve accurate results.

7. Conclusion

7.1 Introduction

The following will be the conclusions made from the tests, static and dynamic, as well as suggestions for further work on the topic.

7.2 Conclusions static tests

- Average static capacity for the unreinforced specimens was 505,8 kN, with a standard deviation of $\pm 37,6$ kN
- Average static capacity for the reinforced specimens was 736,7 kN, with a standard deviation of $\pm 16,9$ kN.
- According to DNV-OS-C502, the effect from partially loaded areas allowed an amplification factor of 1,44 to the compression capacity. As expected, the unreinforced specimens did not show any increase, while the reinforced specimens showed a factor of 1,48. This means that the partial effect from DNV design rules is documented.

NS-EN-1992-1-1 however, allows an amplification factor of 1,73 to the compression capacity. This is far from the factor achieved in this study. Nonetheless, it is reasonable to assume that this study would achieve a factor higher than 1,73 if the amount of reinforcement was sufficient.

- The reinforcement was activated at around 380 kN, which represent 78% of static strength for unreinforced specimens. As expected the reinforcement in the lower layer was activated before the reinforcement in the upper layer.
- In the static tests the critical cracks in the reinforced specimens developed on the outer side of the reinforcement, most likely due to a confining effect from the stirrups that denied the cracks to develop inside the stirrups. In the unreinforced specimens the critical cracks developed in the middle at the top of the specimen and further develop towards the sides. This confirms the confining effect of the stirrups.

7.3 Conclusions dynamic tests

- The C1-factor in the DNV's design code, which takes water into account, seems to be of appropriate scale, as the results were fairly close to the calculated number of cycles with DNV-OS-C502. However, by including concrete strength development in the calculations, C1 seems to be inadequate.

Compared to the results the DNV design code is more conservative regarding specimens tested in air, than specimens tested in water. Most other codes do not even take water into account.

- An effect from partially loaded areas is present in the dynamic life, because the dynamic load levels are based on the static results where the effect of partial loading is present. This is only applicable for the reinforced specimens, as the confinement from the stirrups are essential for this effect.

The proposed partial amplification factor for fatigue of 1,3, is of appropriate scale. However, by including concrete strength development in the calculations, C1 seems to be inadequate for unreinforced specimens. Thus, splitting reinforcement is required.

- The stroke and LVDT lifetime is clearly divided into 3 phases. One non-linear start phase, one linear middle phase and one non-linear end phase. The duration of the three phases varies between the different load levels and type of specimen. The last phase of reinforced specimens represented 10% of its lifetime. In unreinforced specimens, the last phase was almost non-existing, causing sudden failure. Therefore it is important to emphasize the need of a minimum of reinforcement.
- The impact in the strain gauges were generally low in the dynamic tests due to P_{max} (maximum dynamic load) being lower than the static yield load, and crack development outside reinforcement.
- The splitting reinforcement leads to higher static capacity and ductility. Thus dynamic loads can be increased for the same load level compared to unreinforced specimens. The fatigue life (number of cycles before failure) is not particularly affected in any other way.
- The crack patterns in the dynamic tests showed similarities to the static tests. The critical cracks in the reinforced specimens developed outside the reinforcement, while in the middle at the top in the unreinforced specimens.

7.4 Suggestions for further work

- The results in this thesis showed big variations. A higher quantity of specimens will give less uncertainties. A study with tests in water as well as dry will give a better foundation to compare the two types.
- This study included tests with relatively high load levels and low number of load cycles. Tests with lower load levels and a higher number of cycles could have been beneficial.
- To measure the effect of the confinement, the same test should be performed with specimens without confinement as well.

8. References

- Afseth, Jeffrey G. (1993). "High cycle (fatigue) resistance of reinforced concrete beams with lap splices". Master thesis at Department of Civil Engineering, University of Saskatchewan.
- Alexander Furnes and Ole Martin Hauge (2011) "Fatigue capacity of partially loaded areas in concrete structures". Master thesis at Department of Structural Engineering, NTNU, Trondheim, Norway.
- Bères, L (1973). "Failure process of concrete under fatigue loading". Hungarian Institute for Building Science.
- CEB-FIP (2012). "Model Code 2010 Final draft volume 1". International Federation for Structural Concrete (*fib*), Bulletin 65
- CEB-FIP (2012). "Model Code 2010 Final draft volume 2". International Federation for Structural Concrete (*fib*), Bulletin 66
- Claude Bathias and André Pineau (1990). "Fatigue of materials and structures". ISTE Ltd and John Wiley & Sons Inc.
- Claude Bathias and André Pineau (2010). "Fatigue of materials and structures – Fundamentals". ISTE Ltd and John Wiley & Sons Inc.
- C. R. Hendy and D. A. Smith (2007). "Designers guide to EN-1992-2, Eurocode 2: Design of concrete structures, Part 2: Concrete bridges". Thomas Telford Publishing
- Det Norske Veritas (2012). "Offshore standard DNV-OS-C502 Offshore concrete structures". Det Norske Veritas AS.
- EuroLightCon (2000). "Fatigue of normal weight concrete and lightweight concrete". European Union Brite EuRam III.
- European Concrete Platform ASBL (2008). "Commentary to Eurocode 2". European Concrete Platform ASBL
- H. L. Wang & Y. P. Song (2010). "Fatigue capacity of plain concrete under fatigue loading with constant confined stress". *Materials and Structures*, 44.
- Hooi, Tan Teng (2000). "Effects of passive confinement on fatigue properties of concrete". *Magazine of Concrete Research*, 52, No. 1.
- Holmen, Jan Ove (1979). "Fatigue of concrete by constant and variable amplitude loading". Dr.ing dissertation, The Norwegian Institute of Technology, Trondheim.
- Hsu, Thomas T. C. (1984) "Fatigue and microcracking of concrete". *Matériaux et Construction*. Volume 17, Issue 1, pp 51-54.

Jan Arve Øverli, Paula Mayorca, Alexander Furnes and Ole Martin Hauge (2011). "Static and Fatigue Capacity of Partially Loaded Areas in Concrete Structures". Department of Structural Engineering, NTNU, Trondheim, Norway.

John P. Lloyd, James L. Lott and Clyde E. Kesler (1968). "Fatigue of concrete". Urbana, University of Illinois, College of Engineering.

Norges Byggstandardiseringsråd, 6th Edition (2003). "NS 3473 – Design of concrete structures. Design- and detailing rules". Pronorm AS

Payman Ameen & Mikael Szymanski (2006). "Fatigue in Plain Concrete - Phenomenon and Methods of Analysis". Master thesis at Chalmers University of Technology.

S.S. Manson & G.R. Halford (2006). "Fatigue and durability of structural materials". ASM International.

SINTEF (1990). "High strength concrete SP5 – Design application – Report 5.3". Papers prepared and presented by SINTEF FCB and NTH at the Second International Symposium on Utilization of High Strength Concrete in Berkeley, California 1990.

SINTEF (1992). "High strength concrete SP3 – Fatigue – Report 3.2". SINTEF

SINTEF (1993). "High strength concrete SP3 – Fatigue – Report 3.4". SINTEF

SINTEF (1995). "High strength concrete SP5 – Fatigue – Report 5.1". SINTEF

Standard Norway (2008). "NS-EN-1992-1-1:2004+NA:2008, Eurocode 2: Design of concrete structures. Part 1-1: General rules and rules for buildings". Standards Norway

Tokyo Sokki Kenkyujo CO., Ltd, URL: <http://www.tml.jp/e/>

Tarun R. Naik, V.M. Malhotra, Shiw S. Singh, and Bruce W. Ramme (1997). "Flexural fatigue behaviour of concrete containing various sources of fly ash"

9. Attachments

A1 – Calculations of necessary splitting reinforcement	1
A2 – Calculations of centre of gravity of splitting reinforcement	3
A3 – Reinforcement in specimen with splitting reinforcement	4
A4 – Reinforcement in specimen without splitting reinforcement	5
A5 – Compression test of cubes in Trondheim	6
A6 – Fatigue life according to various standards and formulas – unreinforced specimens	8
A7 – Fatigue life according to various standards and formulas – reinforced specimens	12
A8 – Comparison between different SN-curves	16
A9 – Theoretical load level due to concrete strength development	17
A10 – Crack propagation in static tests	23
A11 – Crack propagation in dynamic tests	25

A1 – Calculations of necessary splitting reinforcement

Planned cube-strength of concrete 25 MPa:

$$f_{\text{cm,cube1}} := 25.0 \frac{\text{N}}{\text{mm}^2}$$

$$f_{\text{cm,cylinder1}} := f_{\text{cm,cube1}} \cdot 0.8 = 20 \cdot \frac{\text{N}}{\text{mm}^2}$$

Plate size

$$b_1 := 70\text{mm} \quad d_1 := 210\text{mm}$$

Specimen size

$$b_2 := \min(210\text{mm}, 3 \cdot b_1) = 210\text{mm} \quad d_2 := \min(210\text{mm}, 3 \cdot d_1) = 210\text{mm} \quad h_2 := 525\text{mm}$$

Partial loaded areas

$$A_{\text{c0}} := b_1 \cdot d_1 = 0.015\text{m}^2 \quad A_{\text{c1}} := b_2 \cdot d_2 = 0.044\text{m}^2$$

$$n := \frac{A_{\text{c1}}}{A_{\text{c0}}} = 3$$

$$F_{\text{Rkul}} := \min(A_{\text{c0}} \cdot f_{\text{cm,cylinder1}} \cdot \sqrt{n}, 3.0 f_{\text{cm,cylinder1}} \cdot A_{\text{c0}}) = 509.223\text{kN}$$

Transverse force and reinforcement planned

$$T_{\text{S1}} := \frac{1}{4} \cdot \frac{b_2 - b_1}{b_2} \cdot F_{\text{Rkul}} = 84.87\text{kN}$$

Reinforcement Ø6

$$f_{\text{sk}} := 500 \frac{\text{N}}{\text{mm}^2} \quad A_{\text{s1}} := \frac{T_{\text{S1}}}{f_{\text{sk}}} = 169.741\text{mm}^2 \quad d_{\text{Ø6}} := 6\text{mm}$$

$$A_{\text{sØ6}} := \left(\frac{d_{\text{Ø6}}}{2} \right)^2 \cdot \pi = 28.274\text{mm}^2 \quad n_{\text{Ø6.1}} := \frac{A_{\text{s1}}}{A_{\text{sØ6}}} = 6.003$$

6 reinforcement bars is necessary

Actual cube-strength of concrete: 42,2 MPa:

$$f_{\text{cm,cube1}} := 42.2 \frac{\text{N}}{\text{mm}^2}$$

$$f_{\text{cm,cylinder1}} := f_{\text{cm,cube1}} \cdot 0.8 = 33.76 \frac{\text{N}}{\text{mm}^2}$$

Plate size

$$b_1 := 70\text{mm} \quad d_1 := 210\text{mm}$$

Specimen size

$$b_2 := \min(210\text{mm}, 3 \cdot b_1) = 210\text{mm} \quad d_2 := \min(210\text{mm}, 3 \cdot d_1) = 210\text{mm} \quad h_2 := 525\text{mm}$$

Partial loaded areas

$$A_{\text{c0}} := b_1 \cdot d_1 = 0.015\text{m}^2 \quad A_{\text{c1}} := b_2 \cdot d_2 = 0.044\text{m}^2$$

$$n := \frac{A_{\text{c1}}}{A_{\text{c0}}} = 3$$

$$F_{\text{Rku1}} := \min(A_{\text{c0}} \cdot f_{\text{cm,cylinder1}} \cdot \sqrt{n}, 3.0 f_{\text{cm,cylinder1}} \cdot A_{\text{c0}}) = 859.568\text{kN}$$

Transverse force and reinforcement planned

$$T_{\text{S1}} := \frac{1}{4} \cdot \frac{b_2 - b_1}{b_2} \cdot F_{\text{Rku1}} = 143.261\text{kN}$$

Reinforcement Ø6

$$f_{\text{sk}} := 500 \frac{\text{N}}{\text{mm}^2} \quad A_{\text{s1}} := \frac{T_{\text{S1}}}{f_{\text{sk}}} = 286.523\text{mm}^2 \quad d_{\text{Ø6}} := 6\text{mm}$$

$$A_{\text{sØ6}} := \left(\frac{d_{\text{Ø6}}}{2} \right)^2 \cdot \pi = 28.274\text{mm}^2 \quad n_{\text{Ø6.1}} := \frac{A_{\text{s1}}}{A_{\text{sØ6}}} = 10.134$$

10 reinforcement bars is necessary

A2 – Calculation of centre of gravity of splitting reinforcement

NS-EN 1992-1-1 does not cover this subject. NS 3473 gives us the recommendations

Center of gravity from NS 3473 [12.9.4] should ideally be

$$C_g := \frac{210\text{mm}}{2} = 105\text{mm}$$

In our situation we have 5 layers with 80 mm apart, and the last layer have to be modified to be close to C.g

Distance to first layer: $d_1 := 68\text{mm}$

Distance to second layer: $d_2 := 148\text{mm}$

$d := 6\text{mm}$

$$A_S := \left(\frac{d}{2}\right)^2 \cdot \pi = 28.274\text{mm}^2$$

Splitting reinforcement

$$X_{cg} := \frac{3 \cdot A_S \cdot d_1 + 3 \cdot A_S \cdot d_2}{6 \cdot A_S} = 108\text{mm} \quad \text{OK!}$$

A3 - Reinforcement in specimen with splitting reinforcement

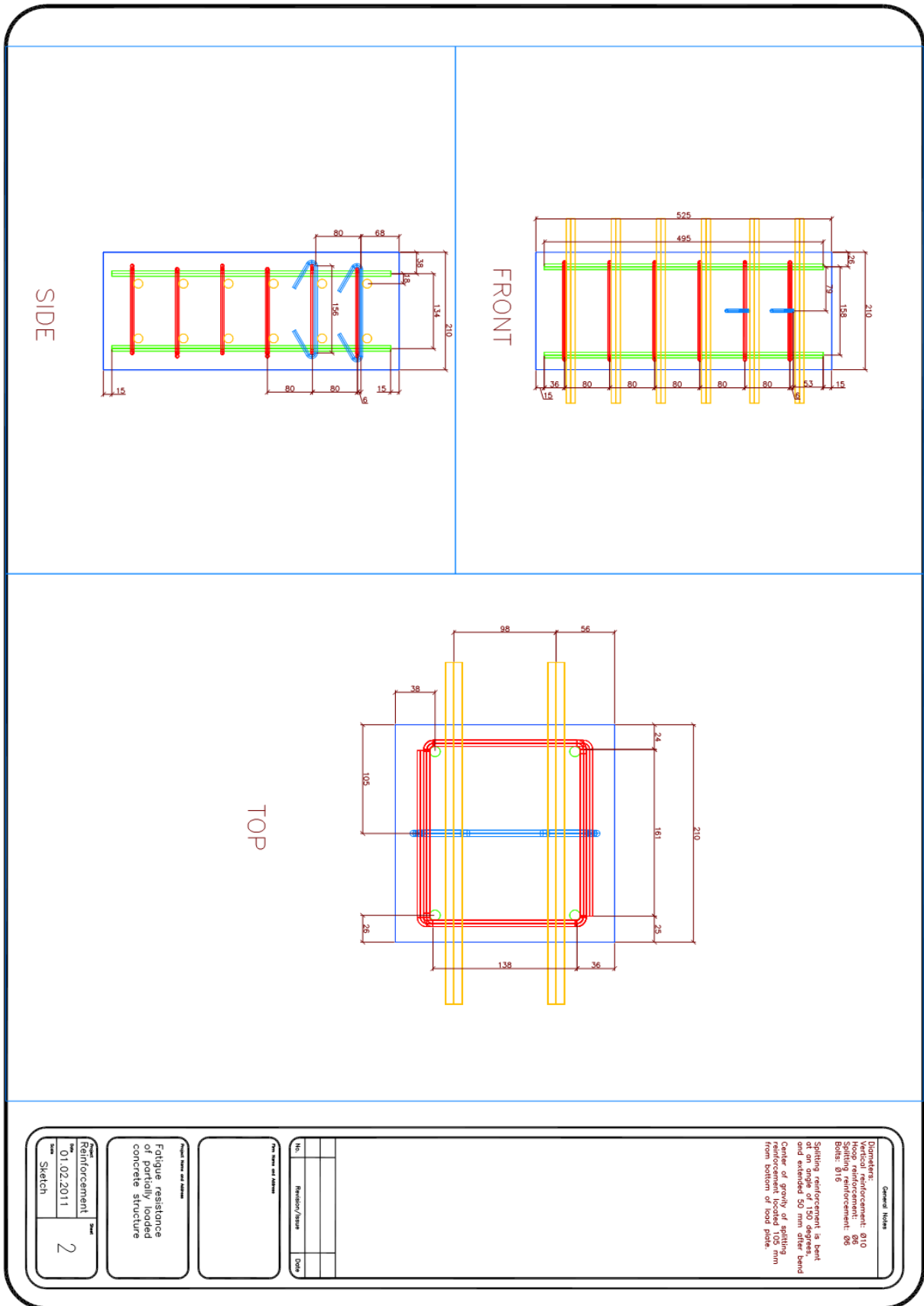


Figure - Reinforcement in specimen with splitting reinforcement. Taken from Furnes and Hauges thesis

A4 - Reinforcement in specimen without splitting reinforcement

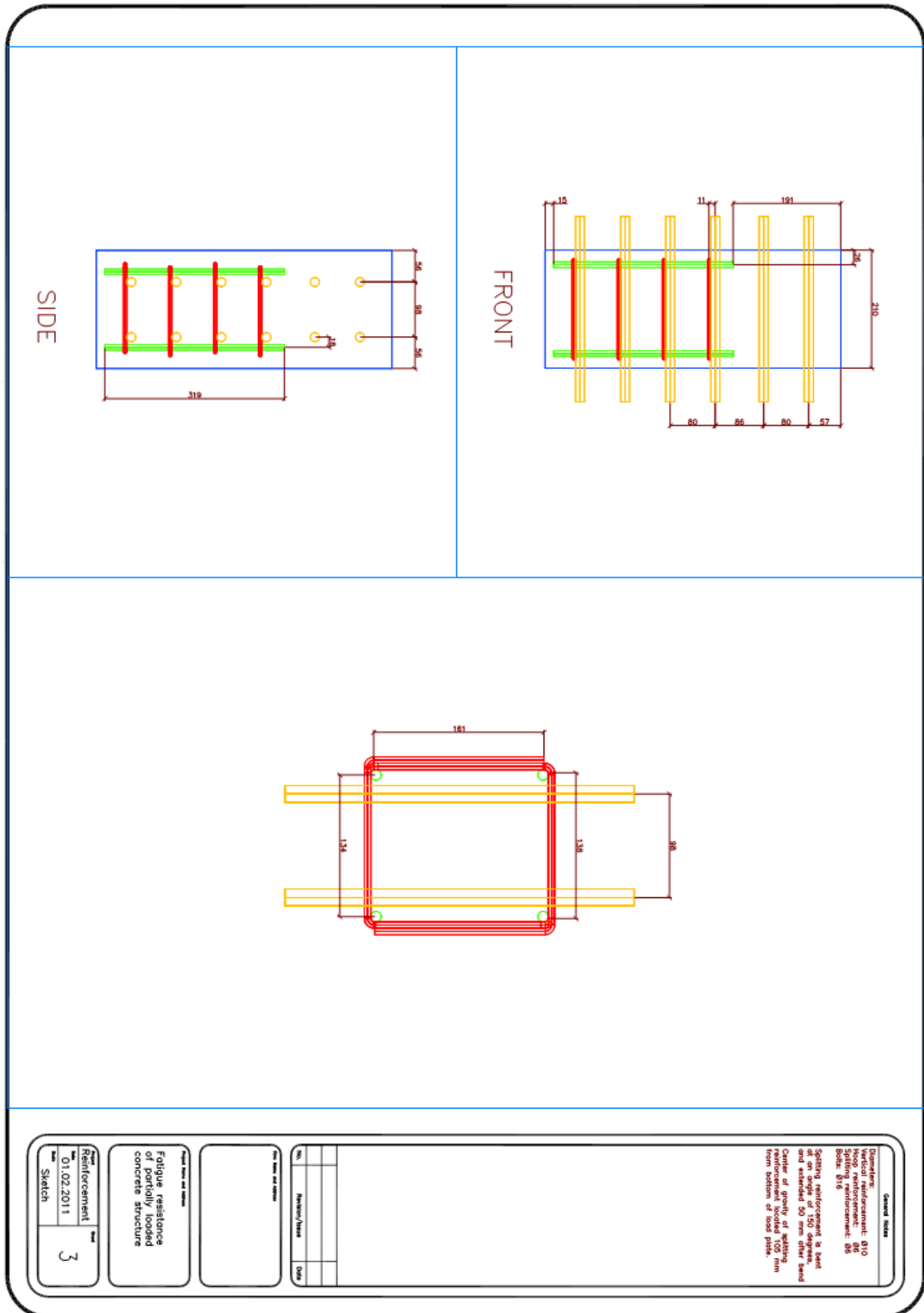


Figure - Reinforcement in specimen without splitting reinforcement. Taken from Furnes and Hauges thesis

A5 – Compression test of cubes in Trondheim

Date	Days since casting	Cube nr.	Failure load (MPa)	Average (MPa)	Cylinder strenght (MPa)
05.03.2014		1,1	42,76		
05.03.2014	33	1,2	41,26	42,20333333	33,76266667
05.03.2014		1,3	42,59		
06.03.2014		2,1	41,97		
06.03.2014	34	2,2	40,45	41,39	33,112
06.03.2014		2,3	41,75		
07.03.2014		3,1	42,69		
07.03.2014	35	3,2	41,68	42,17333333	33,73866667
07.03.2014		3,3	42,15		
10.03.2014		4,1	43,32		
10.03.2014	38	4,2	42,92	42,95333333	34,36266667
10.03.2014		4,3	42,62		
11.03.2014		5,1	46,4		
11.03.2014	39	5,2	42,78	43,53333333	34,82666667
11.03.2014		5,3	41,42		
12.03.2014		6,1	44,23		
12.03.2014	40	6,2	42,5	44,18666667	35,34933333
12.03.2014		6,3	45,83		
14.03.2014		7,1	42,61		
14.03.2014	42	7,2	43,78	43,28333333	34,62666667
14.03.2014		7,3	43,46		
18.03.2014		8,1	45,97		
18.03.2014	46	8,2	45,3	45,26666667	36,21333333
18.03.2014		8,3	44,53		
19.03.2014		9,1	44,12		
19.03.2014	47	9,2	45,56	43,95	35,16
19.03.2014		9,3	42,17		
20.03.2014		10,1	44,86		
20.03.2014	48	10,2	44,61	44,76333333	35,81066667
20.03.2014		10,3	44,82		
21.03.2014		11,1	42,4		
21.03.2014	49	11,2	43,07	43,42333333	34,73866667
21.03.2014		11,3	44,8		

25.03.2014		12,1	45,53		
25.03.2014	53	12,2	46,04	45,84666667	36,67733333
25.03.2014		12,3	45,97		
27.03.2014		13,1	45,29		
27.03.2014	55	13,2	44,84	44,85333333	35,88266667
27.03.2014		13,3	44,43		
28.03.2014		14,1	46,11		
28.03.2014	56	14,2	45,28	46,19	36,952
28.03.2014		14,3	47,18		
31.03.2014		15,1	47,39		
31.03.2014	59	15,2	47,4	47,41333333	37,93066667
31.03.2014		15,3	47,45		
01.04.2014		16,1	47,23		
01.04.2014	60	16,2	46,97	46,78	37,424
01.04.2014		16,3	46,14		

Mean cube strength 44,26 MPa
 Mean cylinder strength 35,41 MPa

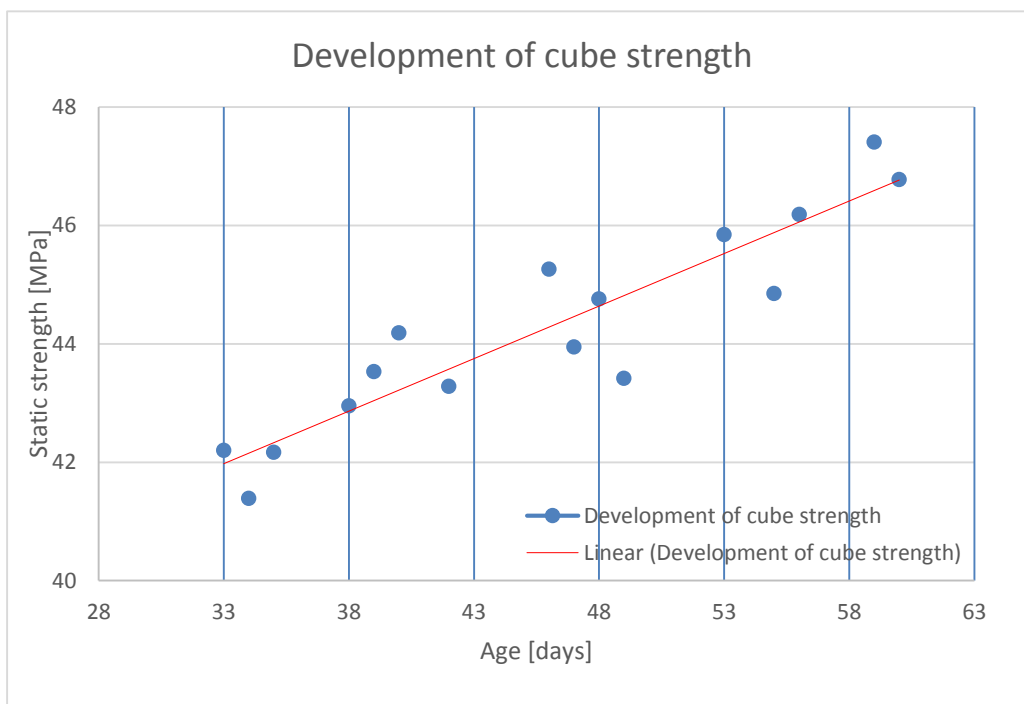


Figure - Development of cube strength

A6 – Fatigue life according to various standards and formulas – unreinforced specimens

According to DNV-OS-C502

- $C_5 := 1.0$ for concrete
- $C_1 := 10.0$ for structures in water for those stress-blocks having stress variation in the compression-compression range
- $f_{rd} := 505.6$ the compression strength for the type of failure in question
- $\sigma_{max} := 505.6$ the numerically largest compressive stress, calculated as the average value within each stress-block
- $\sigma_{min} := 50.6$ the numerically least compressive stress, calculated as the average value within each stress-block

$$\log N := C_1 \cdot \left(\frac{1 - \frac{\sigma_{max}}{C_5 \cdot f_{rd}}}{1 - \frac{\sigma_{min}}{C_5 \cdot f_{rd}}} \right)$$

$$\sigma_{max1} := \begin{pmatrix} 0.6 \\ 0.625 \\ 0.65 \\ 0.675 \\ 0.7 \\ 0.725 \\ 0.75 \\ 0.775 \\ 0.8 \\ 0.825 \\ 0.85 \end{pmatrix} \cdot \sigma_{max} =$$

	0
0	303.36
1	316
2	328.64
3	341.28
4	353.92
5	366.56
6	379.2
7	391.84
8	404.48
9	417.12
10	429.76

$$\sigma_{min1} := \begin{pmatrix} 0.1 \\ 0.1 \\ 0.1 \\ 0.1 \\ 0.1 \\ 0.1 \\ 0.1 \\ 0.1 \\ 0.1 \\ 0.1 \end{pmatrix} \cdot \sigma_{max}$$

$$N_1 := 10 \cdot C_1 \cdot \left(\frac{1 - \frac{\sigma_{max1}}{C_5 \cdot f_{rd}}}{1 - \frac{\sigma_{min}}{C_5 \cdot f_{rd}}} \right) =$$

	27851
	14690
	7749
	4087
	2156
	1137
	600
	316
	167
	88
	46

If the calculated design life log N is larger than the value of X given by the expression

$$X_1 := \frac{C_1}{1 - \frac{\sigma_{\min}}{C_5 \cdot f_{td}} + 0.1 \cdot C_1} = 5.263 \qquad 10^{X_1} = 1.834 \times 10^5 > N$$

Jan Ove Holmen formula

$$S_{\min} := 0.10 \qquad \sigma_{\max 2} := \sigma_{\max 1}$$

$$S_{\max} := \begin{pmatrix} 0.6 \\ 0.625 \\ 0.65 \\ 0.675 \\ 0.7 \\ 0.725 \\ 0.75 \\ 0.775 \\ 0.8 \\ 0.825 \\ 0.85 \end{pmatrix}$$

$$\log N_2 := (1 - S_{\max}) \cdot (12 + 16 \cdot S_{\min} + 8 \cdot S_{\min}^2) =$$

	0
0	5.472
1	5.13
2	4.788
3	4.446
4	4.104
5	3.762
6	3.42
7	3.078
8	2.736
9	2.394
10	2.052

$$N_2 := 10^{\log N_2} =$$

	0
0	2.965 · 10 ⁵
1	1.349 · 10 ⁵
2	6.138 · 10 ⁴
3	2.793 · 10 ⁴
4	1.271 · 10 ⁴
5	5.781 · 10 ³
6	2.63 · 10 ³
7	1.197 · 10 ³
8	544.503
9	247.742
10	112.72

Aas-Jakobsens formel - for ordinary and lightweight concrete

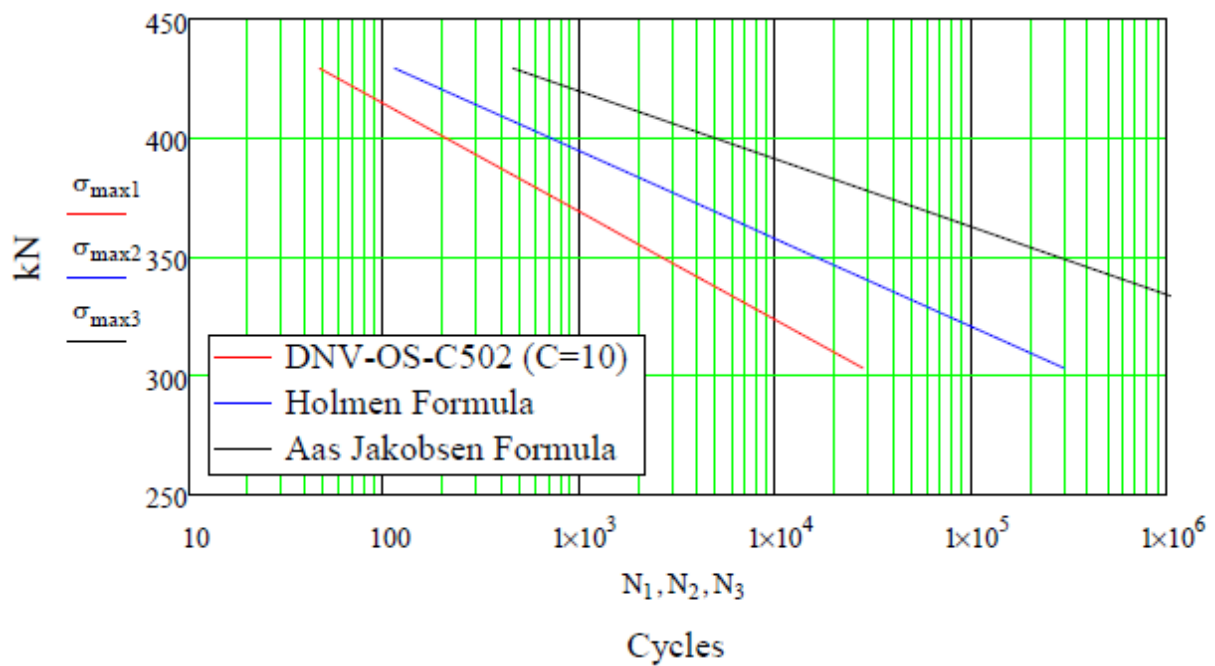
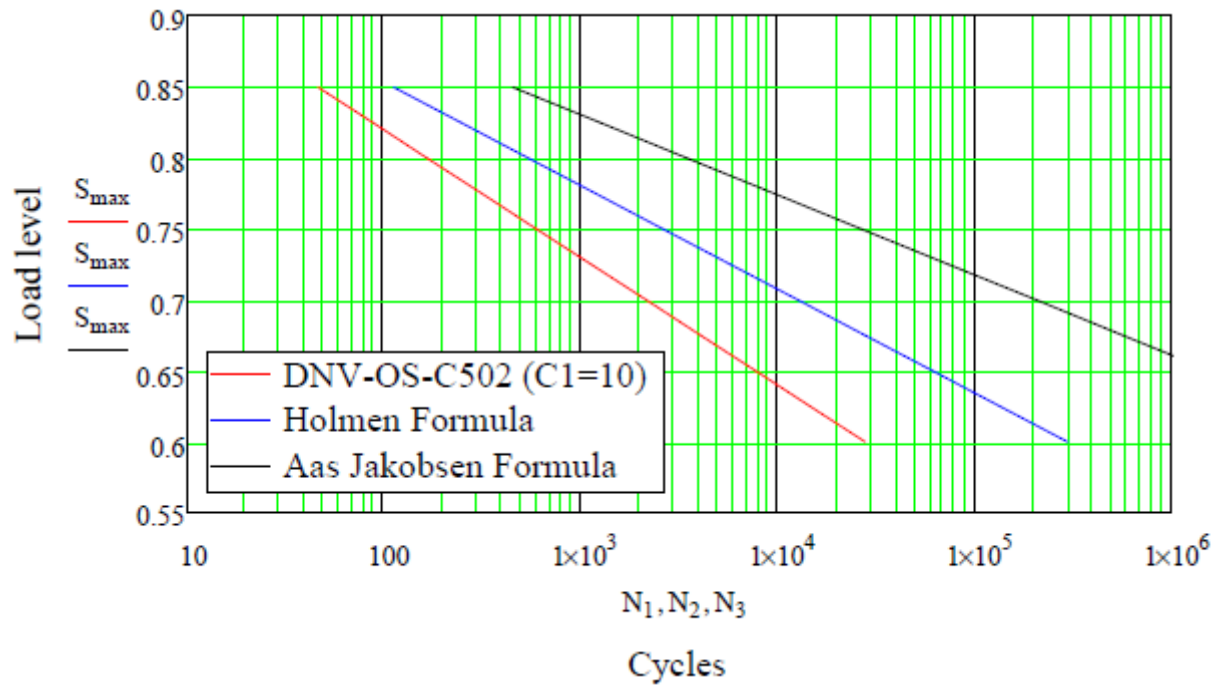
$$\beta := 0.064 \quad \beta_{alt} := 0.0685 \quad \sigma_{max3} := \sigma_{max1} \quad \sigma_{min} = 50.6 \quad \sigma_{rd} := \sigma_{max1} \quad f_c := f_{rd}$$

$$\frac{\sigma_{cdmax}}{f_c} := 1 - \beta(1 - R) \log N_3$$

$$R_1 := \frac{\sigma_{min}}{\sigma_{max3,10}} = 0.118$$

$$\log N_3 := \left(\frac{\sigma_{max1}}{f_c} - 1 \right) \cdot \frac{1}{-\beta \cdot (1 - R_1)} = \begin{pmatrix} 7.08 \\ 6.64 \\ 6.2 \\ 5.76 \\ 5.31 \\ 4.87 \\ 4.43 \\ 3.98 \\ 3.54 \\ 3.1 \\ 2.66 \end{pmatrix}$$

$$N_3 := 10^{\log N_3} = \begin{pmatrix} 1 \times 10^7 \\ 4 \times 10^6 \\ 2 \times 10^6 \\ 569922 \\ 205618 \\ 74183 \\ 26764 \\ 9656 \\ 3484 \\ 1257 \\ 453 \end{pmatrix}$$



A7 – Fatigue life according to various standards – reinforced specimens

According to DNVV-OS-C502

$$C_5 := 1.0$$

For concrete:

$$C_1 := 10.0$$

for structures in water for those stress-blocks having stress variation in the compression-compression range

$$f_{rd} := 736.7$$

the compression strength for the type of failure in question

$$\sigma_{max} := 736.7$$

the numerically largest compressive stress, calculated as the average value within each stress-block

$$\sigma_{min} := 73.6$$

the numerically least compressive stress, calculated as the average value within each stress-block

$$\log N := C_1 \cdot \left(\frac{1 - \frac{\sigma_{max}}{C_5 \cdot f_{rd}}}{1 - \frac{\sigma_{min}}{C_5 \cdot f_{rd}}} \right)^{C_5} \cdot \sigma_{max1} := \begin{pmatrix} 0.6 \\ 0.625 \\ 0.65 \\ 0.675 \\ 0.7 \\ 0.725 \\ 0.75 \\ 0.775 \\ 0.8 \\ 0.825 \\ 0.85 \end{pmatrix} \cdot \sigma_{max} = \begin{matrix} & 0 \\ 0 & 442.02 \\ 1 & 460.438 \\ 2 & 478.855 \\ 3 & 497.273 \\ 4 & 515.69 \\ 5 & 534.108 \\ 6 & 552.525 \\ 7 & 570.942 \\ 8 & 589.36 \\ 9 & 607.778 \\ 10 & 626.195 \end{matrix} \cdot \sigma_{min1} := \begin{pmatrix} 0.1 \\ 0.1 \\ 0.1 \\ 0.1 \\ 0.1 \\ 0.1 \\ 0.1 \\ 0.1 \\ 0.1 \\ 0.1 \\ 0.1 \end{pmatrix} \cdot \sigma_{max}$$

$$N_1 := 10 \cdot C_1 \cdot \left(\frac{1 - \frac{\sigma_{max1}}{C_5 \cdot f_{rd}}}{1 - \frac{\sigma_{min}}{C_5 \cdot f_{rd}}} \right)^{C_5} = \begin{pmatrix} 27796 \\ 14663 \\ 7735 \\ 4081 \\ 2153 \\ 1136 \\ 599 \\ 316 \\ 167 \\ 88 \\ 46 \end{pmatrix}$$

If the calculated design life $\log N$ is larger than the value of X given by the expressior

$$X_1 := \frac{C_1}{1 - \frac{\sigma_{\min}}{C_5 \cdot f_{td}} + 0.1 \cdot C_1} = 5.263$$

$$10^{X_1} = 1.832 \times 10^5 > N$$

Formula proposed by Jan Ove Holmen

$$S_{\min} := 0.10 \quad \sigma_{\max 2} := \sigma_{\max 1}$$

$$S_{\max} := \begin{pmatrix} 0.6 \\ 0.625 \\ 0.65 \\ 0.675 \\ 0.7 \\ 0.725 \\ 0.75 \\ 0.775 \\ 0.8 \\ 0.825 \\ 0.85 \end{pmatrix} \quad \log N_2 := (1 - S_{\max}) \cdot (12 + 16 \cdot S_{\min} + 8 \cdot S_{\min}^2) =$$

	0
0	5.472
1	5.13
2	4.788
3	4.446
4	4.104
5	3.762
6	3.42
7	3.078
8	2.736
9	2.394
10	2.052

$$N_2 := 10^{\log N_2} =$$

	0
0	$2.965 \cdot 10^5$
1	$1.349 \cdot 10^5$
2	$6.138 \cdot 10^4$
3	$2.793 \cdot 10^4$
4	$1.271 \cdot 10^4$
5	$5.781 \cdot 10^3$
6	$2.63 \cdot 10^3$
7	$1.197 \cdot 10^3$
8	544.503
9	247.742
10	112.72

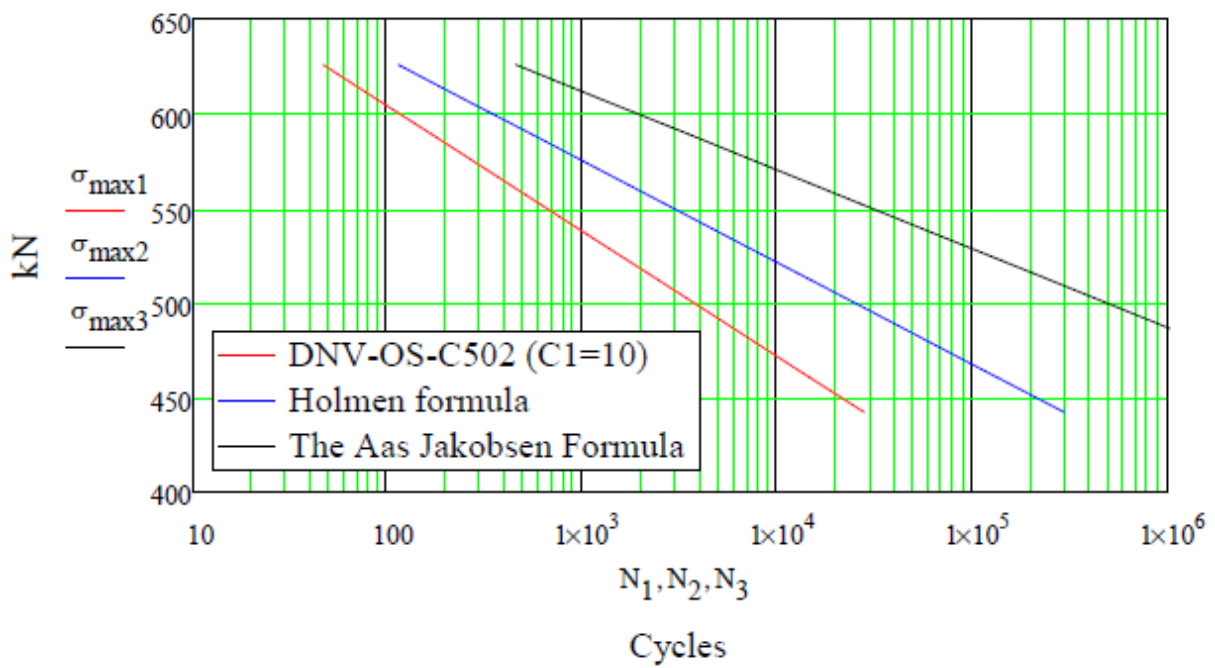
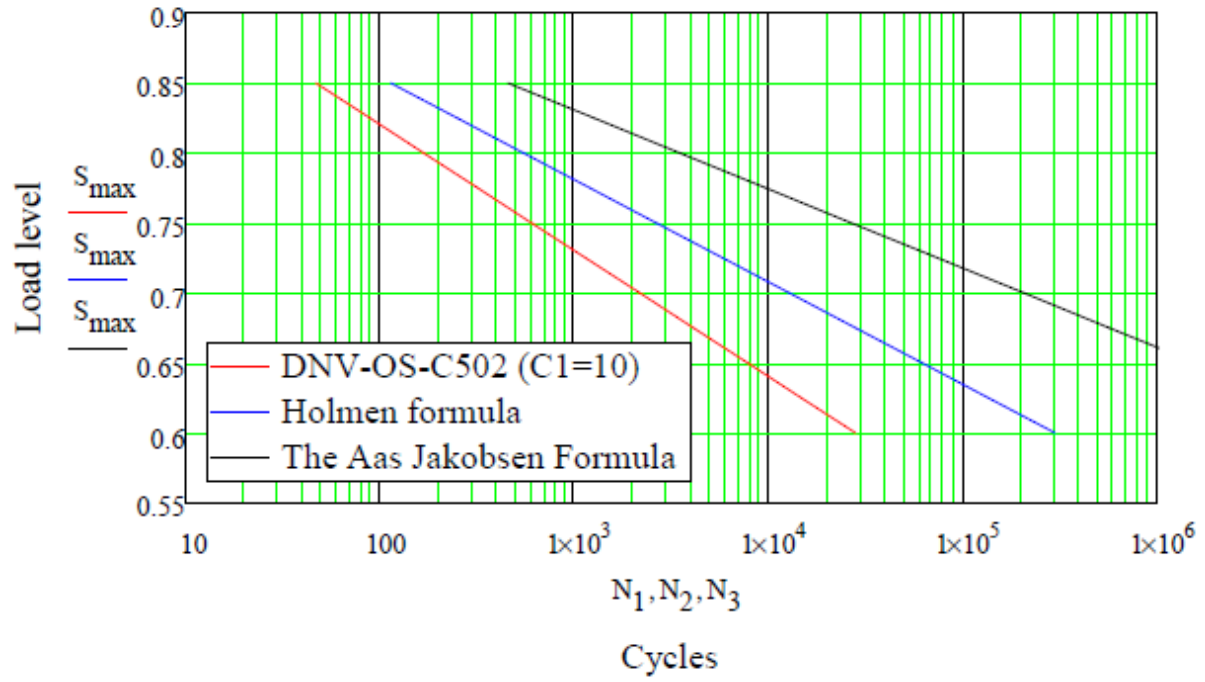
Aas-Jakobsens formel - for ordinary and lightweight concrete

$$\beta := 0.064 \quad \beta_{alt} := 0.0685 \quad \sigma_{max3} := \sigma_{max1} \quad \sigma_{min} = 73.6 \quad \sigma_{rd} := \sigma_{max1}$$

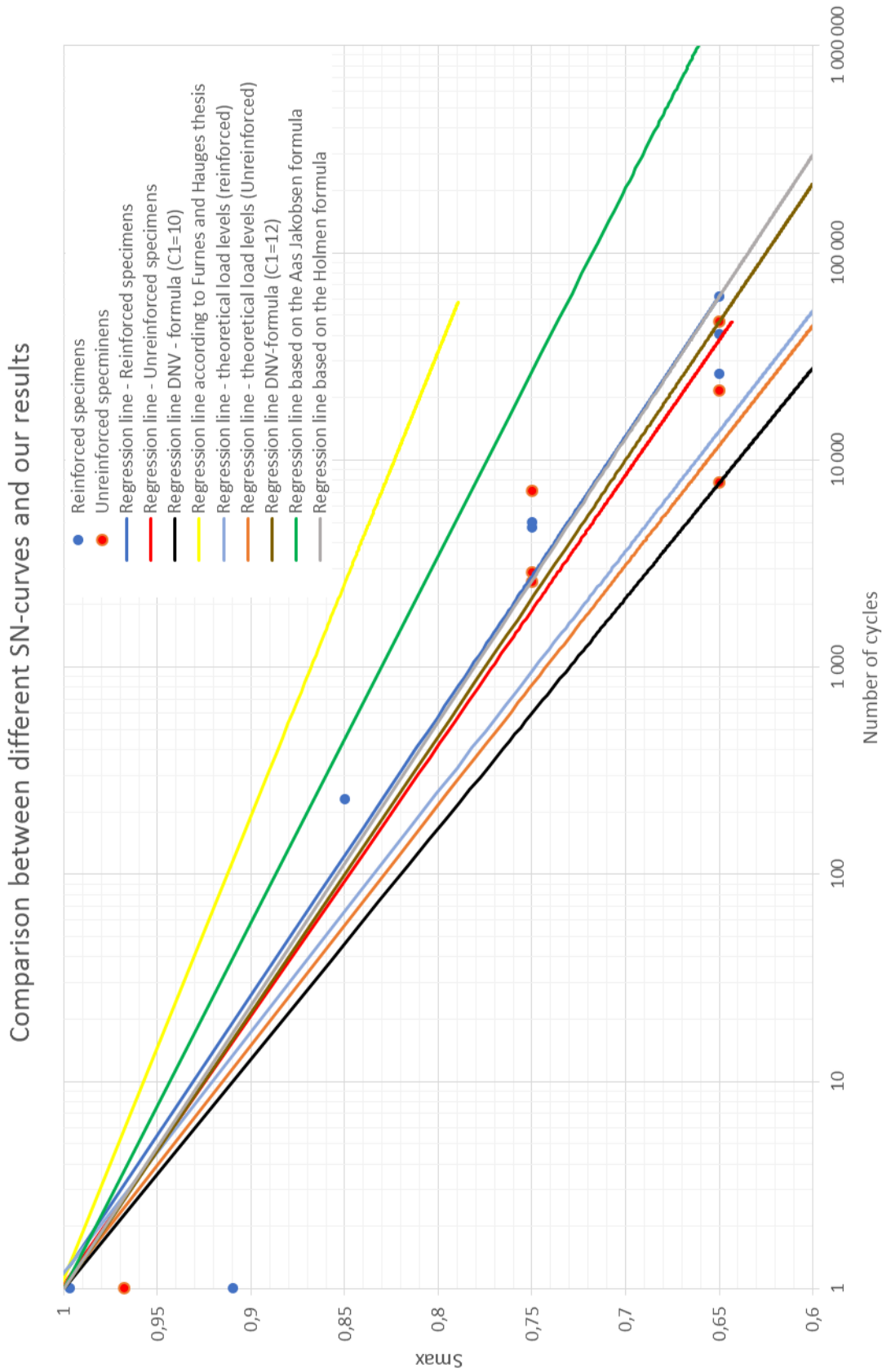
$$f_c := f_{rd} \quad \sigma_{rd} := 0.8 \cdot f_c = 589.36$$

$$\frac{\sigma_{cdmax}}{f_c} := 1 - \beta(1 - R) \log N_3 \quad R_1 := \frac{\sigma_{min}}{\sigma_{max3_{10}}} = 0.118$$

$$\log N_3 := \left(\frac{\sigma_{max1}}{f_c} - 1 \right) \cdot \frac{1}{-\beta \cdot (1 - R_1)} = \begin{pmatrix} 7.08 \\ 6.64 \\ 6.2 \\ 5.75 \\ 5.31 \\ 4.87 \\ 4.43 \\ 3.98 \\ 3.54 \\ 3.1 \\ 2.66 \end{pmatrix} \quad N_3 := 10^{\log N_3} = \begin{pmatrix} 1 \times 10^7 \\ 4 \times 10^6 \\ 2 \times 10^6 \\ 568171 \\ 205035 \\ 73990 \\ 26701 \\ 9635 \\ 3477 \\ 1255 \\ 453 \end{pmatrix}$$



A8 - Comparison between different SN-curves



A9 – Theoretical load levels

Actual strenght of concrete

$$f_{\text{cm.cube.reinforced}} := \begin{pmatrix} 43.53 \\ 43.28 \\ 45.27 \\ 46.19 \\ 47.41 \\ 46.78 \end{pmatrix} \frac{\text{N}}{\text{mm}^2} \quad f_{\text{cm.cylinder1}} := f_{\text{cm.cube.reinforced}} \cdot 0.8 = \begin{pmatrix} 34.824 \\ 34.624 \\ 36.216 \\ 36.952 \\ 37.928 \\ 37.424 \end{pmatrix} \frac{\text{N}}{\text{mm}^2}$$

$$f_{\text{cm.cube.unrein}} := \begin{pmatrix} 43.95 \\ 44.76 \\ 43.42 \\ 45.85 \\ 44.85 \\ 44.85 \end{pmatrix} \frac{\text{N}}{\text{mm}^2} \quad f_{\text{cm.cylinder2}} := f_{\text{cm.cube.unrein}} \cdot 0.8 = \begin{pmatrix} 35.16 \\ 35.808 \\ 34.736 \\ 36.68 \\ 35.88 \\ 35.88 \end{pmatrix} \frac{\text{N}}{\text{mm}^2}$$

Plate size

$$b_1 := 70\text{mm} \quad d_1 := 210\text{mm}$$

Specimen size

$$b_2 := \min(210\text{mm}, 3 \cdot b_1) = 210\text{mm} \quad d_2 := \min(210\text{mm}, 3 \cdot d_1) = 210\text{mm} \quad h_2 := 525\text{mm}$$

Partially loaded areas

$$A_{c0} := b_1 \cdot d_1 = 0.015\text{m}^2 \quad A_{c1} := b_2 \cdot d_2 = 0.044\text{m}^2$$

For armerte
 $n_r := 1.476666666$

For uarmerte
 $n_u := 1.0$

$$F_{\text{Rku1.rein}} := (A_{c0} \cdot f_{\text{cm.cylinder1}} \cdot n_r) = \begin{pmatrix} 755.925 \\ 751.583 \\ 786.141 \\ 802.117 \\ 823.303 \\ 812.363 \end{pmatrix} \cdot \text{kN}$$

$$F_{Rku2.rein} := 3.0 \cdot f_{cm.cylinder1} \cdot A_{c0} = \begin{pmatrix} 1535.7 \\ 1526.9 \\ 1597.1 \\ 1629.6 \\ 1672.6 \\ 1650.4 \end{pmatrix} \cdot \text{kN}$$

$$F_{Rku1.unrein} := (A_{c0} \cdot f_{cm.cylinder2} \cdot n_u) = \begin{pmatrix} 527.189 \\ 536.905 \\ 520.832 \\ 549.98 \\ 537.985 \\ 537.985 \end{pmatrix} \cdot \text{kN}$$

$$F_{Rku2.unrein} := 3.0 \cdot f_{cm.cylinder2} \cdot A_{c0} = \begin{pmatrix} 1550.6 \\ 1579.1 \\ 1531.9 \\ 1617.6 \\ 1582.3 \\ 1582.3 \end{pmatrix} \cdot \text{kN}$$

Theoretical load levels due to development of cube strength

Reinforced

0.85 = 625.5kN

0.75 = 551.9kN

0.65 = 478.9kN

$$L_1 := \frac{625.5 \text{ kN}}{F_{Rku1.rein_0}} = 0.827$$

$$L_4 := \frac{478.9 \text{ kN}}{F_{Rku1.rein_3}} = 0.597$$

$$L_2 := \frac{551.9 \text{ kN}}{F_{Rku1.rein_1}} = 0.734$$

$$L_5 := \frac{478.9 \text{ kN}}{F_{Rku1.rein_4}} = 0.582$$

$$L_3 := \frac{551.9 \text{ kN}}{F_{Rku1.rein_2}} = 0.702$$

$$L_6 := \frac{478.9 \text{ kN}}{F_{Rku1.rein_5}} = 0.59$$

Unreinforced

$$0.75 = 379.4\text{kN}$$

$$0.65 = 328.8\text{kN}$$

$$L_{u1} := \frac{379.4\text{kN}}{F_{Rkul.unrein_0}} = 0.72$$

$$L_{u4} := \frac{328.8\text{kN}}{F_{Rkul.unrein_3}} = 0.598$$

$$L_{u2} := \frac{379.4\text{kN}}{F_{Rkul.unrein_1}} = 0.707$$

$$L_{u5} := \frac{328.8\text{kN}}{F_{Rkul.unrein_4}} = 0.611$$

$$L_{u3} := \frac{379.4\text{kN}}{F_{Rkul.unrein_2}} = 0.728$$

$$L_{u6} := \frac{328.8\text{kN}}{F_{Rkul.unrein_5}} = 0.611$$

$$L_{rein} := \begin{pmatrix} L_1 \\ L_2 \\ L_3 \\ L_4 \\ L_5 \\ L_6 \end{pmatrix} = \begin{pmatrix} 0.827 \\ 0.734 \\ 0.702 \\ 0.597 \\ 0.582 \\ 0.59 \end{pmatrix}$$

$$L_{unrein} := \begin{pmatrix} L_{u1} \\ L_{u2} \\ L_{u3} \\ L_{u4} \\ L_{u5} \\ L_{u6} \end{pmatrix} = \begin{pmatrix} 0.72 \\ 0.707 \\ 0.728 \\ 0.598 \\ 0.611 \\ 0.611 \end{pmatrix}$$

Actual load levels with a partial factor = 1,3 and strengt development

Actual strengt of concrete

$$f_{cm.cube.reinforced} := \begin{pmatrix} 43.53 \\ 43.28 \\ 45.27 \\ 46.19 \\ 47.41 \\ 46.78 \end{pmatrix} \frac{\text{N}}{\text{mm}^2}$$

$$f_{cm.cylinder1} := f_{cm.cube.reinforced} \cdot 0.8 = \begin{pmatrix} 34.824 \\ 34.624 \\ 36.216 \\ 36.952 \\ 37.928 \\ 37.424 \end{pmatrix} \frac{\text{N}}{\text{mm}^2}$$

$$f_{cm.cube.unrein} := \begin{pmatrix} 43.95 \\ 44.76 \\ 43.42 \\ 45.85 \\ 44.85 \\ 44.85 \end{pmatrix} \frac{\text{N}}{\text{mm}^2}$$

$$f_{cm.cylinder2} := f_{cm.cube.unrein} \cdot 0.8 = \begin{pmatrix} 35.16 \\ 35.808 \\ 34.736 \\ 36.68 \\ 35.88 \\ 35.88 \end{pmatrix} \frac{\text{N}}{\text{mm}^2}$$

Plate size

$$b_1 := 70\text{mm} \quad d_1 := 210\text{mm}$$

Specimen size

$$b_2 := \min(210\text{mm}, 3 \cdot b_1) = 210\text{mm}$$

$$d_2 := \min(210\text{mm}, 3 \cdot d_1) = 210\text{mm}$$

$$h_2 := 525\text{mm}$$

Partially loaded areas

$$A_{c0} := b_1 \cdot d_1 = 0.015\text{m}^2 \quad A_{c1} := b_2 \cdot d_2 = 0.044\text{m}^2$$

For reinforced

$$n_r := 1.3$$

For unreinforced

$$n_u := 1.0$$

$$F_{Rku1.rein} := (A_{c0} \cdot f_{cm.cylinder1} \cdot n_r) = \begin{pmatrix} 665.487 \\ 661.665 \\ 692.088 \\ 706.153 \\ 724.804 \\ 715.173 \end{pmatrix} \cdot \text{kN}$$

$$F_{Rku2.rein} := 3.0 \cdot f_{cm.cylinder1} \cdot A_{c0} = \begin{pmatrix} 1535.7 \\ 1526.9 \\ 1597.1 \\ 1629.6 \\ 1672.6 \\ 1650.4 \end{pmatrix} \cdot \text{kN}$$

$$F_{Rku1.unrein} := (A_{c0} \cdot f_{cm.cylinder2} \cdot n_u) = \begin{pmatrix} 516.852 \\ 526.378 \\ 510.619 \\ 539.196 \\ 527.436 \\ 527.436 \end{pmatrix} \cdot \text{kN}$$

$$F_{Rku2.unrein} := 3.0 \cdot f_{cm.cylinder2} \cdot A_{c0} = \begin{pmatrix} 1550.6 \\ 1579.1 \\ 1531.9 \\ 1617.6 \\ 1582.3 \\ 1582.3 \end{pmatrix} \cdot \text{kN}$$

Theoretical load levels due to development of cube strength

Reinforced specimens

$$L_1 := \frac{625.5 \text{ kN}}{F_{Rkul.rein_0}} = 0.94$$

$$L_4 := \frac{478.9 \text{ kN}}{F_{Rkul.rein_3}} = 0.678$$

$$L_2 := \frac{551.9 \text{ kN}}{F_{Rkul.rein_1}} = 0.834$$

$$L_5 := \frac{478.9 \text{ kN}}{F_{Rkul.rein_4}} = 0.661$$

$$L_3 := \frac{551.9 \text{ kN}}{F_{Rkul.rein_2}} = 0.797$$

$$L_6 := \frac{478.9 \text{ kN}}{F_{Rkul.rein_5}} = 0.67$$

Unreinforced specimens

$$L_{u1} := \frac{379.4 \text{ kN}}{F_{Rkul.unrein_0}} = 0.734$$

$$L_{u4} := \frac{328.8 \text{ kN}}{F_{Rkul.unrein_3}} = 0.61$$

$$L_{u2} := \frac{379.4 \text{ kN}}{F_{Rkul.unrein_1}} = 0.721$$

$$L_{u5} := \frac{328.8 \text{ kN}}{F_{Rkul.unrein_4}} = 0.623$$

$$L_{u3} := \frac{379.4 \text{ kN}}{F_{Rkul.unrein_2}} = 0.743$$

$$L_{u6} := \frac{328.8 \text{ kN}}{F_{Rkul.unrein_5}} = 0.623$$

$$L_{rein} := \begin{pmatrix} L_1 \\ L_2 \\ L_3 \\ L_4 \\ L_5 \\ L_6 \end{pmatrix} = \begin{pmatrix} 0.94 \\ 0.834 \\ 0.797 \\ 0.678 \\ 0.661 \\ 0.67 \end{pmatrix}$$

$$L_{unrein} := \begin{pmatrix} L_{u1} \\ L_{u2} \\ L_{u3} \\ L_{u4} \\ L_{u5} \\ L_{u6} \end{pmatrix} = \begin{pmatrix} 0.734 \\ 0.721 \\ 0.743 \\ 0.61 \\ 0.623 \\ 0.623 \end{pmatrix}$$

Actual load levels with a partial factor = 1,3 and fck.cube=42,2Mpa

Strength of concrete after 28 days

$$f_{cm.cube.reinforced} := 42.2 \frac{\text{N}}{\text{mm}^2}$$

$$f_{cm.cylinder1} := f_{cm.cube.reinforced} \cdot 0.8 = 33.76 \frac{\text{N}}{\text{mm}^2}$$

$$f_{cm.cube.unrein} := 42.2 \frac{\text{N}}{\text{mm}^2}$$

$$f_{cm.cylinder2} := f_{cm.cube.unrein} \cdot 0.8 = 33.76 \frac{\text{N}}{\text{mm}^2}$$

Plate size

$$b_1 := 70 \text{ mm} \quad d_1 := 210 \text{ mm}$$

Specimen size

$$b_2 := \min(210 \text{ mm}, 3 \cdot b_1) = 210 \text{ mm} \quad d_2 := \min(210 \text{ mm}, 3 \cdot d_1) = 210 \text{ mm} \quad h_2 := 525 \text{ mm}$$

Partially loaded areas

$$A_{c0} := b_1 \cdot d_1 = 0.015 \text{ m}^2 \quad A_{c1} := b_2 \cdot d_2 = 0.044 \text{ m}^2$$

Partial factor

Reinforced specimens Unreinforced specimens
 $n_r := 1.3$ $n_u := 1.0$

Calculated capacity of specimens

$$F_{Rku1.rein} := (A_{c0} \cdot f_{cm.cylinder1} \cdot n_r) = 645.154 \text{ kN}$$

$$F_{Rku2.rein} := 3.0 \cdot f_{cm.cylinder1} \cdot A_{c0} = 1488.8 \text{ kN}$$

$$F_{Rku1.unrein} := (A_{c0} \cdot f_{cm.cylinder2} \cdot n_u) = 496.272 \text{ kN}$$

$$F_{Rku2.unrein} := 3.0 \cdot f_{cm.cylinder2} \cdot A_{c0} = 1488.8 \text{ kN}$$

Reinforced specimens

$$L_1 := \frac{625.5 \text{ kN}}{F_{Rku1.rein}} = 0.97 \qquad L_4 := \frac{478.9 \text{ kN}}{F_{Rku1.rein}} = 0.742$$

$$L_2 := \frac{551.9 \text{ kN}}{F_{Rku1.rein}} = 0.855 \qquad L_5 := \frac{478.9 \text{ kN}}{F_{Rku1.rein}} = 0.742$$

$$L_3 := \frac{551.9 \text{ kN}}{F_{Rku1.rein}} = 0.855 \qquad L_6 := \frac{478.9 \text{ kN}}{F_{Rku1.rein}} = 0.742$$

Unreinforced specimens







$$L_{u1} := \frac{379.4 \text{ kN}}{F_{Rku1.unrein}} = 0.765 \qquad L_{u4} := \frac{328.8 \text{ kN}}{F_{Rku1.unrein}} = 0.663$$

$$L_{u2} := \frac{379.4 \text{ kN}}{F_{Rku1.unrein}} = 0.765 \qquad L_{u5} := \frac{328.8 \text{ kN}}{F_{Rku1.unrein}} = 0.663$$

$$L_{u3} := \frac{379.4 \text{ kN}}{F_{Rku1.unrein}} = 0.765 \qquad L_{u6} := \frac{328.8 \text{ kN}}{F_{Rku1.unrein}} = 0.663$$







$$L_{rein} := \begin{pmatrix} L_1 \\ L_2 \\ L_3 \\ L_4 \\ L_5 \\ L_6 \end{pmatrix} = \begin{pmatrix} 0.97 \\ 0.855 \\ 0.855 \\ 0.742 \\ 0.742 \\ 0.742 \end{pmatrix} \qquad L_{unrein} := \begin{pmatrix} L_{u1} \\ L_{u2} \\ L_{u3} \\ L_{u4} \\ L_{u5} \\ L_{u6} \end{pmatrix} = \begin{pmatrix} 0.765 \\ 0.765 \\ 0.765 \\ 0.663 \\ 0.663 \\ 0.663 \end{pmatrix}$$







A10 - Crack propagation in static tests

Specimen 1	Specimen 2	Specimen 3
Front view	Front view	Front view
		
Rear view	Rear view	Rear view
		

Specimen 4	Specimen 5	Specimen 6
Front view	Front view	Front view
		
Rear view	Rear view	Rear view
		

A11 - Crack propagation in dynamic tests

Specimen 7	Specimen 8	Specimen 9
Front view	Front view	Front view
		
Rear view	Rear view	Rear view
		

Specimen 10	Specimen 11	Specimen 12
Front view	Front view	Front view
		
Rear view	Rear view	Rear view
		

Specimen 13	Specimen 14	Specimen 15
Front view	Front view	Front view
		
Rear view	Rear view	Rear view
		

Specimen 16	Specimen 17	Specimen 18
Front view	Front view	Front view
Rear view	Rear view	Rear view